AD_____

Award Number:

W81XWH-05-1-0115

TITLE:

Angiogenesis Research to Improve Therapies for Vascular Leak Syndromes, Intra-abdominal Adhesions, and Arterial Injuries

PRINCIPAL INVESTIGATOR:

Judah Folkman, M.D.

CONTRACTING ORGANIZATION:

Children's Hospital
Boston, MA 02115

REPORT DATE:

April 2008

TYPE OF REPORT:

Final Report

PREPARED FOR: U.S. Army Medical Research and Materiel Command
Fort Detrick, Maryland 21702-5012

DISTRIBUTION STATEMENT:

Approved for public release; distribution unlimited

REPORT DOCUMENTATION PAGE

Form Approved
OMB No. 0704-0188

1. REPORT DATE *(DD-MM-YYYY)*	**2. REPORT TYPE**	**3. DATES COVERED** *(From - To)*
01-04-2008	Final	Jan 24 2005 – Mar 23 2008

4. TITLE AND SUBTITLE
Angiogenesis Research to Improve Therapies for Vascular Leak Syndromes, Intra-abdominal Adhesions, and Arterial Injuries

5a. CONTRACT NUMBER
W

5b. GRANT NUMBER
W81XWH-05-1-0115

5c. PROGRAM ELEMENT NUMBER

6. AUTHOR(S)
Judah Folkman, M.D., Mark Puder, M.D., Ph.D., Joyce Bischoff, Ph.D.

5d. PROJECT NUMBER
W23RYX-4299-N601

5e. TASK NUMBER

5f. WORK UNIT NUMBER

7. PERFORMING ORGANIZATION NAME(S) AND ADDRESS(ES)

Children's Hospital
300 Longwood Ave.
Boston, MA 02115

8. PERFORMING ORGANIZATION REPORT NUMBER

9. SPONSORING / MONITORING AGENCY NAME(S) AND ADDRESS(ES)

U.S. Army Medical Research and Materiel Command
Fort Detrick, Maryland 21702-5012

10. SPONSOR/MONITOR'S ACRONYM(S)

11. SPONSOR/MONITOR'S REPORT NUMBER(S)

12. DISTRIBUTION / AVAILABILITY STATEMENT

Approved for public release; distribution unlimited

13. SUPPLEMENTARY NOTES

14. ABSTRACT
The three goals of this project are: (i) to discover and develop novel drugs which could prevent or reverse the vascular leak syndrome; (ii) to develop angiogenesis inhibitors which would inhibit post-operative abdominal adhesions; and, (iii) to isolate endothelial progenitor cells from blood, capable of being expanded in vitro and applied to vascular grafts. Progress has been made in each category: we have demonstrated that the widely used antibiotic, doxycyline, is a potent inhibitor of VEGF-induced vascular leak, and that a combination of Lodamin and doxycycline have additive effects and inhibit vascular leakage by greater than 80%; we have established that sunitinib likely does prevent intra-abdominal postoperative adhesions in rabbits; and, we have isolated and characterized mesenchymal progenitor cells (MPCs) from human adult bone marrow and from human cord blood; showed expansion potential suitable for tissue engineering and tissue regeneration applications.

15. SUBJECT TERMS
Lodamin; doxycycline; Caplostatin; vascular leak; sunitinib; adhesions; circulating endothelial cells; mesenchymal and endothelial progenitor cells; mesenchymal stem cells; tissue-engineering.

16. SECURITY CLASSIFICATION OF:			**17. LIMITATION OF ABSTRACT**	**18. NUMBER OF PAGES**	**19a. NAME OF RESPONSIBLE PERSON**
a. REPORT	**b. ABSTRACT**	**c. THIS PAGE**			Donald Ingber
Unclassified	Unclassified	Unclassified	Unlimited	89	**19b. TELEPHONE NUMBER** *(include area code)* 617-919-2223

Standard Form 298 (Rev. 8-98)
Prescribed by ANSI Std. Z39.18

Table of Contents

DoD Congressional Grant
Annual Report *(01/24/07 – 01/23/08)*

Project I: New Therapy for Vascular Leak Syndromes

Judah Folkman, M.D., *Principal Investigator*
Kwan-Hyuck Baek, Ph.D., *Research Fellow*
Ofra Benny-Ratsaby, Research Fellow
Christiana DelloRusso, Ph.D., *Research Fellow*
Kashi Javaherian, Ph.D., *Research Associate*
Sandra Ryeom, Ph.D., *Research Associate*
Sarah Short, Ph.D., *Research Associate*
Alexander Zaslavsky, Ph.D., *Research Fellow*

I. INTRODUCTION

Vascular leak syndrome induced by blast injuries, burns, asphyxiation, and other injuries lead to progressive pulmonary edema, as well as tissue and limb swelling that contribute to morbidity and mortality of soldiers on the battlefield. The goal of this research remains the development and validation of novel therapies to prevent and reverse vascular leak syndromes. During the past year we continued to use an in vivo permeability assay to investigate the potential value of treating vascular leak syndromes using anti-angiogenic therapies, including Endostatin, Caplostatin (polymer-conjugated form of TNP-470), and a newly developed nanoparticle formulation of TNP-470, called 'Lodamin', as well as the widely used antibiotic, doxycycline. Our ongoing studies include the use of transgenic mouse models to determine the mechanism by which these therapies prevent or block increases in vascular permeability, as this knowledge could lead to even more effective therapies in the future.

II. BODY

Our research accomplishments during this past year include:

Task 1: To determine the mechanism of Caplostatin function in protecting against vascular leak.

We have previously demonstrated that Caplostatin, a form of TNP-470 (a synthetic analog of fumagillin) that is covalently linked to the polymer HPMA (hydroxy-propyl methacrylamide), is a potent anti-angiogenic agent when administered by subcutaneous injection. Over the past year, we developed an improved nanoparticle form of TNP-470 by conjugating it to a biodegradable poly-lactic acid (PLA) polymer via pegylation, which self-assembles into nanometer-sized micelles. This nanotechnology-based form of Caplostatin, which has been named "Lodamin", can be administered orally or by injection. The development of an oral anti-vascular leak therapy is highly

desirable since it raises the possibility of providing a preventative therapy that might be administered immediately before soldiers enter into heavy action, and it could be administered even if needles and syringes were not available on the battlefield.

To ensure that Lodamin would be a suitable oral drug, we examined the intestinal absorption of fluorescently labeled-PEG-PLA micelles. Mice were orally gavaged with polymeric nanomicelles (8 nm diameter), and after 2 hours they were euthanized and their small intestines were harvested, fixed and imaged by fluorescence microscopy. These studies demonstrated that the nanoparticles were effectively taken up by the epithelium lining the luminal side of the small intestine and transported into the lamina propria near the vasculature. These data confirm that these drug-containing nanomicelles are absorbed across the intestinal epithelium.

Initial studies have investigated the anti-vascular leak efficacy of Lodamin after treatment of wild-type mice by oral gavage for 5 days using the Miles permeability assay. This assay has been described in detail in our previous progress reports and publications. The Miles assay revealed that mice treated with oral Lodamin demonstrated a 59% inhibition of VEGF-induced vascular permeability, as compared to mice treated with unconjugated polymer alone.

Objective II. To determine the mechanism by which Fc-endostatin protects against vascular leak by identifying its functional dependence on the endogenous angiogenesis inhibitor thrombospondin-1, identifying its receptor(s) on endothelial cells and identification of genes regulated by endostatin treatment.

Our work has focused on development of a stable form of endostatin that uses the N-terminal peptide domain of this endogenous angiogenesis inhibitor conjugated to the Fc-domain of IgG. The addition of an Fc domain to a recombinant endostatin peptide has increased its half-life to greater than one week. We have used tumor studies as a bioassay to optimize Fc-endostatin treatment dose, timing, and toxicity, with the goal of using these same conditions to assess anti-vascular permeability efficacy.

This past year we have identified a biphasic anti-tumor effect of Fc-endostatin, such that the optimal anti-tumor dose is observed at a moderate concentration of Fc-endostatin (0.67 mg/kg/day). Our studies demonstrated that both lower (0.167 mg/kg/day) and higher (2.6 mg/kg/day) doses of Fc-endostatin were much less effective in suppressing tumor growth, as compared to a moderate dose of Fc-endostatin. Studies are currently underway to determine if these Fc-endostatin regimens have a similar biphasic effect on vascular permeability.

Objective III. To examine the anti-vascular leak effect of the antibiotic doxycycline.

While not included in our Statement of Work from 2007, this past year we discovered that the clinically approved and widely used antibiotic, Doxycycline, which is known to be anti-angiogenic also has potent anti-vascular leak properties. This work

was initially described in our second quarter progress report (May 2007). We have investigated this previously unknown effect of doxycycline in the *in vivo* Miles permeability assay using VEGF as an agonist. Our studies confirmed that doxycycline (80 mg/kg/day) administered by oral gavage to wild-type mice suppressed VEGF-induced vascular permeability by 54% in the Miles assay. Moreover, combined therapy using doxycycline and Lodamin (15 mg/ kg/day) resulted in an even greater (82%) inhibition of VEGF-induced vascular permeability in this assay.

We also have investigated the mechanism by which doxycycline may protect against vascular leak in studies with cultured endothelial cells. Our preliminary results suggest that the endothelial junctional protein, VE-cadherin is significantly upregulated after doxycycline treatment. VE-cadherin is an endothelial cell transmembrane protein expressed at the cell surface and is known to play a critical role in physically linking cells, thereby maintaining the barrier function of endothelial cell monolayers. Therefore, our data suggest that upregulation of VE-cadherin may be one of the mechanisms by which doxycycline blocks vascular permeability.

III. KEY RESEARCH ACCOMPLISHMENTS

- Generation of an improved orally available version of TNP470 and Caplostatin renamed Lodamin.
- Validation of the oral absorption and bioavailability of Lodamin.
- Demonstration of Lodamin's ability to suppress VEGF-induced vascular permeability *in vivo*.
- Optimization of the anti-tumor dose and timing of a Fc-conjugated endostatin peptide
- Demonstration that the widely used antibiotic, doxycyline, is a potent inhibitor of VEGF-induced vascular leak.
- Preliminary identification of VE-Cadherin as a mediator of the effects of doxycycline on vascular permeability
- Demonstration that combination of Lodamin and doxycycline have additive effects and inhibit vascular leakage by greater than 80%

IV. REPORTABLE OUTCOMES

Manuscripts:

1. Lee TL, Sjin RMT, Movahedi S, Ahmed B, Pravda EA, Lo KM, Gillies SD, Folkman J and Javaherian K. (2008) Linking antibody Fc domain to endostatin significantly improves endostatin half-life and efficacy**.** ***Clin. Cancer Res****.* -in press.

2. Folkman J. Angiogenesis: an organizing principle for drug discovery? **Nat Rev Drug Discov.** 2007; 6: 273-286.

3. Folkman, J. Endostatin finds a new partner: nucleolin. **Blood** 2007; 110(8): 2786 -2787.

4. Benny O, Fainaru O , Adini A , Bazinet L , Adini I, Cassiola F, Pravda E, Koirala S , D'Amato R, Corfas G , Folkman J. LodaminTM: a novel formulation for oral administration of TNP-470 as a potent inhibitor of angiogenesis, tumor growth and metastasis. **Nat Biotech**, *in review. Will forward to DOD once accepted.*

5. Fainaru O, Adini I, Benny O, Lauren Bazinet, Adini A, D'Amato RJ, Folkman J. Doxycycline induces the expression of VE-cadherin and prevents vascular permeability in mice*. (manuscript in preparation—will forward to DOD once accepted.)*

Presentations:

1. Boston Medical Center Ground Rounds, Boston, MA. (January 25, 2007). "Angiogenesis-dependent Diseases".

2. Bruce Terman Annual Lectureship, Albert Einstein College of Medicine, New York, NY. (February 8, 2007). "Angiogenesis: An organize principle in biomedicine?"

3. 8Th World Congress for Microcirculation, Milwaukee, WI. (August 16, 2007). "Endogenous Angiogenesis Inhibitors".

4. Emory University School of Medicine's Winship Cancer Institute, Atlanta, GA. (October 25, 2007). "Angiogenesis: A Paradigm for Translating from the Laboratory to the Clinic and Back".

V. CONCLUSION

Our studies utilizing an oral nanoparticle formulation of TNP470 called Lodamin suggest that this agent may be an even more effective anti-vascular leak agent than Caplostatin. We also discovered that the FDA-approved antibiotic doxycycline is a potent anti-vascular leak drug, which produces even more potent effects when co-administered with Lodamin. The use of these orally available therapies to prevent or treat vascular leak syndromes as a result of trauma or other injuries sustained during combat may allow rapid self-treatment by soldiers or other wounded personnel, and might potentially be used as prophylaxis before entering into battle. We also will continue to optimize dosing for Lodamin and doxycycline separately, and in combination, using the *in vivo* Miles permeability assay; we also will examine the effects of Fc-endostatin in this model system. To explore the utility of these agents in a more physiologically relevant model of vascular leak syndromes, we will also examine their effects in a mouse model of IL-2 induced pulmonary edema; we recently received approval for our mouse protocol to utilize this model. Our plans for next year include the testing of Lodamin, doxycycline and Fc-endostatin to prevent IL-2 induced pulmonary edema in wild-type mice. Data from these mouse studies will form the basis

for future translation of this therapy into clinical testing. We will initiate discussions with members of the military medical command to explore how to best translate these discoveries into new therapies for soldiers with pulmonary leak syndrome.

"SO WHAT" SECTION:

The significance of this work lies in the discovery that non-toxic angiogenesis inhibitors, including one that is currently FDA-approved for human use, may be used to prevent or treat vascular leak syndrome. These oral agents might be self-administered by soldiers before they enter battle to prevent vascular leak syndrome in the case of injury. They also may be injected subcutaneously or by gavage in badly injured soldiers to prevent this life-threatening syndrome.

VI. REFERENCES None

Project II: Prevention of Post-operative and Traumatic Abdominal Adhesions

Mark Puder, M.D. Ph.D., *Primary Investigator*
Sendia Kim, M.D., *Research Fellow*
Arin Greene, M.D., *Research Fellow*
Hau Le, M.D., *Research Fellow*
Jonathan Meisel, M.D., *Research Fellow*

I. INTRODUCTION

Postoperative intra-abdominal adhesions are a major problem causing high morbidity in the general surgery and trauma patient populations. It costs the U.S. hundreds of millions of dollars annually. Several approaches have been attempted to inhibit intra-abdominal adhesion formation, most with limited success [1, 2]. Most recently, our attention has been turned towards a recently FDA approved class of drugs called tyrosine kinase inhibitors that have both anti-angiogenic and anti-tumor properties. In clinical practice, this class of drugs is approved for use in advanced stages of renal cell carcinoma and gastrointestinal stromal tumors. Sunitinib (sunitinib malate or SU11248; Pfizer Inc.) inhibits vascular endothelial growth factor receptors (VEGFR) 1 and 2, which are angiogenesis mediators that may potentially be involved in adhesion formation. We felt that the inhibition of VEGFR may also have significance in the prevention of surgical adhesions, as VEGF, among other factors, is up-regulated in adhesion formation.

II. BODY

During the first two quarters of 2007, animal protocols were being reviewed by the Animal Research committee at Children's Hospital, Boston, and animal work could not be initiated until protocol approval was secured. The previous year's protocol used celecoxib, a COX-2 inhibitor that targets the expressed COX-2 enzyme on the newly proliferating vasculature, to prevent adhesions. The change in drug from celecoxib to sunitinib required multiple levels of review.

In the second half of 2007, the previous research fellow in the lab finished her fellowship and moved on. Drs. Jonathan Meisel and Hau Le, general surgery residents at Beth Israel Deaconess Medical Center and the University of Medicine and Dentistry of New Jersey respectively, began their research fellowships in Dr. Puder's lab. They were required to attend several animal research training sessions and to learn the operative techniques used on the rabbits.

Work with the experimental drug sunitinib began late in the 3rd quarter and continued through the end of the year. Preliminary results are promising. The uterine horn model for abdominal adhesions was used. The procedure is as follows: The

abdomen is prepped and draped in the normal sterile fashion. A lower midline incision is made and the uterine horns brought out through the incision. Using a number 10 blade scalpel, the uterus and fallopian tubes are abraded until punctuate hemorrhages appear. A small collateral blood vessel in the mesosalpinx is tied off with a 5-0 silk tie. The uterus is then returned to normal anatomic position, and the peritoneum and skin are closed.

A total of ten rabbits were randomly assigned to receive either sunitinib (40mg/kg/day) once a day, or a placebo. The medication was mixed with water and given by orogastric gavage. The control rabbits were gavaged with water only. All rabbits received the first dose 24 hours prior to surgery and continued daily for 10 days postoperatively. The rabbits were sacrificed on postoperative day 10 and the adhesions were blindly scored by 2 individual scorers based on a well accepted scoring system: tenacity to the uterine horns (none = 0, fell apart = 1, lysed with traction = 2, lysed with blunt dissection = 3, lysed with sharp dissection = 4) and percent covered (0 = 0, <25% = 1, 25-50% = 2, 50-75% = 3, >75% = 4).

Results showed that all 5 control rabbits developed adhesions. Their mean total adhesion score was 6.5 and ranged from 5-8 (0 being no adhesions, 8 being the most extensive adhesions possible). The rabbits treated with sunitinib were all adhesion free, however, three of them died unexpectedly, prior to post-operative day (POD) 10. One died on POD 2, another on POD 5, and the third on POD 8. The first was witnessed to have a seizure. The last 2 were found dead in their cage. Necropsy revealed no cause of death. They were all adhesion free. The most severe known side effect of sunitinib in humans is hypertension and congestive heart failure. Cardiac toxicity was the likely cause of death in the rabbits.

The next step is to perform a pilot study to determine the appropriate non-toxic dose of sunitinib. This new protocol amendment is currently under review but the Animal Care committee.

Over the next year we hope to determine the appropriate dose for preventing adhesions in the rabbits, as well as assess the drug's effect on wound strength. We will also attempt to determine the long-term effect of sunitinib on adhesions by carrying out the experiments to 6-8 weeks. Next we hope to look at bowel anastamosis strength as well. Finally we'd like to determine the role of sunitinib in preventing reoperative adhesions.

III. KEY RESEARCH ACCOMPLISHMENTS

● Established that sunitinib likely does prevent intra-abdominal postoperative adhesions in rabbits.

IV. REPORTABLE OUTCOMES

None

V. CONCLUSION

The anti-angiogenic effects of sunitinib seem to prevent postoperative adhesions in rabbits. The appropriate safe dose has yet to be determined.

"SO WHAT" SECTION:

Adhesions are the major cause of intestinal obstruction, which can lead to prolonged hospital stays and often additional abdominal surgery, which only perpetuates the problem. Adhesions also increase the morbidity and mortality of each subsequent surgery because they lead to increased blood loss and injury to internal organs. In the United States, the total cost from complications from adhesions is over $1 billion a year, and accounts for over 846,000 inpatient care days [3]. The prevention of adhesions would profoundly decrease the morbidity and reduce health care costs across a broad range of medical disciplines [4].

VI. REFERENCES

1. Montz FJ, Holschneider CH, Bozuk M, Gotlieb WH, Martinez-Maza O (1994) Interleukin 10: ability to minimize postoperative intraperitoneal adhesion formation in a murine model. Fertil Steril 61: 1136-1140.
2. Rodgers KE, Johns DB, Girgis W, Campeau J, diZerega GS (1997) Reduction of adhesion formation with hyaluronic acid after peritoneal surgery in rabbits. Fertil Steril 67: 553-558.
3. Ray NF, Denton WG, Thamer M, Henderson SC, Perry S (1998) Abdominal adhesiolysis: inpatient care and expenditures in the United States in 1994. J Am Coll Surg 196: 1-9.
4. Menzies D, Parker M, Hoare R, Knight A (2001) Small bowel obstruction due to postoperative adhesions: treatment patterns and associated costs in 110 hospital admissions. Ann R Coll Surg Engl 83: 40-46.

Project III: Creating New Blood Vessels using Blood-derived Endothelial and Mesenchymal Progenitor Cells

Joyce Bischoff, Ph.D., *Principal Investigator*
Juan Martin-Melero, Ph.D., *Research Fellow*

I. INTRODUCTION

Tissue engineering of blood vessels, cardiovascular structures and whole organs holds promise as a new approach to replace damaged or diseased tissues. Using sheep as a model system, we showed that endothelial progenitor cells (EPCs) isolated from a small amount of peripheral blood can be used to create non-thrombogenic long-lasting functional blood vessels (1). The success of this project encouraged us to develop methods for isolating EPCs from human blood, and also to pursue the isolation and characterization of mesenchymal progenitor cells (MPCs). We postulated that the MPCs can be used to form the smooth muscle layer in tissue-engineered blood vessels surrounding the EPCs that form the blood vessel lumen. Towards this end, we have developed isolation and cell expansion techniques for these human progenitor cells and quantitative measures of blood vessel forming potential in vivo.

With DOD funding, we showed that human cord blood-derived EPCs were able to form functional blood vessel networks in vivo, within 7 days, when combined with mature human saphenous vein endothelial cells (2). In addition, we showed that EPCs from adult peripheral blood had the same vasculogenic potential when combined with human smooth muscle cells(2). In the past funding year, we isolated and characterized MPCs from adult bone marrow and from cord blood and showed that MPCs could substitute for the mature human smooth muscle cells (3; Melero-Martin et al., submitted). This has brought us one step closer to our goal of building blood vessel networks from human progenitor cells obtained without sacrifice of healthy tissues, veins or arteries. Advancing this research could lead to strategies for creating tissue-engineered blood vessels and microvascular networks as needed for damaged organs and tissues suffered by injured soldiers.

II. BODY

Objective 1. To optimize growth conditions for adult EPCs isolated from peripheral blood. Success in this objective will advance our goal of using autologous EPCs for creating arteries and microvessels for tissue repair.

We showed that adult EPCs grow well in culture and can be expanded to 10^8 cells from a starting blood sample of 50-100 mls of blood (2). Experiments performed for Objective 3 (below), and now submitted for publication, show that adult EPCs have the same robust blood vessel forming potential in vivo as cord blood EPCs when the adult EPCs are supported by human MPCs. These encouraging results suggest that it

might not be necessary to use higher numbers of adult EPCs to achieve in vivo blood vessel formation, and so we focused our attention on Objectives 2 and 3.

Objective 2: To use our in vivo model for blood vessel formation to quantitate and test the blood-vessel forming capability of blood-derived progenitors.

In this Objective, our plan was to optimize various parameters using EPCs combined with human saphenous vein smooth muscle cells – as described in our 2007 publication (2). However, since we were able to move rapidly on Objective 3, and show that our MPCs are able to substitute for the human saphenous vein smooth muscle cells, we used this two cell system - EPCs and MPCs - to optimize parameters and to quantify the blood vessel forming potential of the progenitor cell populations.

Objective 3: To identify culture conditions under which the MPCs from blood will be able to function as smooth muscle cells in the in vivo assay.

We have isolated, expanded and fully characterized human MPCs from umbilical cord blood (cbMPCs) and from adult bone marrow (bmMPCs), and have shown that MPCs substitute for human saphenous vein smooth muscle cells. This work has been submitted for publication. In the manuscript, we describe the formation of functional microvascular beds in immunodeficient mice by co-implantation of human EPCs and MPCs isolated from blood and bone marrow. Evaluation of implants after one week revealed an extensive network of human blood vessels containing erythrocytes, indicating the rapid formation of functional anastomoses with the host vasculature. The implanted EPCs were restricted to the luminal aspect of the vessels; MPCs were found on their abluminal surface, confirming their role as perivascular cells. Importantly, the engineered vascular networks remained patent at 4 weeks *in vivo*. This rapid formation of long-lasting microvascular networks by postnatal progenitor cells obtained from non-invasive sources constitutes an important step forward in the development of clinical strategies for tissue vascularization, a critical requirement for wound healing and tissue regeneration.

III. KEY RESEARCH ACCOMPLISHMENTS

- Isolated and characterized mesenchymal progenitor cells (MPCs) from human adult bone marrow and from human cord blood; showed expansion potential suitable for tissue engineering and tissue regeneration applications
- Demonstrated potential for MPCs to differentiate towards a smooth muscle phenotype in vitro.
- Demonstrated ability of the MPCs combined with EPCs to form vascular networks in vivo: optimized the EPC/MPC ratio for in vivo blood vessel formation.
- Demonstrated the durability of the EPC/MPC vascular networks in vivo over a four week time period.
- Showed that adult blood-derived EPCs combined with adult MPCs formed vascular networks in vivo at the same rate and density as cord blood EPCs.

IV. REPORTABLE OUTCOMES

Manuscripts:

1. Melero-Martin JM, Khan ZA, Picard A, Wu X, Paruchuri S Bischoff J. 2007; In vivo vasculogenic potential of human blood-derived endothelial progenitor cells. Blood, 109: 4761-4768.

2. Melero-Martin JM, De Obaldia ME, Kang S-Y, Khan ZA, Yuan L, Oettgen P, Bischoff J. 2008; Engineering vascular networks *in vivo* with human postnatal progenitor cells isolated from blood and bone marrow, *submitted*

3. Melero-Martin, JM, Santhalingam S, Al-Rubeai M, 2008; Methodology for optimal in vitro cell expansion in tissue engineering, *submitted*

Abstracts:

Melero-Martin JM, Khan ZA, Bischoff J. In vivo vasculogenic potential of blood-derived endothelial progenitor cells: potential applications for tissue engineering. 2nd Annual Methods in Bioengineering Conference, July 2007, Cambridge, MA USA

Melero-Martin JM, De Obaldia ME, Kang S-Y, Khan ZA, Bischoff J. Engineering vascular networks in vivo by combination of human endothelial and mesenchymal progenitor cells isolated from blood and bone marrow. Gordon Research Conference: Angiogenesis and Microcirculation. August 2007, Newport, RI, USA

Presentations:

Juan Melero-Martin, Invited Speaker, Harvard Stem Cell Institute (HSCI) Cardiovascular Symposium, April 2007, Cambridge, MA, USA
Title: In vivo vasculogenic potential of blood-derived progenitor cells: potential applications to tissue-engineering.

Juan Melero-Martin, Poster Presentation, Center for Integration of Medicine & Innovative Technology (CIMIT) 2007 Innovation Congress, Nov 2007, Boston, MA USA
Title: Engineering vascular networks in vivo by combination of human endothelial and mesenchymal progenitor cells isolated from blood and bone marrow.

Joyce Bischoff, Invited Speaker, NAVBO Vascular Matrix Biology and BioEngineering, March 2007, British Columbia, Canada
Title: Blood-derived Progenitor Cells for Tissue Vascularization

Joyce Bischoff, Keynote Speaker, NATO Advanced Research Workshop on Nanoengineered Systems for Regenerative Medicine, Sept. 2007, Varna, Bulgaria
Title: Blood-derived Endothelial and Smooth Muscle Progenitor Cells for Creating Vascular Networks In Vivo

Joyce Bischoff, Seminar Speaker, Dept. Molecular Biology and Biochemistry, UC-Irvine, November 2007, Irvine, CA, USA
Title: Tissue Vascularization using Blood-derived and Bone Marrow-derived Progenitor Cells

Patents:

Title: Methods for Promoting Neovascularization*
Inventors: Juan Melero-Martin and Joyce Bischoff
International Application no.: PCT/US2007/88110
Filing Date: December 19, 2007
CMCC Reference # 1495*
A provisional patent application was filed last year, December 19, 2006 for the same technology but under a different title: Isolation and Expansion of Human Progenitors from Cord Blood and Adult Peripheral Blood.

V. CONCLUSION

In our *in vivo* model for *de novo* blood vessel formation (i.e, vasculogenesis), subcutaneous co-implantation of human EPCs and MPCs, suspended as single cells in Matrigel, into immunodeficient mice resulted in the creation of extensive microvascular beds that rapidly formed anastomoses with the host vasculature. We showed that the MPCs obtained from both human adult bone marrow and human cord blood serve as perivascular/smooth muscle cells and are essential for rapid and high density blood vessel formation. Furthermore, our study shows that adult blood-derived EPCs achieve the same blood vessel density as cord blood EPCs when combined with human MPCs. This study constitutes a step forward in the clinical development of therapeutic vasculogenesis by showing the feasibility of using human postnatal progenitor cells as the basic cellular building blocks to create functional vascular networks *in vivo*.

"SO WHAT" SECTION:

Our goal is to build vascular networks from human endothelial progenitor cells (EPCs) and mesenchymal progenitor cells (MPCs) to rebuild damaged tissues and organs. We have shown that human EPCs and MPCs can be obtained from blood or bone marrow and expanded in the laboratory without difficulty. Our published and preliminary data demonstrate the vasculogenic capability of these cells in vivo. In the future, we envision use of a patient's own EPCs and MPCs for a variety of tissue-engineering applications and for in situ regeneration of vascular networks in ischemic or injured tissue. For tissue-engineering, vascular networks created from EPCs/MPCs would be incorporated into tissue-engineered constructs in vitro such that upon implantation in vivo, anastomoses with the host circulation occur rapidly to establish blood flow. For tissue regeneration in situ, EPCs/MPCs would be delivered to the site in vivo where they will undergo vasculogenesis and connect to ends of remaining functional vascular networks. In summary, we envision our two-cell system as an

enabling technology that can be applied to many different tissues/organs where new functional blood vessel networks are required for repair and regeneration.

VI. REFERENCES

1. Kaushal S, Emiel G, Guleserian KJ, Shapira OM, Perry T, Sutherland FW, Rabkin E, Moran AM, Schoen FJ, Atala A, Soker S, Bischoff J, Mayer J. 2001; Functional small diameter neovessels created using endothelial progenitor cells expanded ex vivo. Nature Medicine, 7: 1035-1040.
2. Melero-Martin JM, Khan ZA, Picard A, Wu X, Paruchuri S Bischoff J. 2007; In vivo vasculogenic potential of human blood-derived endothelial progenitor cells. Blood, 109: 4761-4768.

3. Melero-Martin JM, De Obaldia ME, Kang S-Y, Khan ZA, Yuan L, Oettgen P, Bischoff J. 2008; Engineering vascular networks *in vivo* with human postnatal progenitor cells isolated from blood and bone marrow, *submitted*

VII: APPENDICES:

Project I:

Lee TL, Sjin RMT, Movahedi S, Ahmed B, Pravda EA, Lo KM, Gillies SD, Folkman J and Javaherian K. (2008) Linking antibody Fc domain to endostatin significantly improves endostatin half-life and efficacy**.** ***Clin. Cancer Res****.* -in press.

Folkman J. Angiogenesis: an organizing principle for drug discovery? **Nat Rev Drug Discov.** 2007; 6: 273-286.

Folkman, J. Endostatin finds a new partner: nucleolin. **Blood** 2007; 110(8): 2786 -2787.

Project II:

None

Project III:

Melero-Martin JM, Khan ZA, Picard A, Wu X, Paruchuri S Bischoff J. 2007; In vivo vasculogenic potential of human blood-derived endothelial progenitor cells. **Blood**, 109: 4761-4768.

Melero-Martin JM, De Obaldia ME, Kang S-Y, Khan ZA, Yuan L, Oettgen P, Bischoff J. 2008; Engineering vascular networks *in vivo* with human postnatal progenitor cells isolated from blood and bone marrow, *submitted*

Linking Antibody Fc Domain to Endostatin Significantly Improves Endostatin Half-life and Efficacy

Tong-Young Lee,[1] Robert M. Tjin Tham Sjin,[1] Shahla Movahedi,[1] Bissan Ahmed,[1] Elke A. Pravda,[1] Kin-Ming Lo,[2] Stephen D. Gillies,[2] Judah Folkman,[1] and Kashi Javaherian[1]

Abstract

Purpose: The half-life of the antiangiogenic molecule endostatin that has been used in clinical trial is short (~2 h). In addition, ~50% of the clinical grade endostatin molecules lack four amino acids at their NH_2 termini. Lack of these amino acids gives rise to a molecule that is devoid of zinc, resulting in no antitumor activity. Our goal was to develop a new version of endostatin that does not show such deficiency.

Experimental Design: A recombinant human endostatin conjugated to the Fc domain of IgG was constructed and expressed in mammalian cell culture. The presence of Fc has been shown by previous investigators to play a major role in increasing the half-life of the molecule. Fc-endostatin was tested in tumor-bearing mice, and its half-life was compared with the clinical grade endostatin.

Results: The antitumor dose of Fc-endostatin was found to be ~100 times less than the clinical grade endostatin. The half-life of Fc-endostatin in the circulation was found to be weeks rather than hours, as observed for endostatin alone. In addition, a U-shaped curve was observed for antitumor activity of endostatin as a function of endostatin concentration delivered to the animals.

Conclusion: Fc-endostatin is a superior molecule to the original clinical endostatin. Due to its long half-life, the amount of protein required is substantially reduced compared with the clinically tested endostatin. Furthermore, in view of the U-shaped curve of efficacy observed for endostatin, we estimate that the requirement for Fc-endostatin is ~700-fold less than endostatin alone. The half-life of endostatin is similar to that of vascular endothelial growth factor – Trap and Avastin, two other antiangiogenic reagents. We conclude that a new clinical trial of endostatin, incorporating Fc, may benefit cancer patients..

Q2

Endostatin, a proteolytic fragment from collagen 18, has been shown to be a potent antiangiogenic protein (1, 2). The antitumor activity of endostatin is well-established. At the time of this writing, there are >950 publications on endostatin. The antitumor properties of endostatin have been confirmed in the vast majority of these publications using a large variety of tumor models (2). The protein does not cause toxicity in patients.

The mechanism of endostatin action is still not clear. Integrin $\alpha5\beta1$ has been implicated by binding endostatin and inhibiting angiogenesis (3). More recently, it has been shown that endostatin is not a passive inhibitor. Its generation from collagen 18 is regulated by cell pathways initiated by the master tumor suppressor p53 (4, 5). P53 up-regulates transcription of α (II) collagen prolyl-4-hydroxylase, releasing tumstatin and endostatin from collagen 4 and 18, respectively.

Clinical trials of human endostatin in phase I and II used a recombinant molecule that was expressed in yeast. This formulation of endostatin carried two major handicaps. The half-life of the protein in circulation was very short. The decay of endostatin represented a biexponential model that resulted in a half-life ($t_{1/2}$) of 42.3 min and a β $t_{1/2}$ of 12.9 h (6). The second problem, which has not been appreciated, is the fact that ~50% of the injected recombinant human endostatin used in the original clinical trials lacked four amino acids at the NH_2 terminus of the molecule (7). Deletion of these four amino acids gave rise to a molecule, which did not bind zinc and consequently showed a relatively decreased antitumor activity (8).

To overcome these two deficiencies, we have constructed a molecule of endostatin that is fused to the Fc region of an IgG molecule (9, 10). The presence of Fc increases the half-life to longer than a week, analogous to the two angiogenesis inhibitors Avastin and vascular endothelial growth factor (VEGF)-Trap. Both of these reagents contain an Fc domain that increases the half-lives of the proteins to weeks rather than hours (11, 12). In this connection, it is relevant to point out that a Fab fragment of Avastin, which lacks Fc, has a half-life of ~2 h [the molecule is called Lucentis (Ranibizumab) and is

Authors' Affiliations: [1]Vascular Biology Program, Department of Surgery, Children's Hospital Boston and Harvard Medical School, Boston, Massachusetts and [2]EMD Lexigen Research Center, Billerica, Massachusetts

Received 6/20/07; revised 10/18/07; accepted 12/7/07.

Grant support: Breast Cancer Research Foundation, Department of Defense grant W81XWH-05-1-0115, and NIH grant RO1 CA064481 (J. Folkman).

The costs of publication of this article were defrayed in part by the payment of page charges. This article must therefore be hereby marked *advertisement* in accordance with 18 U.S.C. Section 1734 solely to indicate this fact.

Requests for reprints: Kashi Javaherian, Karp Family Research Laboratories, Room 11.213, 1 Blackfan Circle, Boston, MA 02115. Phone: 617-919-2392; Fax: 617-730-0231; E-mail: kashi.javaherian@childrens.harvard.edu.

doi:10.1158/1078-0432.CCR-07-1530

produced by Genentech for the treatment of age-related macular degeneration; ref. 13].

Another aspect of endostatin, its biphasic, U-shaped antitumor activity (14, 15), is also revealed for recombinant human Fc-endostatin (hFc-endostatin) here. We show here that Fc-endostatin, when its biphasic, U-shaped antitumor activity is taken into account, can achieve optimum antitumor efficacy when administered at doses that are at least 100-fold lower than endostatin lacking Fc.

We anticipate that by using Fc-endostatin, it should be possible to reach endostatin concentrations in tens of μg/mL in the circulation of patients, analogous to Avastin and VEGF-Trap (11, 16). Finally, we report the antitumor activities for two endostatin mutants. One of the mutants has alanine substitutions of two histidines responsible for its zinc binding (H1A and H3A). The second mutant lacks heparin binding due to replacement of two critical arginines by alanines (R27A and R139A). Both of these mutants decrease antitumor activity of the native endostatin. The zinc-deficient mutant is more effective than the heparin-deficient endostatin. The improved formulation of endostatin reported here may provide for more effective clinical trials.

Materials and Methods

Expression and purification. Construction, expression, and purification of hFc-endostatin and mouse Fc-endostatin (mFc-endostatin) have been described previously (9, 10). The recombinant constructs were prepared by placing the Fc regions at the NH_2 terminus of endostatin. Stable cell lines of these constructs were produced in NS/0 murine myeloma cells. The proteins were expressed and secreted into the medium. Protein A was used for purification of the recombinant proteins (at least 90% purity; refs. 9, 10). We obtained ~50 mg/liter of Fc-endostatin by using fermentors of 10- to 18-liter capacity.

hFc-endostatin (H1A and H3A) is a mutant in which the histidines 1 and 3 of endostatin are substituted by alanines, resulting in a molecule that lacks zinc binding. The expression plasmid for hFc-endostatin (H1A and H3A) was constructed by using a synthetic HindIII-SexA1 oligonucleotide duplex containing the two codon substitutions to replace the corresponding restriction fragment in pdCs-Fc(D4K)-endostatin (9). The sense strand has the sequence 5′-AGCTT**GCT**AGC**GCA**CGCGACTTCCAGCCGGTGCTCCA, and the nonsense strand has the sequence 5′-CCAGGTGGAGCACCGGCTG-GAAGTCGCG**TGC**GCT**AGC**A, where the H1A and H3A codons and anticodons are in bold. The resultant construct was used to transfect NS/0 murine myeloma cells. hFc-endostatin (H1A and H3A) was purified from conditioned medium of stable clones as previously described (9). Construction, expression, and purification of endostatin deficient in heparin binding have been previously described (17). We have previously reported the inhibition of endothelial cell migration *in vitro* and the reduction of tumor vessel density *in vivo* by Fc-endostatin (8, 14).

Animal studies. All animal procedures were carried out in compliance with Children's Hospital Boston guidelines. Protocols were approved by the Institutional Animal Care and Use Committee. Male (24-27 g) immunocompetent C57Bl/6J (Jackson Laboratory) and immunocompromised severe combined immunodeficiency (SCID) mice (Massachusetts General Hospital) were used. Mice were ages 7 to 9 weeks. Mice were acclimated, caged in groups of five in a barrier care facility, and fed animal chow and water *ad libitum*. Animals were euthanized by CO_2 inhalation.

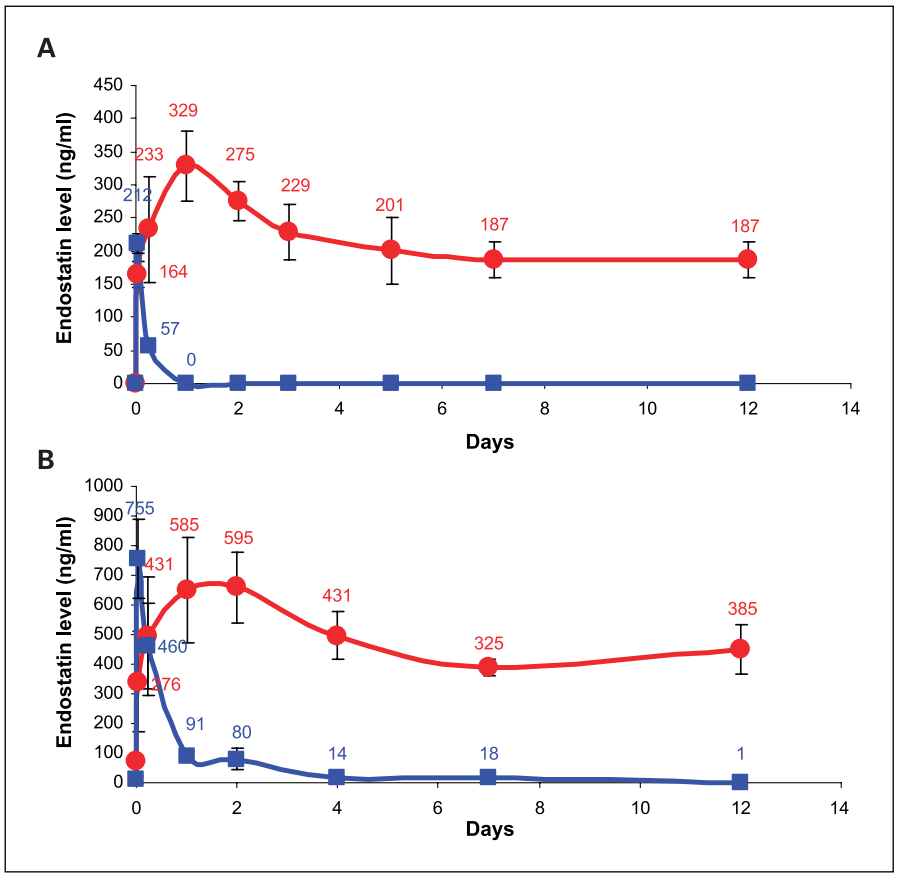

Fig. 1. Pharmacokinetics of endostatin and Fc-endostatin. PBS of endostatin (100 μg/0.2 mL) was injected s.c. into C57Bl/6J.mice, and concentrations of the circulating protein were monitored by ELISA (Cytimmune). Three mice were in each group. *A,* hFc-endostatin (●) and human endostatin (■). *B,* mFc-endostatin (●) and mouse endostatin (■). The measured concentrations of mouse endostatin were corrected for baseline endostatin (60 ng/mL). Mouse endostatin was prepared by treating mFc-endostatin with enterokinase and purified on Pharmacia Sepharose S-100 (9).

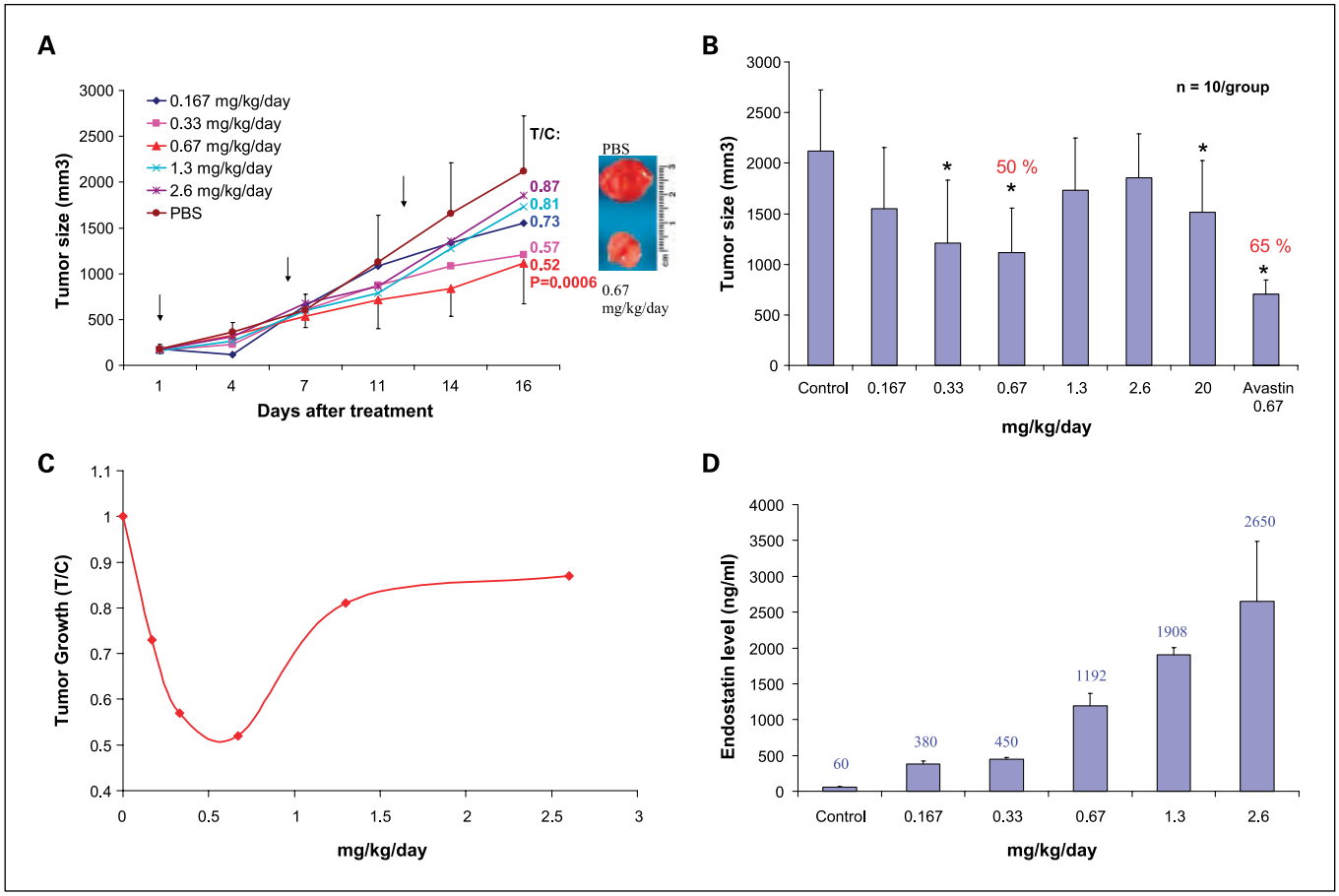

Fig. 2. Treatment of human melanoma cancer cells (A2058) with hFc-endostatin. Ten SCID mice in each group. S.c. injections were delivered in 0.2 mL volume of PBS once every 6 days; $n = 10$. *A,* tumor size as a function of time and concentration of endostatin. The ratio of T/C is shown for each group. *B,* tumor size is plotted as a function of concentration of the delivered protein. The Avastin dose is the same as endostatin at its optimum efficacy (0.67 mg/kg/d). Daily injection of endostatin at 0.5 mg per mouse day (20 mg/kg/d). *C,* the U-shaped curve for data of *B*. *D,* ELISA of endostatin 3 days after the last injection.

ELISA determination of Fc-endostatin. Serum samples were obtained by retroorbital puncture with nonheparinized capillary tubes under anesthesia. Samples were placed at 4°C overnight, and serum was collected after centrifugation at 10,000 rpm for 10 min. Concentrations were determined by competition ELISA (Cytimmune Sciences) following the manufacturer's protocol.

Tumor models. Human melanoma A2058 and ASPC-1 (a human pancreatic tumor cell line) were cultured in DMEM and RPMI 1640 with L-glutamine, respectively and supplemented with 10% FCS and antibiotics. SCID mice were shaved and the dorsal skin was cleaned with ethanol before cell injection. A suspension of 5×10^6 tumor cells in 0.1 mL of PBS was injected s.c. into the dorsa of mice at the proximal midline. Mice were weighed and tumors were monitored twice a week in 2 diameters with a digital calipers. Tumor volumes were determined using $a^2 \times b \times 0.52$ (where a is the shortest and b is the longest diameter). Tumors were allowed to grow to ~100 mm^3 and mice were randomized. Treatment was by bolus s.c. injections. Concentrations of Fc-endostatin were corrected for the Fc contribution. Consequently, all indicated concentrations refer to concentrations of endostatin in Fc-endostatin. After experiments were completed, tumors were excised and fixed in either 4% paraformaldehyde or were snap frozen. Ten mice were treated with each dose of endostatin.

Unless specified otherwise, antitumor studies were done with injection doses delivered every 6 days. The dose amounts were converted into mg/kg/d to compare with our previous published data for endostatin alone (no Fc).

Immunohistology. Melanomas (A2058) were removed and fixed with 4% paraformaldehyde for 2 h and then incubated in 30% sucrose in PBS overnight. Tumors were embedded in ornithine carbamyl transferase medium (Tissue-Tek). Sections were treated with proteinase K (20 μg/mL) for 20 min before staining. hFc-endostatin was detected by FITC-labeled polyclonal antibody against human Fc fragment (Sigma). Blood vessels were visualized with monoclonal antibody against CD-31 (BD PharMingen). The primary antibody was detected by biotin-labeled goat anti-rat antibody (Vector) followed by Alexa 594–labeled streptavidin (Molecular Probes). The sections were imaged by confocal microscopy (model DM IRE2; Leica).

Terminal deoxynucleotidyltransferase–mediated dUTP nick end labeling assay. Apoptosis was examined by use of the terminal deoxynucleotidyltransferase–mediated dUTP nick end labeling (TUNEL) assay (18). To detect apoptotic cells *in vivo*, frozen tumor sections were treated with proteinase K (20 μg/mL) for 20 min, and the slides were stained by manufacturer's protocol (Promega). Hoescht 33258 (Molecular Probes) was used as a counter stain. Quantitative results were expressed as the number of apoptotic cells per total cells at magnification ×200.

Statistical method. Data are expressed as mean ± SD. Statistical significance was assessed by using the Student's t test.

Results

Pharmacokinetics of Fc-endostatin versus endostatin alone is significantly different. We used mouse endostatin, human

endostatin, and their Fc counterparts to investigate their pharmacokinetics. Immunocompetent mice received a single injection s.c. and they were bled at indicated time intervals. The concentration of endostatin in serum was detected by ELISA. F1 The data in Fig. 1A show that in contrast to human endostatin alone (*blue*), which has a half-life of 1 to 2 h, the half-life of hFc-endostatin (*red*) is at least a week and a half and possibly longer; a phenomenon known for Fc containing proteins and antibodies (19, 20). The maximum endostatin concentration is 329 ng/mL and decreases to 187 ng/mL by day 7. Similar data were obtained for mouse endostatin and mFc-endostatin (Fig. 1B). In the case of murine endostatin, the highest endostatin concentration was 585 ng/mL, which decreased to 385 ng/mL by day 12. Mouse endostatin concentrations have been corrected for the baseline value of 20 to 60 ng/mL.

Antitumor activity of hFc-endostatin in a melanoma cancer model requires much less protein and shows a U-shaped curve. Human melanoma cells (A2058) were injected into SCID mice, and the animals were treated with hFc-endostatin at doses delivered once every 6 days. We show here that smaller doses administered at longer intervals resulted in optimum antitumor activity. The tumor volumes as a function of F2 endostatin dosage are presented in Fig. 2A. The optimum antitumor effect is observed at 0.67 mg/kg/d [100 μg of endostatin per mouse every 6 days; treated versus control (T/C) = 0.52; P = 0.0006]. In Fig. 2B, the data are presented as a histogram at the completion of the experiment (8). Anti-VEGF monoclonal Avastin was used for comparison in Fig. 2B. The T/C for Avastin is 0.35 at the dose of 0.67 mg/kg/d. In Fig. 2C, the same data are shown by a U-shaped curve. The antitumor efficacy drops below and above the optimum concentration; consistent with a biphasic curve of efficacy.

For comparison of endostatin levels in the circulation corresponding to different doses of recombinant hFc-endostatin, we carried out an ELISA analysis (Fig. 2D). The optimum concentration (1.192 ng/mL) is a function of endostatin concentration of the dose and the frequency.

Treatment of mice bearing pancreatic tumor cell line ASPC-1 with hFc-endostatin yields similar results to those of melanoma-treated mice. For a second tumor model, we used a human pancreatic cancer cell line ASPC-1. The cells were injected into the dorsa of SCID mice. After tumors reached a mean volume of F3 ~100 mm^3, the mice were treated with hFc-endostatin (Fig. 3). The optimum antitumor activity was achieved with a dose of 0.67 mg/kg/d (100 μg of endostatin per mouse every 6 days; Fig. 3A). In Fig. 3B, the tumor sizes are plotted as a function of endostatin doses (8). The U-shaped curve for these data are presented in Fig. 3C.

We conclude that the U-shaped curve is a property of endostatin in a number of tumor models, based on our data presented here, our previous data, and those generated by another group of investigators in our laboratory (14, 15).

Histidine and arginine mutations in hFc-endostatin affect antitumor activity of endostatin. We previously reported that the antitumor activity of endostatin is mimicked by a 25-amino-acid peptide corresponding to the NH_2 terminus of the molecule (8). Substitution of histidines 1 and 3 by alanines in this peptide eliminated its antitumor activity. This result showed that zinc binding of endostatin is required for its activity. The zinc binding requirement has been controversial and has been reviewed by us (8). Boehm et. al. (21) reported the first evidence for the criticality of zinc binding for the antitumor activity of endostatin. For antitumor activity, the authors used an *Escherichia coli* suspension of endostatin that was poorly soluble. The data showed that zinc binding was necessary for antiangiogenic and antitumor activity but did not include comparison to a soluble form of endostatin.

In the construct reported here, we have substituted alanines for the two crucial histidine residues essential for zinc binding (H1A and H3A). The antitumor activity of this mutant in the ASPC-1 tumor model is shown in Fig. 3 (A and B). Consistent with our previous data, we conclude that zinc binding of endostatin is critical for its antitumor activity. Substitution for the two histidine residues reduces this activity from 50% to 20%.

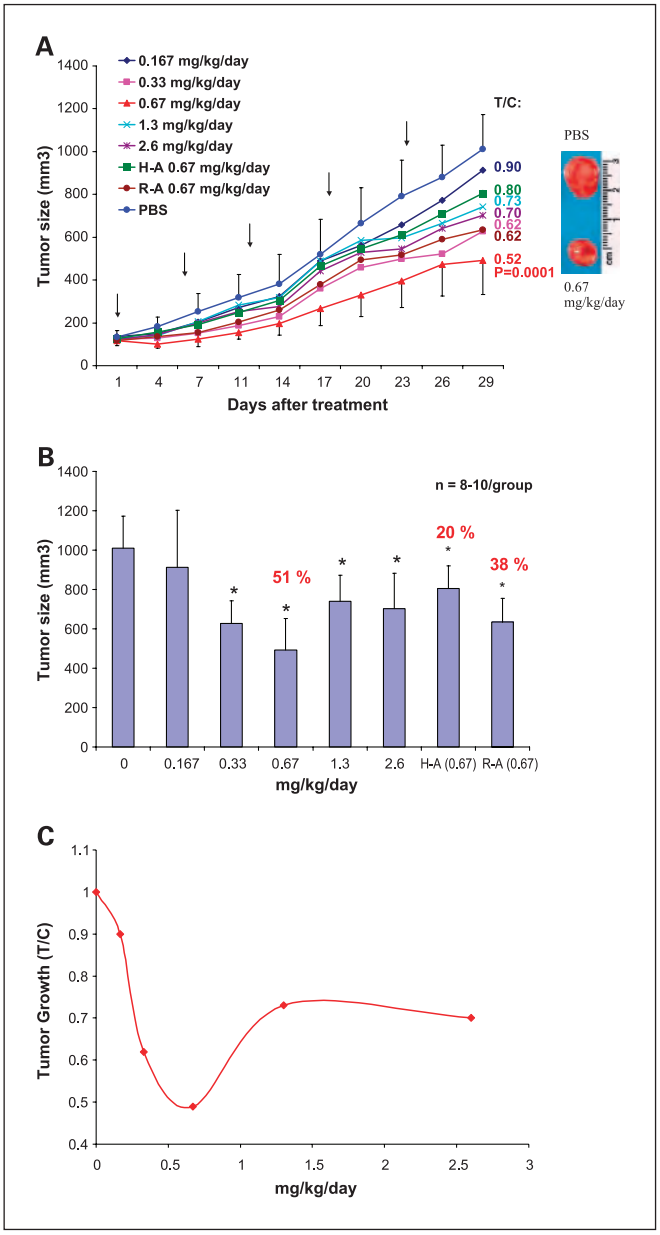

Fig. 3. Treatment of mice bearing human pancreatic tumor cells (ASPC-1) with hFc-endostatin. The protocol was identical to that in Fig. 2 except a different tumor cell line was used. H-A, endostatin mutants H1A and H3A; R-A, endostatin mutants R27A and R139A.

The U-shaped curve of ASPC-1 is not as symmetrical as that of a melanoma (compare Figs. 2C and 3C). The antitumor activity of the mutant endostatin resembles the nonoptimum doses of the wild-type molecule. Based on these data, in addition to the zinc binding contribution to the antitumor activity, other constituents of the endostatin molecule may play a smaller role in such an activity.

The heparin binding domain of endostatin is clustered on the protein surface (which cannot be mimicked by a linear peptide). We prepared a mutant of endostatin lacking heparin binding (R27A and R139A) in the context of hFc-endostatin as described previously (17). Mutation of these two arginines eliminates the heparin binding property of endostatin (22). Antitumor activity of this mutant, using ASPC-1 tumor cells, is shown in Fig. 3A and B. We observed 38% tumor inhibition for mice treated with endostatin (deficient for heparin binding), in contrast to 50% tumor inhibition for mice treated with wild-type endostatin. Both zinc-binding and heparin-binding mutant Fc-endostatin will need to be tested in a number of tumor models to reach a more definite conclusion.

Clinical grade yeast–expressed endostatin shows a doublet on PAGE with ~50% of endostatin having reduced antitumor activity. It has been reported that the endostatin protein used in clinical trials showed a doublet on PAGE (7). Based on their animal studies, the authors concluded that deletion of four amino acids from the NH_2 terminus (HSHR), which included two zinc-binding histidines in endostatin, did not affect its antitumor activity. In this study, it was found that histidine-deleted endostatin bound two atoms of zinc, whereas wild-type endostatin bound 10 atoms of zinc. However, the zinc binding data are inconsistent with the crystal structure of human endostatin and our zinc measurements of native endostatin where one atom of zinc is bound to the endostatin molecule (9). We conclude that the reported high zinc-binding endostatin was probably the result of nonspecific interactions between zinc and endostatin. This artifact occurs when certain conditions are not met during the reconstitution of endostatin with zinc. For example, during reconstitution of zinc with endostatin, the protein should be dialyzed against a large volume of buffer containing low zinc concentration to allow a gradual addition of the metal ion to the protein.

We previously reported that endostatin antitumor activity requires zinc binding (8, 21). In Fig. 4, clinical grade endostatin and hFc-endostatin are subjected to PAGE. The faster migrating protein in endostatin (*lane 2*) lacks four amino acids HSHR (data not shown). Based on PAGE, we speculate that the antiangiogenic and antitumor activity of recombinant endostatin used in clinical trials may have been reduced by at least 30%. This is because ~50% of the final endostatin product lacked zinc. In contrast, hFc-endostatin seems to show a single protein band under the same conditions (*lane 3*).

hFc-endostatin accumulates in tumor vessels. To verify the location of exogenous hFc-endostatin, histologic sections of melanoma were incubated with FITC-labeled anti-human Fc fragment antibody (*green*) and anti-mouse CD 31 antibody (*red*). The FITC-labeled antibody reacted with the histologic sections of tumors from mice treated with endostatin but not with the histologic sections of tumors treated only with PBS (Fig. 5A). We conclude that the injected hFc-endostatin is selectively localized in tumor vessels.

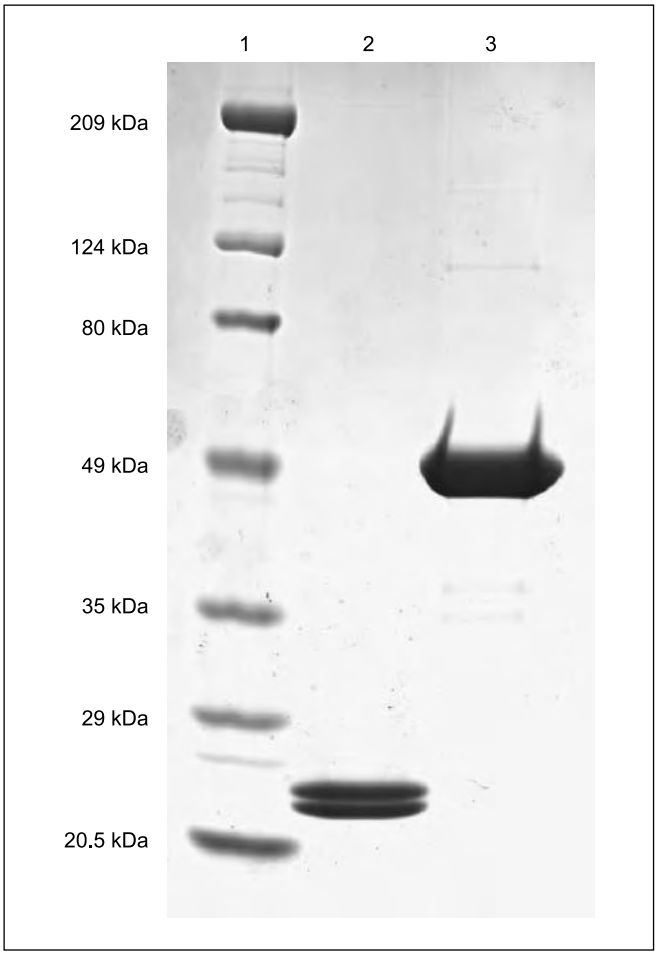

Fig. 4. Electrophoretic analysis of the clinical grade endostatin. Four to 20% gradient PAGE was done (Invitrogen). Lane 1, molecular weight markers. Lane 2, clinical grade endostatin. Lane 3, hFc-endostatin.

TUNEL-positive apoptotic cells are increased after hFc-endostatin treatment. To confirm the role of hFc-endostatin as an apoptosis inducer, we did TUNEL analysis on histologic sections of melanoma (Fig. 5B). TUNEL-positive apoptotic cells were increased in hFc-endostatin–treated sections. The mean percentage of apoptotic tumor cells was 34.7% ± 6.82% in the histologic sections of the hFc-endostatin–treated (0.67 mg/kg/d) mice but was only 8.77% ± 0.87% in PBS-treated tumor sections (Fig. 5C).

Discussion

A major problem observed with clinical grade recombinant human endostatin produced in yeast has been its short half-life. Forty-two patients with advanced neuroendocrine tumors who had failed conventional therapy were treated with daily self-administered subcutaneous injections of recombinant human endostatin (from yeast) in a phase II study at a dose of 90 mg/m^2 day (~2.5 mg/kg/d; ref. 23). There was minimal or no toxicity, and the disease remained stable in 80% of patients. Four patients had stable disease for >3.5 years of uninterrupted therapy. However, there was no partial response to therapy (i.e., 50% tumor regression), as defined by WHO criteria.

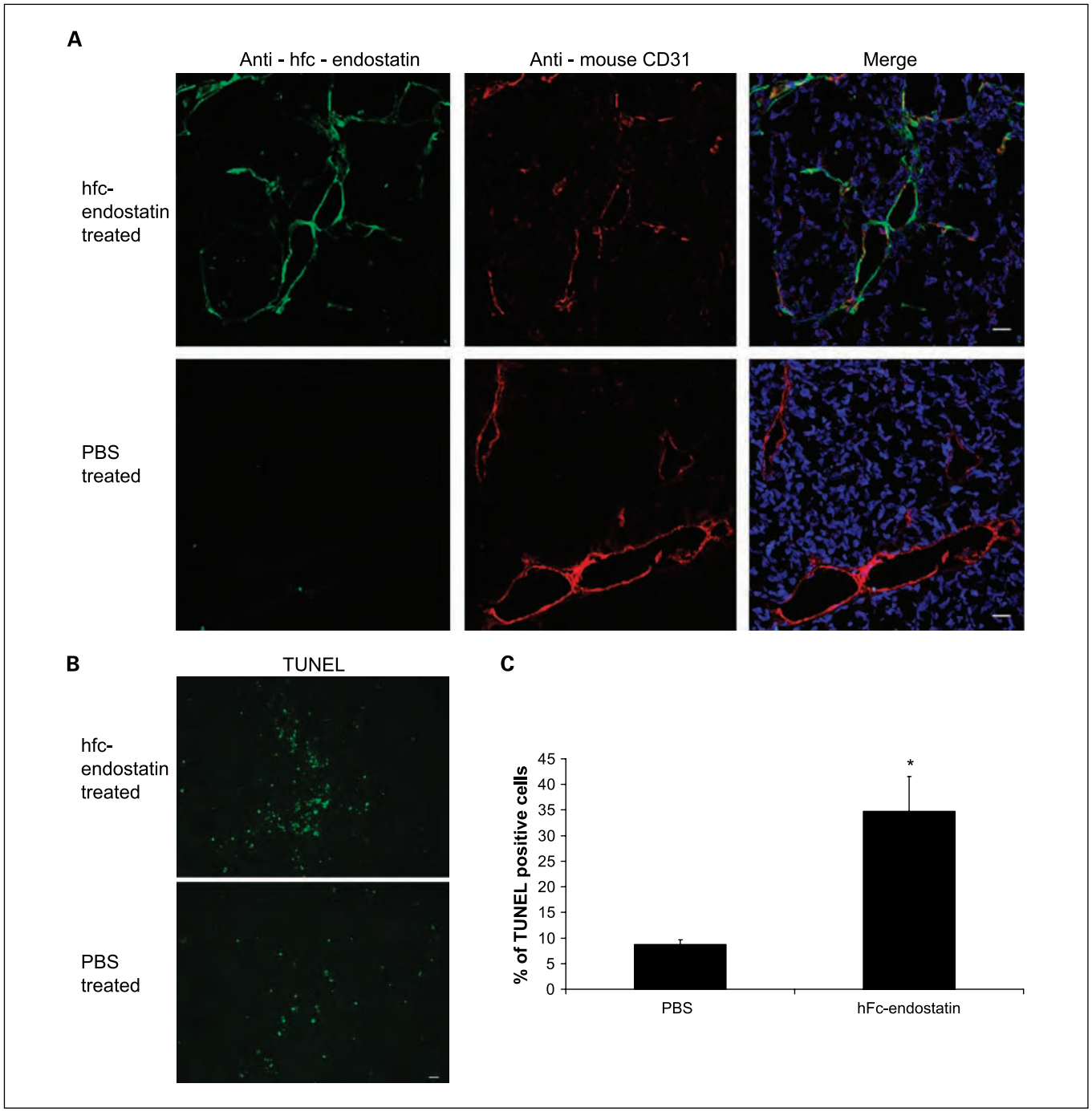

Fig. 5. Immunohistochemistry and TUNEL assay. *A,* immunohistochemistry results for one of the mice treated at 0.67 mg/kg/d and a control mouse. *B* and *C,* TUNEL assay (scale, 20 μm).

The median steady-state trough serum level after dose escalation was 331 ng/mL. The fact that only half of the endostatin bound zinc (deletion of four amino acids at the NH_2 terminus) suggests that the actual median protein concentration of active endostatin was ~200 ng/mL for active endostatin. This estimate is based on the assumption that the ELISA detects both intact and deleted endostatin equally well. The level of endogenous endostatin was reported to be 61 ng/mL. We conclude that the measured median steady-state trough in serum was only 3.3-fold higher than the baseline value.

In contrast, when Avastin (anti-VEGF monoclonal antibody) was administered to cancer patients at a dose of 0.1 to 10 mg/kg, the maximum concentration of circulating antibody was determined to be linear with a range of 2.8 to 284 μg/mL and with a half-life of 3 weeks (11, 24). The dose of antibody administered to patients with colorectal cancer was 5 mg/kg. This translates to 140 μg/mL for maximum circulating antibody. The long half-life of Avastin is mainly due to the presence of the Fc domain. Of interest is that Lucentis, a Fab fragment derived from Avastin, has a half-life of only a few hours (13).

Although the modes of actions of endostatin and Avastin are different, and the requirements for the two drugs are not equivalent, we believe that the poor pharmacokinetics of recombinant endostatin from yeast may be a critical basis for its lack of robust response in patients. Therefore, we have formulated *Fc-endostatin*, in the event that this construct will increase the serum concentration of endostatin in patients by at least 100-fold compared with endostatin lacking the Fc domain. From our experimental results in tumor-bearing mice, we predict that the half-life of Fc-endostatin in humans may be ~2 to 3 weeks, in contrast to hours for endostatin lacking the Fc-fragment. In other words, Fc-endostatin would be expected to have a similar half-life in the circulation as Avastin or VEGF-Trap.

For VEGF-Trap, treatment of patients with 0.8 mg/kg of the protein resulted in a maximum concentration of ~14 μg/mL with a half-life of 25 days (16). Based on the observed linear pharmacodynamics for Avastin in patients (11), at a dose of 0.8 mg/kg of the antibody, the maximum circulating antibody is calculated to be 22 μg/mL with a half-life of ~3 weeks. We conclude that the concentration of endostatin in the serum of cancer patients may have to reach 10 to 100 μg/mL with a 2- to 3-week half-life to achieve optimum antitumor efficacy for endostatin. hFc-endostatin is potentially capable of achieving such a level.

We also report here that the antitumor activity of endostatin is biphasic and reveals a U-shaped curve for efficacy. Other proteins that regulate angiogenesis have also been reported to show similar biphasic curves of antitumor efficacy. These include IFN-α (25), rosiglitazone (26), and thrombospondin (27). In our study of hFc-endostatin in mice, we determined that maximum antitumor activity was achieved by administration of ~0.7 mg/kg/d for the two tumor models. We compared Fc-endostatin from this study with clinical endostatin in the tumor models ASPC-1 and BxPC-3 (15). Maximum antitumor activity was achieved with Fc-endostatin at 0.67 mg/kg/d. In contrast, maximum antitumor activity for endostatin lacking the Fc-fragment was achieved at ~100 mg/kg/d for BxPC-3 and 500 mg/kg/d for ASPC-1. Thus, the optimum antitumor dose for Fc-endostatin is 150- to 700-fold lower than the optimum antitumor dose for endostatin that lacks the Fc-fusion domain. However, when the clinical grade recombinant lacking the Fc-domain (from yeast) was used in tumor-bearing animals, the authors reported 90% inhibition of tumor growth. We observed ~55% inhibition of tumor growth in mice given recombinant Fc-endostatin and 65% inhibition of tumor growth in mice treated with Avastin.

In conclusion, the new data presented here: (*a*) provide a molecular explanation for why the limited clinical trials of endostatin did not achieve the full potential expected for this broad-spectrum, endogenous antiangiogenic protein (2); (*b*) show that the antitumor potency of human endostatin can be increased by 150- to 700-fold by fusing an Fc domain to the NH_2 terminus, thus increasing the half-life of the protein, stabilizing the terminal histidines, and conserving the zinc affinity of endostatin; (*c*) reveal a biphasic U-shaped curve of antitumor activity for Fc-endostatin, as we previously reported for endostatin lacking the Fc-domain; and (*d*) make a compelling case for initiation of clinical trials of recombinant hFc-endostatin.

Acknowledgments

We thank Sarah Short for her critical reading of the manuscript and for making many helpful suggestions and Catherine Butterfield for technical help.

References

1. O'Reilly MS, Boehm T, Shing Y, et al. Endostatin: an endogenous inhibitor of angiogenesis and tumor growth. Cell 1997;88:277–85.

2. Folkman J. Antiangiogenesis in cancer therapy-endostatin and its mechanisms of action. Exp Cell Res 2006;312:594–607.

3. Wickstrom SA, Alitalo K, Keski-Oja J. Endostatin associates with integrin $\alpha_5\beta_1$ and caveolin-1, and activates Src via a tyrosyl phosphatase-dependent pathway in human endothelial cells. Cancer Res 2002;62:5580–9.

4. Teodoro JG, Parker AE, Zhu X, Green MR. p53-mediated inhibition of angiogenesis through up-regulation of a collagen prolyl hydroxylase. Science 2006;313:968–71.

5. Folkman J. Tumor suppression by p53 is mediated in part by the antiangiogenic activity of endostatin and tumstatin. Sci STKE 2006;354:pe35.

6. Thomas JP, Arzoomanian RZ, Alberti D, et al. Phase I pharmacokinetic and pharmacodynamic study of recombinant human endostatin in patients with advanced solid tumors. J Clin Oncol 2003;21:223–31.

7. Sim BK, Fogler WE, Zhou XH, et al. Zinc ligand-disrupted recombinant human endostatin: potent inhibition of tumor growth, safety and pharmacokinetic profile. Angiogenesis 1999;3:41–51.

8. Tjin Tham Sjin RM, Satchi-Fainaro R, Birsner AE, Sadagopa Ramanujam VM, Folkkman J, Javaherian K. A 27-amino-acid synthetic peptide corresponding to the NH_2-terminal zinc-binding domain of endostatin is responsible for its antitumor Activity. Cancer Res 2005;65:3656–63.

9. Ding Y-H, Javaherian K, Lo K-M, et al. Zinc-dependent dimers observed in crystals of human endostatin. Proc Natl Acad Sci U S A 1998;95:10443–8.

10. Bergers G, Javaherian K, Lo K-M, Folkman J, Hanahan D. Effects of angiogenesis inhibitors on multistage carcinogenesis in mice. Science 1999;284:808–12.

11. Gordon MS, Margolin K, Talpaz M, et al. Phase I safety and pharmacokinetic study of recombinant human anti-vascular endothelial growth factor in patients with advanced cancer. J Clin Oncol 2001;19:843–50.

12. Holash J, Davis S, Papadopoulos N, et al. VEGF-Trap: a VEGF blocker with potent antitumor effects. Proc Natl Acad Sci U S A 2002;99:11393–8.

13. Stone EM. A very effective treatment for neovascular macular degeneration. N Engl J Med 2006;355:1493–5.

14. Tjin Tham Sjin RM, Naspinski J, Birsner AE, et al. Endostatin therapy reveals a U-shaped curve for antitumor activity. Cancer Gene Ther 2006;13:619–27.

15. Celik I, Sürücü O, Dietz C, et al. Therapeutic efficacy of endostatin exhibits a biphasic dose-response curve. Cancer Res 2005;65:11044–50.

16. Dupont J, Schwartz L, Koutcher J, et al. Phase I and pharmacokinetic study of VEGF Trap administered subcutaneously (sc) to patients (pts) with advanced solid malignancies [abstract]. J Clin Oncol 2004;22:14s.

17. Javaherian K, Park SY, Pickl WF, et al. Laminin modulates morphogenic properties of the collagen XVIII endostatin domain. J Biol Chem 2002;277:45211–8.

18. Gavrieli Y, Sherman Y, Ben-Sasson SA. Identification of programmed cell death *in situ* via specific labeling of nuclear DNA fragmentation. J Cell Biol 1992;119:493–501.

19. Capon DJ, Chamow SM, Mordenti J, et al. Designing CD4 immunoadhesins for AIDS therapy. Nature 1989;337:525–31.

20. Lo K-M, Sudo Y, Chen J, et al. High level expression and secretion of Fc-X fusion proteins in mammalian cells. Protein Eng 1998;11:495–500.

21. Boehm T, O'Reilly MS, Keough K, Shiloach J, Shapiro R, Folkman J. Zinc-binding of endostatin is essential for its antiangiogenic activity. Biochem Biophys Res Commun 1998;252:190–4.

22. Sasaki T, Larsson H, Kreuger J, et al. Structural basis and potential role of heparin/heparan sulfate binding to the angiogenesis inhibitor endostatin. EMBO J 1999;18:6240–8.

23. Kulke MH, Bergsland EK, Ryan DP, et al. Phase II study of recombinant human endostatin in patients with advanced neuroendocrine tumors. J Clin Oncol 2006;24:3555–61.

24. Motl S. Bevacizumab in combination chemotherapy for colorectal and other cancers. Am J Health Syst Pharm 2005;62:1021–32.

25. Slaton JW, Perrotte P, Inoue K, Dinney C, Fidler IJ. Interferon-mediated down-regulation of angiogenesis-related genes and therapy of bladder cancer are dependent on optimization of biological dose and schedule. Clin Cancer Res 1999;5:2726–34.

26. Panigrahy D, Singer S, Shen LQ, et al. PPARγ ligands inhibit primary tumor growth and metastasis by inhibiting angiogenesis. J Clin Invest 2002;110:923–32.

27. Motegi K, Harada K, Pazouki S, Baillie R, Schor AM. Evidence of a bi-phasic effect of thrombospondin-1 on angiogenesis. Histochem J 2002;34:411–21.

OPINION

Angiogenesis: an organizing principle for drug discovery?

Judah Folkman

Abstract | Angiogenesis — the process of new blood-vessel growth — has an essential role in development, reproduction and repair. However, pathological angiogenesis occurs not only in tumour formation, but also in a range of non-neoplastic diseases that could be classed together as 'angiogenesis-dependent diseases'. By viewing the process of angiogenesis as an 'organizing principle' in biology, intriguing insights into the molecular mechanisms of seemingly unrelated phenomena might be gained. This has important consequences for the clinical use of angiogenesis inhibitors and for drug discovery, not only for optimizing the treatment of cancer, but possibly also for developing therapeutic approaches for various diseases that are otherwise unrelated to each other.

The term angiogenesis is generally applied to the growth of microvessel sprouts the size of capillary blood vessels, a process that is orchestrated by a range of angiogenic factors and inhibitors (FIG. 1). Although proliferating endothelial cells undergoing DNA synthesis are a common hallmark of angiogenic microvascular sprouts, extensive sprouts can grow for periods of time, mainly by the migration of endothelial cells[1]. Physiological angiogenesis is distinct from arteriogenesis and lymphangiogenesis and occurs in reproduction, development and wound repair. It is usually focal, such as in blood coagulation in a wound, and self-limited in time, taking days (ovulation), weeks (wound healing) or months (placentation). By contrast, pathological angiogenesis can persist for years. Pathological angiogenesis is necessary for tumours and their metastases to grow beyond a microscopic size and it can give rise to bleeding, vascular leakage and tissue destruction. These consequences of pathological angiogenesis can be responsible, directly or indirectly, for the symptoms, incapacitation or death associated with a broad range of 'angiogenesis-dependent diseases'[2]. Examples of such diseases include cancer, autoimmune diseases, age-related macular degeneration and atherosclerosis (TABLE 1).

The concept of angiogenesis-dependent diseases originated in 1972 with the recognition that certain non-neoplastic diseases, such as the chronic inflammatory disease psoriasis, depend on chronic neovascularization to provide a conduit for the continual delivery of inflammatory cells to the inflammatory site[3–5]. Subsequently, other non-neoplastic diseases were recognized to be in part angiogenesis dependent, for example, infantile haemangiomas[6], peptic ulcers[7], ocular neovascularization[8], rheumatoid arthritis[9] and atherosclerosis[3,10,11]. This led to a more general understanding that the process of angiogenesis itself could be considered as an 'organizing principle'. Organizing principles are common in the physical sciences, and are now starting to be recognized in biology — other examples might be inflammation or apoptosis, which are also aspects of many otherwise unrelated diseases. The heuristic value of such a principle is that it permits connections between seemingly unrelated phenomena. For example, the discovery of a molecular mechanism for one phenomenon might be more rapidly demonstrated for a second phenomenon if one understands *a priori* that the two are connected. Furthermore, when the mechanisms underlying different diseases can be related in this way, the development of therapeutics for one disease could aid the development of therapeutics for others. Although it remains to be determined to what extent treating pathological angiogenesis in different angiogenesis-dependent diseases will be successful, the recent approval of ranibizumab (Lucentis; Genentech) — an antibody fragment based on the anti-angiogenic cancer drug bevacizumab (Avastin; Genentech) — for age-related macular degeneration suggests that such strategies merit investigation.

Here, I provide an overview of the current state of drug development of angiogenesis inhibitors, as well as certain drugs that have varying degrees of anti-angiogenic activity in addition to their other functions, and highlight examples of anti-angiogenic strategies in unrelated diseases. Furthermore, I discuss burgeoning new directions in angiogenic research, the optimization of anti-angiogenic strategies and how viewing angiogenesis as an organizing principle might uncover fruitful connections for future drug discovery.

A brief history of angiogenesis inhibitors

The attempt to discover angiogenesis inhibitors became possible after my group and others had developed bioassays for angiogenesis during the 1970s. These included the long-term culture of vascular endothelial cells[12], the development of the chick-embryo chorioallantoic-membrane bioassay[13], the development of sustained-release polymers[14] and the implantation of these polymers as pellets in the rabbit[15] and murine[16] cornea to quantify the angiogenic activity of tumour-derived proteins.

The first angiogenesis inhibitors were reported in the 1980s from the Folkman laboratory, during a study that continued over 25 years[17,18] (TIMELINE). No angiogenesis inhibitors existed before 1980, and few scientists thought at that time that such molecules would ever be found. However, the effort to isolate and purify them was driven by preliminary data that led to the 1971 hypothesis that tumour growth is dependent on angiogenesis[19]. This effort was also informed by preliminary data that the removal of an angiogenic sustained-release pellet from the rabbit cornea led to a rapid regression (weeks) of neovascularization that was induced by the pellet[20].

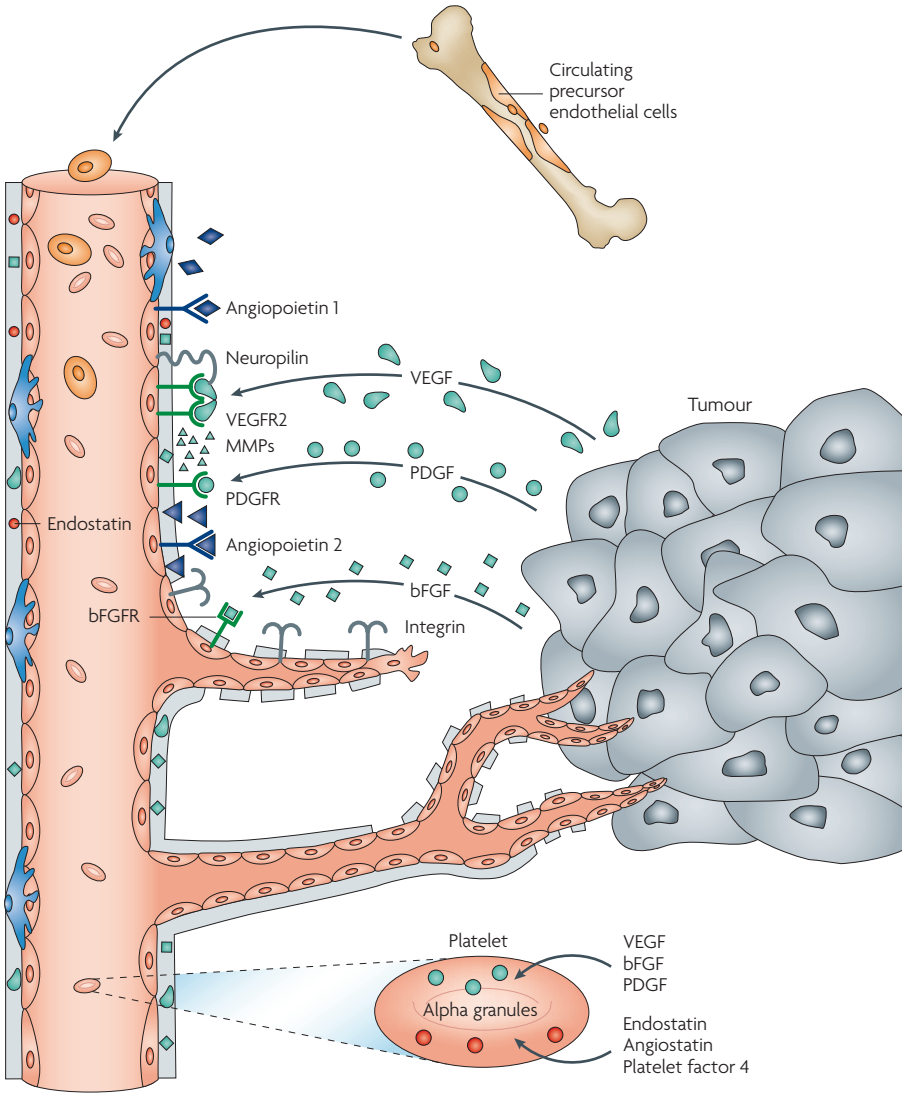

Figure 1 | **Key steps in tumour angiogenesis.** Angiopoietin 1 (ANGPT1), expressed by many cells, binds to the endothelial TIE2 (also known as TEK) receptor and helps maintain a normalized state in blood vessels. Vascular endothelial growth factor (VEGF) is secreted by tumour cells and binds to its receptor (VEGFR2) and to neuropilin on endothelial cells. It is the most common of at least six other pro-angiogenic proteins from tumours. Matrix metalloproteinases (MMPs) are released from tumour cells, but also by VEGF-stimulated endothelial cells. MMPs mobilize pro-angiogenic proteins from stroma, but can also cleave endostatin from collagen 18 in the vessel wall and participate in the cleavage of angiostatin from circulating plasminogen. Tumour cells secrete angiopoietin 2 (ANGPT2), which competes with ANGPT1 for binding to the endothelial TIE2 receptor. ANGPT2 increases the degradation of vascular basement membrane and migration of endothelial cells, therefore facilitating sprout formation. Platelet-derived growth factor (PDGF), an angiogenic protein secreted by some tumours, can upregulate its own receptor (PDGFR) on endothelial cells. Basic fibroblast growth factor (bFGF; also known as FGF2) is secreted by other tumours. Integrins on endothelial cells carry signals in both directions. Integrins facilitate endothelial cell binding to extracellular membranes, a requirement for the cells to maintain viability and responsiveness to growth regulatory proteins. Endothelial cells are among the most anchorage-dependent cells. Certain pro-angiogenic proteins upregulate endothelial integrins and are thought to sustain endothelial cell viability during the intermittant detachments that are required to migrate towards a tumour and to simultaneously increase their sensitivity to growth regulators — both mitogenic (VEGF or bFGF) and anti-mitogenic (endostatin). New endothelial cells do not all originate from neighbouring vessels. A few arrive as precursor bone-marrow-derived endothelial cells. Endothelial growth factors are not all delivered to the local endothelium directly from tumour cells. Some angiogenic regulatory proteins (both pro- and anti-angiogenic) are scavenged by platelets, stored in alpha granules and seem to be released within the tumour vasculature. It was recently discovered that pro- and anti-angiogenic proteins are stored in different sets of alpha granules (depicted in green and red respectively)[63].

After the mid-1980s, we and others began to discover additional angiogenesis inhibitors[21–29] (TIMELINE). By the mid-1990s, new drugs with anti-angiogenic activity entered clinical trials. These drugs began to receive Food and Drug Administration (FDA) approval in the United States by 2003. Bevacizumab, which received FDA approval for colorectal cancer in 2004, was the first drug developed solely as an angiogenesis inhibitor[30]. However, certain non-endothelial cells (haematopoietic-derived cells that colonize tumour stroma and some cancer cells, such as those in pancreatic cancer) can also express receptors for vascular endothelial growth factor (VEGF; also known as VEGFA), raising the possibility that this drug might also have direct antitumour effects[31,32]. At the time of writing this article, 10 new drugs — in which anti-angiogenic activity is considered to be central to their therapeutic effects — have been approved by the FDA in the United States, and by equivalent agencies in 30 other countries, for the treatment of cancer and age-related macular degeneration (TABLE 2). At least 43 other drugs that have varying degrees of anti-angiogenic activity are currently in clinical trials in the United States for different types of cancer, ten of which are in Phase III (TABLE 3). Other FDA-approved drugs revealed anti-angiogenic activity in addition to anticancer activity directed against tumour cells. For example, bortezomib (Velcade; Millennium Pharmaceuticals), approved as a proteasome inhibitor for the treatment of multiple myeloma, was subsequently demonstrated to also have potent anti-angiogenic activity[33].

As the treatment range of angiogenesis inhibitors covers not only many types of cancer, but also unrelated diseases such as age-related macular degeneration and possibly others, angiogenesis inhibitors, or drugs that have varying degrees of anti-angiogenic activity, might be defined as a class of drugs that specifically target an organizing principle in biomedicine.

Angiogenesis as an organizing principle

Clinical advantages to understanding angiogenesis as an organizing principle.
There are important clinical advantages to viewing angiogenesis as an organizing principle. For example, if a clinician recognizes that a patient's disease might be partly angiogenesis-dependent, it is conceivable that an angiogenesis inhibitor approved for one type of tumour could be used for a different type of tumour, or even used off-label for a different disease.

Table 1 | **Angiogenesis-dependent diseases**

Disease	Symptoms
Diabetic retinopathy	Loss of vision
Rheumatoid arthritis[2]	Pain and immobility from destroyed cartilage
Atherosclerotic plaques[3]	Chest pain, dyspnoea
Endometriosis[4,5]	Abdominal pain from intraperitoneal bleeding
Crohn's disease[6]	Intestinal bleeding
Psoriasis[7]	Persistent severe itching
Uterine fibroids	Vaginal bleeding, abdominal pain
Benign prostatic hypertrophy	Urinary retention
Cancer	Bleeding, thrombosis, anaemia, abdominal ascites, bone pain, seizures from cerebral oedema around a tumour and others

An example of the former is the use of bevacizumab in colorectal cancer and also in non-small-cell lung cancer, and an example of off-label use is its use for age-related macular degeneration. Oncologists might also benefit from knowing that certain anticancer drugs (for example, cyclophosphamide) that were originally developed to target cancer cells also have anti-angiogenic activity.

A connection between colorectal cancer and macular degeneration. Bevacizumab is an antibody that neutralizes VEGF and was approved by the FDA for colorectal cancer in 2004 (REFS 30,34). Ranibizumab is a fragment of bevacizumab. In randomized clinical trials, ranibizumab injected into the eye at monthly intervals showed dramatic success in patients with age-related macular degeneration. In patients who were legally blind, with an average visual acuity of ~20/300, approximately 40% recovered their sight and improved to a visual acuity of 20/40 (sufficient for some to drive a car). In ~90–95% of patients, the disease was arrested, and there was no further loss of sight. By contrast, patients who were treated with a placebo continually lost visual acuity over a 12-month period, as was expected[35–40] (FIG. 3a). Pegaptanib (Macugen; OSI Pharmaceuticals), an anti-VEGF aptamer, was the first anti-VEGF drug to be approved by the FDA (2004) for the treatment of age-related macular degeneration. More than 75,000 patients with age-related macular degeneration have been treated with pegaptanib since its approval, and in the past year more than 50,000 patients have been treated with either intravitreal ranibizumab or off-label bevacizumab.

This might be the first time that a relatively non-toxic anticancer drug has been injected into the eye to treat ocular neovascularization. It is rare to treat diseases as diverse as colorectal cancer and age-related macular degeneration with the same agent — with the exception that the target for each was known to be VEGF[41–44].

Discovery of dual roles for cancer drugs. The cancer drugs erlotinib (Tarceva; Genentech, OSI Pharmaceuticals, Roche), cetuximab (Erbitux; Bristol–Myers Squibb, Merck) and vandetanib were originally developed as inhibitors of the epidermal growth factor receptor (EGFR) tyrosine kinase. For this reason, they are also known as anti-oncoprotein signal-transduction inhibitors[45]. However, they were subsequently found to also inhibit tumour angiogenesis by blocking the VEGF receptor. Cetuximab, an anti-EGFR agent, produces an antitumour effect *in vivo* that is due to the direct blockade of the EGFR-dependent mitogenic pathway and in part to the inhibition of secretion of various pro-angiogenic proteins such as VEGF, basic fibroblast growth factor (bFGF; also known as FGF2) and transforming growth factor-α (TGFα)[46].

Timeline | **Discovery of angiogenesis inhibitors**

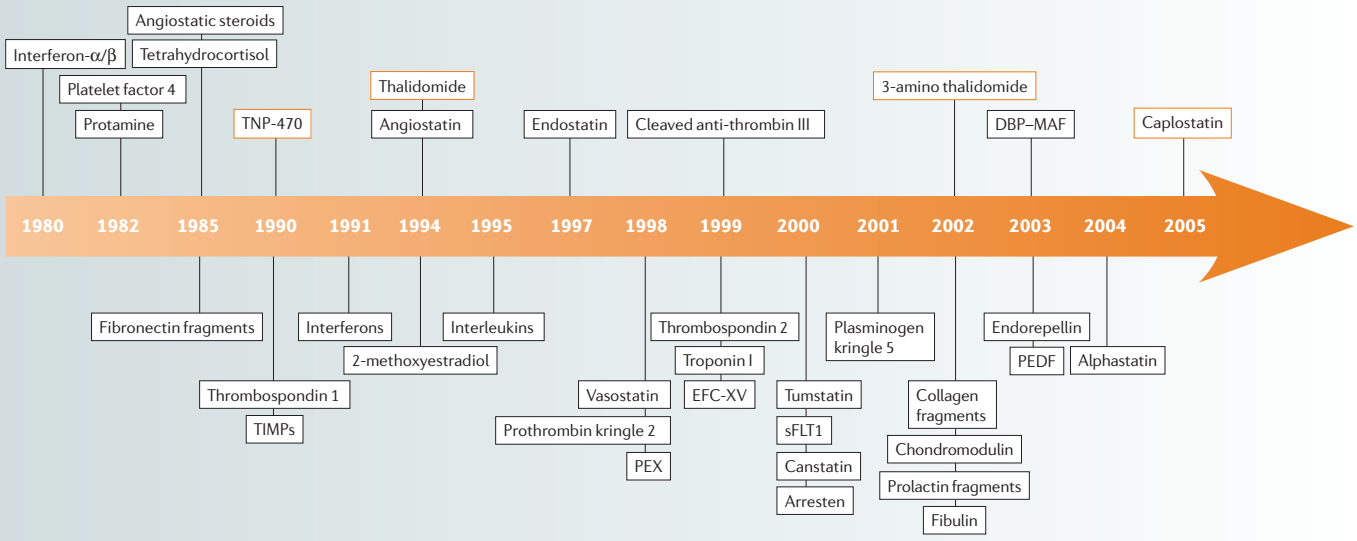

Synthetic angiogenesis inhibitors (orange keyline) and endogenous angiogenesis inhibitors that were identified in the Folkman laboratory are depicted above the timeline. Examples of additional endogenous angiogenesis inhibitors discovered in other laboratories are depicted below the timeline. The first drugs with anti-angiogenic activity were approved in 2003 (TABLE 2). DBP–MAF, vitamin-D-binding protein–macrophage-activating factor; EFC-XV, endostatin-like fragment from type XV collagen; PEDF, pigment epithelium-derived factor (also known as SERPINF1); PEX, haemopexin C domain autolytic fragment of matrix metalloproteinase 2; sFLT1, soluble fms-related tyrosine kinase 1; TIMP, tissue inhibitors of matrix metalloproteinase.

With this knowledge of their dual role[45], these drugs might be used more effectively by oncologists who could follow guidelines for dose-efficacy of angiogenesis inhibitors, which differ from conventional cytotoxic chemotherapies (see below).

Emerging research directions

The usefulness of recognizing an underlying organizing principle during angiogenesis research is illustrated by several fascinating insights into diverse biological processes. Some examples of these are new insights into platelet biology[47], metastases[22], endothelial control of tissue mass[48,49,72], the concept of oncogene dependence[50] and the surprising discovery that some of the ligand–receptor pairs that mediate axon-pathway finding also mediate

Table 2 | **Anti-angiogenic drugs approved for clinical use and phase of clinical trials for other indications**

Drug (Trade name; company)	Approved*	Phase III	Phase II	Phase I
Bortezomib (Velcade; Millennium Pharmaceuticals)	Multiple myeloma (2003)	NSCLC, multiple myeloma, NHL	Multiple myeloma, NHL, NSCLC, lymphoma, gliomas, melanoma, Waldenstrom's macroglobinaemia, prostate, head and neck, breast, liver, nasopharyngeal, gastric, pancreatic, colorectal, cervical/vaginal cancer, and others	Lymphoma, myelodysplasia, multiple myeloma, NHL, solid tumours, head and neck, cervical, colorectal, ovarian, prostate cancer, and others
Thalidomide (Thalomid; Celgene Corporation)	Multiple myeloma (2003‡)	Multiple myeloma, brain metastases, SCLC, NSCLC, prostate, kidney, ovarian, hepatocellular cancer	Soft tissue sarcoma, multiple myeloma, ALS, melanoma, neuroendocrine tumours, leukaemia, glioma, glioblastomas, paediatric neuroblastoma, NSCLC, NHL, paediatric solid tumours, myelofibrosis, myelodysplastic syndrome, AML, CLL, SCLC, Hodgkin's disease, paediatric brain stem, liver, colorectal, kidney, neuroendocrine, endometrial, thyroid, uterine, ovarian cancer, and others	Solid tumours, glioma
Bevacizumab (Avastin; Genentech)	Colorectal cancer (2004), lung cancer (2006)	NSCLC, GIST, diabetic retinopathy, vascular occlusions, retinopathy of prematurity, colorectal, breast, ovarian, peritoneal, pancreatic, prostate, kidney cancer	Glioblastoma, glioma, mesothelioma, NSCLC, AML, CLL, CML, lymphoma, angiosarcoma, melanoma, billary tumours, SCLC, Kaposi's sarcoma, sarcomas, NHL, carcinoid, oesophagogastric, gastric, renal cell, head and neck, rectal, hepatocellular, bladder, pancreatic, gall bladder, breast, neuroendocrine, cervical, ovarian, endometrial cancer, and others	NSCLC, pancreatic, solid tumours, head and neck tumours, VHL, retinal tumours
Erlotinib (Tarceva; Genentech, OSI Pharmaceuticals, Roche)	Lung cancer (2004)	NSCLC, colorectal, pancreatic, ovarian, head and neck, oral cancer	NSCLC, mesothelioma, glioblastoma, glioma, gall bladder, GIST, biliary tumours, bladder cancer prevention, malignant peripheral nerve sheath tumours, endometrial, colorectal, pancreatic, breast, renal cell, prostate, ovarian, head and neck, gastric/oesophageal, liver cancer, and others	NSCLC, glioblastoma, solid tumours, colorectal, pancreatic, head and neck cancer
Pegaptanib (Macugen; OSI Pharmaceuticals)	Age-related macular degeneration (2004)			
Endostatin (Endostar)	Lung cancer (2005§)			
Sorafenib (Nexavar; Onyx Pharmaceuticals)	Kidney cancer (2005)	Kidney, melanoma, hepatocellular cancer	Melanoma, glioblastoma, GIST, SCLC, thyroid, neuroendocrine, mesothelioma, soft tissue sarcoma, NSCLC, CLL, multiple myeloma, cholangiocarcinoma, NHL, kidney, colorectal, prostate, ovarian, peritoneal, pancreatic, breast, gastric, head and neck, uterine, gall bladder, bladder cancer, and others	Solid tumours, melanoma, glioblastoma, NHL, glioma, multiple myeloma, Kaposi's sarcoma, ALL, CML, MDS
Lenalidomide (Revlimid; Celgene Corporation)	Myelodysplastic syndrome (2005)	Multiple myeloma, myelodysplastic syndrome	NSCLC, NHL, multiple myeloma, CLL, myelofibrosis, myelodysplastic syndrome, glioblastoma, ocular melanoma, AML, mantle-cell lymphoma, Waldenstrom's macroglobinaemia, ovarian/peritoneal, thyroid, prostate cancer	Multiple myeloma, prostate cancer, melanoma, myelodysplastic syndrome, solid tumours, paediatric CNS tumours
Sunitinib (Sutent; Pfizer)	GIST, kidney cancer (2006)	Renal cell cancer, GIST	Melanoma, VHL/solid tumour, NSCLC, GIST, hepatocellular, colorectal, prostate, breast, renal cell, gastric, neuroendocrine cancer, and others	Melanoma, solid tumours, colorectal, breast cancer
Ranibizumab (Lucentis; Genentech)	Age-related macular degeneration (2006)			

*Year of first approval by the US Food and Drug Administration, unless stated otherwise. ‡Australia, approved by US Food and Drug Administration in 2006. §China State Food and Drug Administration. ALS, amyotrophic lateral sclerosis (or Lou Gehrig's disease); ALL, acute lymphoblastic leukaemia; AML, acute myeloid leukaemia; CLL, chronic lymphocytic leukaemia; CML, chronic myeloid leukaemia; CNS, central nervous system; GIST, gastrointestinal stromal tumour; MDS, myelodysplastic syndromes; NSCLC, non-small-cell lung cancer; NHL, non-Hodgkin's lymphoma; SCLC, small-cell lung cancer; VHL, von Hippel Lindau.

angiogenesis[51]. Furthermore, genetic variations in the expression of angiogenic proteins between different groups of individuals[52] provide further clues about the role of these angiogenesis-regulatory proteins in different diseases.

Endothelium and neurons share regulatory proteins. In 1998, Klagsbrun and colleagues reported that neuropilin, a cell-surface protein originally identified as a receptor for a signal that guides growing nerves, is also a receptor for VEGF[53,54]. This marked the beginning of a merger between the fields of neural guidance and angiogenesis. It was discovered that various ligand–receptor pairs that mediate axon-pathway finding also mediate angiogenesis[51].

Also, during development, sensory nerves determine the pattern of arterial differentiation in blood-vessel branching in the skin[55]. It was found that in the highly vascular dorsal root ganglia, neuronal VEGF interacts with endothelial cell VEGF receptor 2 (VEGFR2; also known as KDR)[56], which is necessary for endothelial survival. As the interactions of growth and motility proteins for neurons and endothelial cells are gradually uncovered, they might have important roles in drug discovery, for example, for drugs that can repair spinal-cord injuries, reverse Alzheimer's disease or broaden the efficacy of currently approved angiogenesis inhibitors.

New platelet biology. In a review in 2001, my colleagues and I assembled the reports that showed that most of the endogenous angiogenesis-regulatory proteins known at that time were contained in platelets or were on the platelet surface[57]. Several studies subsequently reported that circulating platelets in mice take up and sequester angiogenesis regulatory proteins, such as VEGF, bFGF and connective-tissue-activating peptide, when a microscopic human tumour is present in a mouse[58–60].

The angiogenisis-regulatory proteins are sequestered in alpha granules of platelets at a significantly higher concentration than in plasma. In fact, when radiolabelled VEGF is implanted subcutaneously in a Matrigel pellet in mice, platelet lysates take up virtually all of the radiolabelled VEGF and none is found in plasma[58]. Mouse platelets live for ~3–4 days. Nevertheless, platelets seem to recycle the angiogenesis-regulatory proteins they have scavenged, because the concentration of these proteins increases in the platelets over time (weeks to months), as long as the source of an angiogenesis-regulatory protein is present. Also, a single intravenous injection of thrombospondin 1 (THBS1) (2 μg) into *THBS1*-null mice continues to appear in platelet lysates for weeks (S. Ryeom, personal communication). Furthermore, it was recently reported that in patients with cancer who were receiving bevacizumab, the antibody was taken up by platelets where it was bound to VEGF[61].

This new platelet property, quantifiable by mass spectroscopy of platelet lysates, might permit the development of a biomarker for early detection of tumour recurrence. In tumour-bearing mice, the platelet-angiogenesis proteome detects microscopic tumours at a millimetre size, before they have become angiogenic, but when they are generating angiogenic proteins (VEGF, bFGF and platelet-derived growth factor; PDGF) and anti-angiogenic proteins (endostatin or THBS1)[58,62].

Italiano *et al.* have recently discovered that angiogenesis-regulatory proteins are in fact segregated among two sets of alpha granules in platelets: positive regulators of angiogenesis in one set of alpha granules and negative regulators in the other set[63]. This previously unknown function of platelets links them with the process of angiogenesis. A new opportunity lies ahead to determine whether and how platelets release pro-angiogenic proteins at a wound site and then later release anti-angiogenic proteins. Furthermore, the putative role of platelet release of angiogenesis-regulatory molecules in tumours remains to be elucidated. It might also be possible to develop drugs that selectively release anti-angiogenic proteins from platelets trapped in haemangiomas or in cancer. It is likely that in the future novel angiogenesis-regulatory molecules that could be developed into drugs will be discovered in platelets.

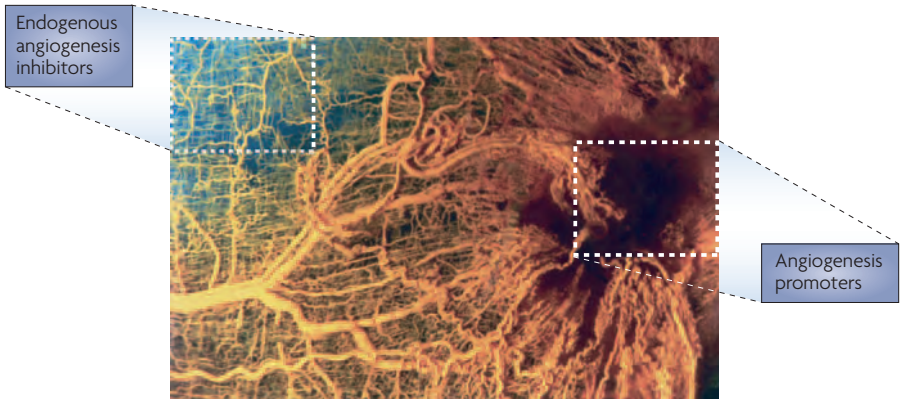

Figure 2 | **Angiogenesis in rat sarcoma.** In this micrograph, blood vessels grow towards a sarcoma (dark area at right) in rat muscle. This contrasts with the normal grid-like pattern of blood vessels that appears at the upper left. (Courtesy of L. Heuser and R. Ackland, University of Louisville, USA)[141].

A new mechanism for site specificity of metastasis. It is known that THBS1 is a potent angiogenesis inhibitor[64] that is expressed by fibroblasts and other stromal cells in many tissues. It is also clear that reduction of THBS1 expression in a tumour bed is a necessary prerequisite for induction of neovascularization and for a microscopic tumour to become neovascularized and to grow[65,66]. Watnick and colleagues recently found that certain human tumours produce a novel protein that specifically represses THBS1 in the stromal tissue to which the tumour is subsequently able to metastasize[67]. Suppression of anti-angiogenic activity at the future metastatic site facilitates the initiation of angiogenesis by metastatic tumour cells. If this discovery can be generalized to other tumours, it could be the basis for the development of drugs such as antibodies that could neutralize the THBS1 suppressor protein produced by the primary tumour.

When a new angiogenesis-based metastatic mechanism is uncovered, it is prudent to ask whether the new cancer mechanism could have a physiological counterpart. As in normal tissues, THBS1 is highly expressed under normal conditions in the endometrium[68]. It is not known whether THBS1 is suppressed before the implantation of a fertilized ovum or of a blastocyst, and if so, by what mechanism. This is a topic of current investigation, and there are potential clinical implications. More than 10% of all pregnancies miscarry early in the first trimester. Some women have repeated early miscarriages and are unable to carry a baby to term. *In vitro* fertilization often requires multiple cycles of ovum implantation. Could these problems be the result of insufficient suppression of endometrial THBS1, or of some other endogenous angiogenesis

Table 3a | **Clinical trials of drugs that have shown anti-angiogenic activity in preclinical models**

Inhibitor (Company)	Target/mechanism	Clinical development
2-methoxyestradiol-EntreMed (EntreMed)	Inhibits HIF1α and tubulin polymerization	• Phase I: Breast cancer and solid tumours • Phase II: Glioblastoma, multiple myeloma, neuroendocrine, renal cell, prostate, ovarian cancer
A6 (Angstrom Pharmaceuticals)	Binds to uPA cell-surface receptor	• Phase II: History of ovarian cancer with rising CA125
Abergrin (MedImmune)	Anti αvβ3 antibody	• Phase I: Melanoma, solid tumours, colorectal cancer • Phase II: Melanoma, prostate cancer, psoriasis, arthritis
ABT-510 (Abbott Laboratories)	Thrombospondin 1 receptor CD36	• Phase I: Head and neck cancer, solid tumours • Phase II: Lymphoma, renal cell, head and neck, NSCLC, soft tissue sarcoma
Actimid (Celgene Corporation)	Downregulates TNF	• Phase II: Prostate cancer (completed)
AG-013736 (Pfizer)	VEGFR, PDGFR	• Phase I: Breast cancer • Phase II: NSCLC, melanoma, thyroid, breast, pancreatic, renal cell cancer
AMG706 (Amgen)	VEGFR, PDGFR, KITR, RETR	• Phase I: Lymphoma, solid tumours, NSCLC, breast, colorectal cancer • Phase II: Solid tumours, NSCLC, gastrointestinal stromal tumours (GIST), breast, thyroid cancer
AP23573 (Ariad Pharmaceuticals)	mTOR, VEGF	• Phase I: Glioma, sarcoma, solid tumours, multiple myeloma • Phase II: Endometrial cancer, prostate cancer, haem malignancies
AS1404 (Antisoma)	Vascular disrupting agent, releases TNF and vWF	• Phase II: Prostate cancer
ATN-161 (Attenuon)	α5β1 antagonist	• Phase II: Renal cell cancer, malignant glioma
AZD2171 (AstraZeneca)	VEGFR1, VEGFR2, VEGFR3, PDGFR	• Phase I: NSCLC, AML, colorectal, head and neck cancer, CNS tumours (child) • Phase II: Solid tumours, NSCLC, glioblastoma, melanoma, mesothelioma, neurofibromatosis, ovarian, CLL, colorectal, breast, kidney, liver, SCLC • Phase III: NSCLC
BMS-275291 (Bristol–Myers Squibb)	MMP inhibitor	• Phase I: Kaposi's sarcoma • Phase II: Kaposi's sarcoma, prostate cancer, NSCLC • Phase III: NSCLC
CCI-779 (Wyeth)	mTOR, VEGFR	• Phase I: Solid tumours, prostate cancer, CML, and others • Phase II: CLL, melanoma, glioblastoma, multiple myeloma, GIST, SCLC, NHL, NSCLC, neuroendocrine tumours, breast, pancreatic, endometrial cancer, and others
CDP-791 (Imclone Systems)	VEGFR2, KDR	• Phase II: NSCLC
Celecoxib (Pfizer)	Increases endostatin	• Phase I: NSCLC, pancreatic, prostate cancer, solid tumours • Phase II: Head and neck cancer prevention, breast cancer prevention, lung cancer prevention, NSCLC, paediatric solid tumours, Ewing's sarcoma, glioma, skin cancer prevention, basal cell nevus syndrome, Barrett's oesophagus, hepatocellular, oesophogael, prostate, cervical, colorectal, head and neck, breast, thyroid, nasopharyngeal cancer, and others • Phase III: Colon, prostate, bladder cancer, NSCLC, and others
Cilengitide (EMD Pharmaceuticals)	αvβ3 and 5 antagonist	• Phase I: Solid tumours, lymphomas, paediatric brain tumours • Phase II: Glioblastoma, gliomas
Combretastatin (Oxigene)	VE-cadherin	• Phase I: Solid tumours • Phase II: Solid tumours, anaplastic thyroid cancer
E7820 (Eisia Medical Research Inc.)	Inhibits integrin α2 subunit on endothelium	• Phase I: Lymphoma • Phase II: Colorectal cancer
Everolimus (Novartis)	VEGFR, mTOR	• Phase I: Breast cancer, solid tumours, lymphoma • Phase II: NSCLC, melanoma, AML, ALL, CML, lymphoma, glioblastoma, prostate, colorectal, neuroendocrine, breast, endometrial, kidney cancer, paediatric tumours, solid tumours • Phase III: Islet cell pancreas II/III, and others
Genistein (National Cancer Institute (NCI), USA)	Suppresses VEGF and neuropilin and MMP9 in tumour cells, upregulates CTAP	• Phase I: Melanoma, kidney, prostate, bladder, breast cancer
Homoharringtonine (ChenGenex Therapeutics)	Downregulates VEGF in leukaemic cells	• Phase II: CML, APML • Phase III: CML
IMC-1121b (Imclone Systems)	VEGFR2, KDR	• Phase I: Solid tumours
INGN 241 (Introgen Therapeutics)	MDA7, VEGF	• Phase II: Melanoma

Table 3b | **Clinical trials of drugs that have shown anti-angiogenic activity in preclinical models**

Inhibitor (Company)	Target/mechanism	Clinical development
Interleukin-12 (NCI)	Upregulates IP10	• Phase I: Solid tumours, melanoma, paediatric neuroblastoma, kidney, breast cancer • Phase II: Melanoma, NHL, multiple myeloma, breast, ovarian, peritoneal, prostate cancer
Enzastaurin (Eli Lilly and Company)	VEGF	• Phase I: Solid tumours, gliomas • Phase II: Gliomas, lymphoma, brain tumours, NSCLC, pancreatic, colorectal cancer • Phase III: Lymphoma prevention, glioblastoma
Neovastat (Aeterna Zentaris)	MMP inhibitor	• Phase II: Multiple myeloma • Phase III: Kidney, NSCLC
NM-3 (Genzyme Corporation)	Inhibits VEGF expression by tumour cells, inhibits endothelial proliferation	• Phase I: Solid tumours
NPI-2358 (Nereus Pharmaceuticals)	β-tubulin	• Phase I: Solid tumours
Phosphomannopentaose sulphate (Progen Industries, Medigen Biotechnology)	bFGF, stimulates release of TFP1	• Phase II: Melanoma, NSCLC, prostate, hepatocellular cancer
PKC412 (Novartis)	VEGFR2	• Phase I: AML • Phase II: Mast-cell leukaemia
PPI-2458 (Praecis)	METAP2	• Phase I: Solid tumours, NHL
Prinomastat (Agouron Pharmaceuticals)	MMP inhibitor	• Phase II: Glioblastoma
PXD101 (CuraGen Corporation)	HDAC inhibitor	• Phase I: Solid tumours, haem malignancies • Phase II: Multiple myeloma, myelodysplastic syndrome, lymphoma, AML, NHL, ovarian/peritoneal, liver cancer
Suramin (NCI)	IGF1, EGFR, PDGFR, TGFβ, inhibits VEGF and bFGF	• Phase I: Bladder, breast, kidney cancer • Phase II: Glioblastoma, breast, kidney, adrenocortical cancer • Phase III: Prostate cancer
Tempostatin (Collard Biopharmaceuticals)	Extracellular matrix proteins	• Phase I: Solid tumours • Phase II: Kaposi's sarcoma
Tetrathiomolybdate (Sigma–Aldrich)	Copper chelator	• Phase II: Prostate, oesophageal, breast, colorectal cancer • Phase III: Psoriasis
TKI-258 (Novartis, Chiron Corporation)	FGFR3, VEGFR	• Phase I: Multiple myeloma, AML, melanoma
Vatalanib (Novartis)	VEGFR1,2, PDGFR	• Phase I: Solid tumours, NSCLC, gynaelogic tumours • Phase II: GIST, AML, CML, solid tumours, NSCLC, VHL, haemangioblastoma, mesothelioma, breast, prostate, pancreatic, neuroendocrine cancer, glioblastoma, meningioma, myelodysplastic syndrome, multiple myeloma, age-related macular degeneration • Phase III: Colorectal cancer
VEGF Trap (Regeneron Pharmaceuticals)	VEGF	• Phase I: NHL, age-related macular degeneration, diabetic macular oedema • Phase II: Kidney, ovarian cancer, NSCLC, age-related macular degeneration • Phase III: Ovarian cancer
XL184 (Exelixis)	MMET, VEGFR, RTK, FLT3, TIE2	• Phase I: Solid tumours
XL880 (Exelixis)	C-met, RTK	• Phase I: Solid tumours • Phase II: Papillary renal cell carcinoma
XL999 (Exelixis)	VEGFR, PDGFR, EGFR, FLT3, Src	• Phase I: Solid tumours • Phase II: Multiple myeloma, colorectal, ovarian, renal cell cancer, AML, NSCLC
ZD6474 (AstraZeneca)	VEGFR2, EGFR	• Phase I: Glioma • Phase II: Breast cancer, NSCLC, SCLC, thyroid, gliomas, multiple myeloma • Phase III: NSCLC

AML, acute myeloid leukaemia; APML, acute promyelocytic leukaemia; bFGF, basic fibroblast growth factor; CML, chronic myeloid leukaemia; CLL, chronic lymphocytic leukaemia; CNS, central nervous system; CTAP, connective tissue activation peptide; EGFR, epidermal growth factor receptor; FGFR3, fibroblast growth factor receptor 3; FLT3, fms-related tyrosine kinase 3; HDAC, histone deacetylase; HIF1, hypoxia-inducible factor 1; IGF1, insulin-like growth factor 1; IP10, inducible protein 10; KDR, kinase insert domain receptor; MDA7, interleukin-24; METAP2, methionyl aminopeptidase 2; MMP, matrix metalloproteinase; mTOR, mammalian target of rapamycin; NHL, non-Hodgkin's lymphoma; NSCLC, non-small-cell lung cancer; PDGFR, platelet-derived growth factor receptor; RETR, ret proto-oncogene (multiple endocrine neoplasia and medullary thyroid carcinoma 1, Hirschsprung disease) receptor; SCLC, small-cell lung cancer; TFP1, transferrin pseudogene 1; TGFβ, transforming growth factor-β; TNF, tumour-necrosis factor; uPA, urokinase-type plasminogen activator; VE-cadherin, vascular/endothelial-cadherin; VEGF(R), vascular endothelial growth factor (receptor); vWF, von Willebrand factor.

inhibitor in the endometrium? If so, could this condition be diagnosed by the measurement of THBS1 in the vaginal fluid? Could endometrial THBS1 then be suppressed, for example, by a vaginal suppository containing a putative short-acting THBS1-suppressor protein? Another intriguing finding is that haemangiomas, benign tumours of infancy, have the gene signature of cells of the fetal placental endothelium, implying that they might originate from the fetal placenta[69,70] (BOX 1). As haemangiomas usually regress spontaneously, they might reveal important clues about the molecular mechanisms of spontaneous regression of new blood vessels.

Endothelial cell control of tissue mass. When approximately 70% of the liver is removed in a rat (hepatectomy), the original mass regenerates completely in approximately 10 days[71]. Hepatocyte proliferation and endothelial cell proliferation are initiated the day after surgery. At approximately day 8, there is a wave of endothelial cell apoptosis, following which hepatocyte proliferation ceases[48]. The liver stops growing at ~10 days. However, if an angiogenic protein, such as VEGF or bFGF, is administered systemically, endothelial cells continue to proliferate and the liver continues to grow beyond its normal size. By contrast, if a specific inhibitor of endothelial proliferation is administered, liver regeneration is prevented and the liver remains at 30% of its normal size. Discontinuation of the endothelial inhibitor is followed immediately by liver regeneration that is complete by 10 days[48]. These experiments indicate that normal tissue and organ regeneration are controlled in part by the microvascular endothelium.

Growth and regression of fat is controlled by endothelial proliferation or apoptosis, respectively[49]. Leptin-deficient mice gain up to approximately 1 gram per day, mainly in fat. Adipocyte enlargement and proliferation is accompanied by endothelial proliferation that is restricted to fat. Systemic administration of an angiogenesis inhibitor (TNP-470 or endostatin) specifically induces endothelial apoptosis and a decrease in fat accompanied by rapid weight loss. When the normal weight for age is reached, weight loss stops. A similar result is obtained when endothelial cells in fat are specifically targeted by a genetically regulated inhibitor of proliferation[72]. Growth of normal prostate is also under endothelial control[73], and so is bone growth[74]. Therefore, it seems that microvascular endothelial cells can control tissue mass, regardless of whether the cells in this mass have a normal genome or a cancer genome[75]. This raises a provocative question: Is there some type of set-point or feedback mechanism in endothelial cells that tells them when a normal organ, such as liver, has reached its normal mass? If so, do tumour cells override this mechanism, and how?

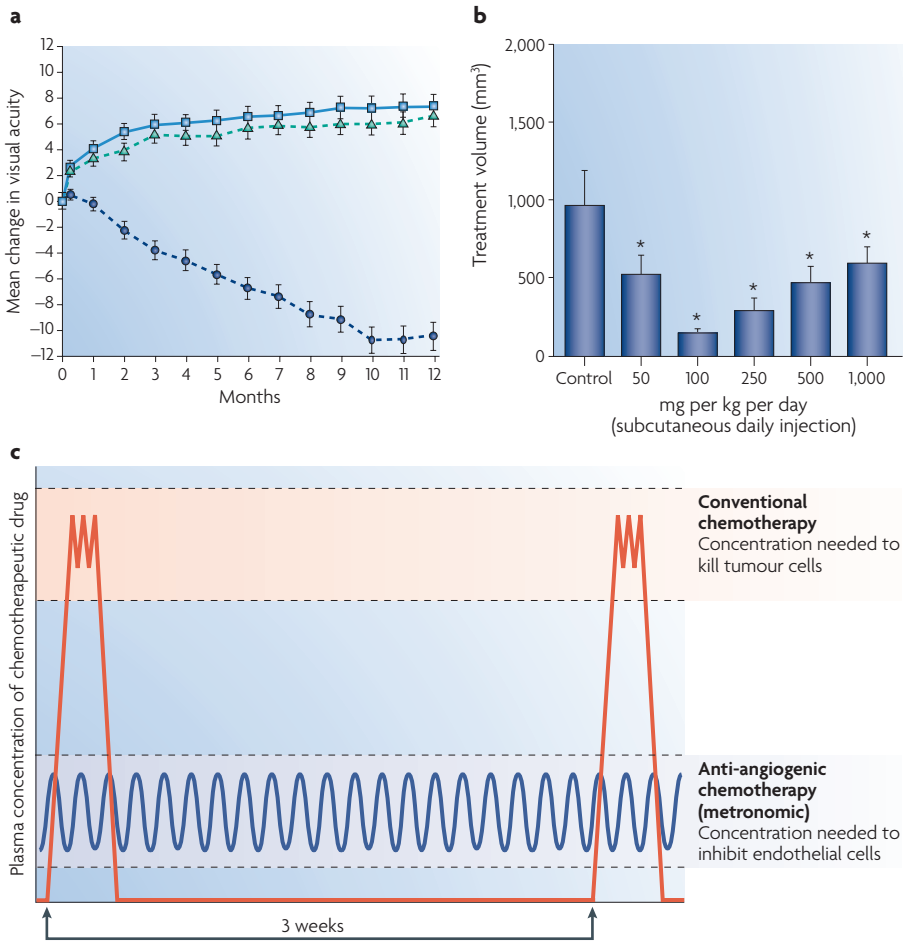

Figure 3 | **Examples of anti-angiogenic therapy. a** | Phase III clinical trial of Lucentis (ranibizumab; Genentech), a fragment of Avastin, an antibody to vascular endothelial growth factor (VEGF). Lucentis is used for intra-ocular injection in patients with age-related macular degeneration[37]. **b** | A biphasic (U-shaped) dose-efficacy curve for human pancreatic cancer in immunodeficient mice treated with endostatin. The tumour cells are also deficient in p53 (adapted from REF. 119). **c** | Dosing schedule differences between conventional chemotherapy (red) and anti-angiogenic (metronomic) chemotherapy (blue) (adapted from REF. 131 and from discussions with R. Kerbel).

What are the implications of this general principle for drug discovery? There is the possibility that specific endothelial inhibitors might be used to control obesity[72], as well as overgrowth of other tissues, such as uterine fibroids, overgrowth of bone caused by lymphangiogenesis and ectopic bone growth (fibrodysplasia ossificans progressiva)[76]. Specific endothelial inhibitors might also be used to control vascular malformations that grow rapidly after puberty or after attempts at surgical excision, and for which there are currently no drugs. The endocrine-specific angiogenesis-regulatory proteins, such as *Bombina variegata* peptide 8 kDa protein[77] (Bv8; also known as PROK2; testicular-cancer-specific), are of particular interest.

Is oncogene dependence angiogenesis dependent? The recognition that endothelial cells control tumour mass is crucial for a more complete understanding of how oncogenes initiate tumour growth. The conventional wisdom is that oncogene activation in a cell leads directly to the formation of large lethal tumours in mice. This concept is reinforced by experiments in which *Ras* or *Myc* oncogenes, under the control of the doxycycline promoter, induce rapid tumour growth when the oncogene is activated, leading to rapid tumour regression when the oncogene is inactivated[78–83]. This phenomenon is called oncogene dependence or oncogene addiction[84].

However, my group has found that during oncogene-induced tumour growth there is intense tumour angiogenesis associated with suppression of THBS1 in the tumour bed. When an oncogene is inactivated, the expression of THBS1, a potent angiogenesis inhibitor, is increased in the tumour bed, leading us to propose that oncogene addiction is angiogenesis dependent[83]. This hypothesis has now been supported by the deletion of THBS1 in the tumour and the host. In these mouse models, an activated oncogene induces more rapid tumour growth than in wild-type mice, but tumours do not regress after the inactivation of the oncogene[82]. Restoration of THBS1 expression in the tumour results in tumour regression upon oncogene inactivation[50].

How could this change in thinking about oncogene addiction provide new opportunities in drug discovery? Conventional wisdom (FIG. 4) suggests that the development of drugs targeted against oncogenes should be sufficient to control cancer. Imatinib (Gleevec; Novartis), which targets the product of the *BCR–ABL* oncogene, has demonstrated proof-of-concept by its success in the treatment of chronic myeloid leukaemia. Furthermore, imatinib targets the product of the oncogene *cKIT*, and has also proved successful in treating gastrointestinal stromal tumours in which this protein has a key role[85,86]. However, many patients eventually develop drug resistance[87], and there are numerous other oncogenes that could be responsible for inducing expression of redundant growth factors in these tumours. The imatinib experience also suggests that drugs will need to be developed against combinations of many oncogenes. A single angiogenesis inhibitor, especially a broad-spectrum angiogenesis inhibitor such as endostatin[28] or caplostatin, or a combination of angiogenesis inhibitors might block the effect of a large family of oncogenes, as the blockade of angiogenesis can prevent tumour growth downstream of oncogene activation. Analysis of 15 of the most studied oncogenes revealed that the majority of them increase the expression of VEGF (and/or bFGF) and decrease the expression of THBS1 in tumour cells[88,89].

Genetic regulation of angiogenesis. Although we all carry endogenous angiogenesis inhibitors in our blood and tissues (at least 29 at the time of writing)[24,25,90], different individuals reveal distinct genetic differences in their angiogenic response to a given stimulus. For example, individuals with Down syndrome are protected against diabetic retinopathy, although they have a similar incidence of diabetes as individuals without Down syndrome[52,91]. They also have higher levels of circulating endostatin (~1.6-fold) than normal individuals because of an extra copy of the gene for the endostatin precursor (collagen XVIII) on chromosome 21 (REFS 91,92). Interestingly, they seem to be among the most protected of all humans against cancer. Although testicular cancer and a megakaryocytic leukaemia have been reported for individuals with Down syndrome, they have the lowest incidence of the other ~200 human cancers compared with age-matched controls[52,91]. Conversely, individuals with a polymorphism in endostatin (specifically arginine substituted for alanine at N104) have a significantly higher risk of breast cancer[93]. The correlation between endostatin levels and cancer susceptibility was demonstrated in mice. Mice that were engineered to genetically overexpress endostatin to mimic individuals with Down syndrome have tumours that grow 300% slower[94], and in mice that had THBS1 deleted, tumours grow approximately 300% more rapidly, and more quickly still if two angiogenesis inhibitors are knocked out (tumstatin and THBS1)[94].

Another interesting finding is that African Americans rarely develop the 'wet' form of age-related macular degeneration. They usually do not have intravitreal haemorrhages and do not go blind from the 'dry' form of this disease[95]. By contrast, African Americans have a similar incidence of diabetic retinopathy. In age-related macular degeneration, neovascularization is in the choroidal layer that is surrounded by melanocytes containing melanin. In diabetic retinopathy, neovascularization arises from the retina. The retinal pigmented epithelial cells contain a lighter form of oxidized melanin, which differs from melanin in the choroid or in the skin. Also, African American infants rarely develop cutaneous haemangiomas compared with white infants.

These correlations suggest that factors linked to pigmentation and melanin are producing an inhibitory influence on the angiogenic balance in the melanin-rich tissues. However, there is no melanin in prostate or breast tissue, and African Americans are not protected from cancer of these organs.

This hypothesis was examined in animal experiments. When the gene for tyrosinase (in the melanin pathway) was deleted from mice, the albino relatives C57Bl/6J-Tyr$^{c\text{-}2J}$ showed intense iris neovascularization and haemorrhage (hyphaema) compared with weak neovascularization and no haemorrhage in the pigmented iris of wild-type mice. The amount of corneal neovascularization was not significantly different between these two strains because the cornea is not a pigmented tissue[96,97].

Genetic variations of angiogenic factors have important consequences for the clinical treatment of angiogenesis-dependent

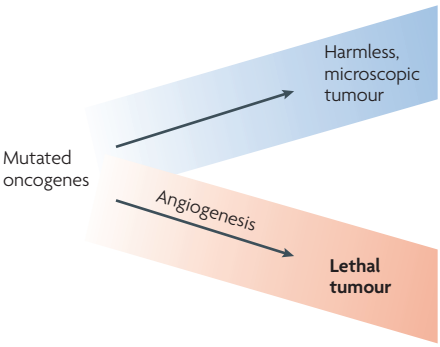

Figure 4 | **Oncogene addiction is angiogenesis dependent.** An oncogene-induced tumour that cannot recruit new blood vessels will remain as a harmless microscopic tumour in experimental animals[50,83].

Box 1 | Are infantile haemangiomas metastases from the placenta?

Haemangiomas are benign tumours made of capillary blood vessels that appear in 1 out of 100 newborns and usually begin to undergo spontaneous regression at approximately the end of the first year[6]. Some haemangiomas can be life threatening if they occur in the brain, airway or liver. The mechanism of haemangioma regression is unclear. Haemangiomas provide the possibility that they might reveal a clue about molecular mechanisms of spontaneous regression of new blood vessels. It was recently reported that all infantile haemangiomas express the glucose receptor GLUT1 (also known as SLC2A1), and that this receptor is also found on the endothelium of the placenta[69]. This observation led to a gene array analysis of endothelial cells from haemangioma and other tissues, which revealed that gene expression of haemangioma endothelium is identical to gene expression of fetal placental endothelium, but not to any other tissue analyzed[70]. The implication is that haemangiomas might be metastases from the fetal placenta. A further implication is that putative endogenous angiogenesis inhibitors that control the regression of placental vasculature at term might also be involved in the regression of haemangiomas. This speculation remains to be tested, but it illustrates how viewing a given process as part of an organizing principle can be useful.

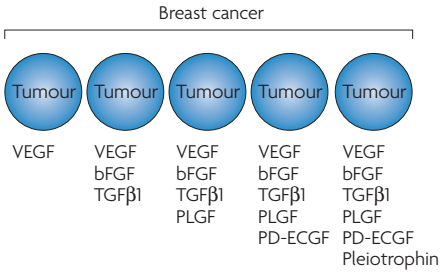

Figure 5 | **Angiogenic proteins in breast cancer.** Human breast cancer can cause the expression of at least six different angiogenic proteins (adapted from REF. 142). bFGF, basic fibroblast growth factor (also known as FGF2); PD-ECGF, platelet-derived endothelial cell growth factor (also known as ECGF1); PLGF, placental growth factor (also known as PGF); TGFβ1, transforming growth factor-β1; VEGF, vascular endothelial growth factor.

diseases. For example, some tumours that seem poorly vascularized and have a low microvessel density will be inhibited by a significantly lower dose of an angiogenesis inhibitor than is required for a highly vascularized tumour with a significantly higher microvessel density[98]. This may be counter-intuitive to clinicians who might inform a patient that their tumour is not very vascular and therefore will not respond to anti-angiogenic therapy. In fact, these tumours might be expressing their own angiogenesis inhibitors[99,100] and might respond to a lower therapeutic dose of angiogenesis inhibitor than would be required for a highly vascularized tumour.

The genetic heterogeneity of the angiogenic response is another reason for the pressing need to develop blood or urine biomarkers[101] to optimize the dosing of anti-angiogenic therapy. Furthermore, when mice are used for preclinical studies of angiogenesis inhibitors, it is crucial to know the genetic background of the mice in regards to their angiogenic responsiveness.

Optimizing anti-angiogenic therapy

Insights into the molecular mechanisms and significance of angiogenesis in different biological contexts are creating exciting new opportunities for drug discovery. However, as in some cases including cancer, anti-angiogenic therapies can also be used in combination with existing drugs. It is important to understand the difference between anti-angiogenic and cytotoxic drugs to optimize efficacy.

Anti-angiogenic therapy and cytotoxic chemotherapy. In February 2004, when the FDA approved bevacizumab for colorectal cancer, M. McClellan, then FDA Commissioner, said: "Anti-angiogenic therapy can now be considered the fourth modality for cancer treatment."[102]. It is a different modality because there are certain notable differences about chemotherapy that do not always readily transfer to anti-angiogenic therapy.

Importantly, anti-angiogenic therapy primarily targets the activated microvascular endothelial cells in a tumour bed rather than the tumour itself. It can accomplish this directly by preventing endothelial cells from responding to angiogenic proteins, as endostatin[28] and caplostatin[103,104] do. Anti-angiogenic therapy can also inhibit endothelial cell proliferation and motility indirectly by suppressing a tumour's production of angiogenic proteins, as erlotinib does[105], or by neutralizing one of these proteins, as bevacizumab does.

Also, although chemotherapy is usually more effective on rapidly growing tumours than on slowly growing tumours, the opposite is often true of anti-angiogenic therapy. More rapidly growing tumours can require higher doses of anti-angiogenic therapy[98]. Furthermore, chemotherapy is optimally given at a maximum tolerated dose, with off-therapy intervals of 1–3 weeks to rescue bone marrow and intestine. Anti-angiogenic therapy might optimally require that endothelial cells be exposed to steady blood levels of the inhibitor[100]. Therefore, daily dosing is optimal for those angiogenesis inhibitors with a short half-life. However, certain antibodies such as bevacizumab can be administered every 2 weeks because of long-lasting antibody levels in plasma, and perhaps because of neutralization of VEGF in platelets by bevacizumab that enters the platelets and binds with VEGF[61]. Zoledronate (Zometa; Novartis) is an amino-bisphosphonate that has been shown to inhibit angiogenesis[106] by targeting matrix metalloproteinase 9 (MMP9)[107], by reducing circulating levels of pro-angiogenic proteins in the circulation[108] or by suppressing multiple circulating pro-angiogenic factors in patients with cancer[109]. It accumulates in bone and can therefore be administered every month. However, after prolonged use, zoledronate may need to be administered less frequently to avoid osteonecrosis of the jaw.

Another important difference concerns the side effects of anti-angiogenic therapy compared with chemotherapy. Bone-marrow suppression, hair loss, severe vomiting and diarrhoea, and weakness are less common with anti-angiogenic therapy, and endostatin has shown minimal or no side effects in animals[110] and in humans[111]. It has to be noted though, that certain angiogenesis inhibitors increase the incidence of thrombotic complications, such as thalidomide (Thalomid; Celgene)[112] and bevacizumab. The risk of thrombosis is increased when these angiogenesis inhibitors are administered together with conventional chemotherapy[113]. Other side effects of inhibitors of VEGF include hypertension, intratumoural bleeding and bowel perforation, especially

Table 4 | **Three types of angiogenesis inhibitors**

Mechanism	Drug	Action
Type I		
Blocks one main angiogenic protein	Avastin (Avastin; Genentech)	Blocks VEGF
	VEGF Trap (Regeneron Pharmaceuticals)	Blocks VEGF
Type II		
Blocks two or three main angiogenic proteins	Sutent (Sutent; Pfizer)	Downregulates VEGF receptor 2, PDGF receptor, cKIT receptor
	Tarceva (Tarceva; Genentech, OSI Pharmaceuticals, Roche)	Downregulates VEGF production, bFGF production, TGFα by tumour cell
Type III		
Blocks a broad range of angiogenic regulators	Endostatin	Downregulates VEGF, bFGF, bFGF receptor, HIF1α, EGF receptor, ID1, neuropilin Upregulates thrombospondin 1, maspin, HIF1α, TIMP2
	Caplostatin	Broad anti-angiogenic and anticancer spectrum

bFGF, basic fibroblast growth factor; EGF, epidermal growth factor; HIF1α, hypoxia-inducible factor 1α; ID1, inhibitor of DNA binding 1, dominant negative helix–loop–helix protein; PDGF, platelet-derived growth factor; TIMP2, tissue inhibitor of metalloproteinase 2; TGFα, transforming growth factor-α; VEGF, vascular endothelial growth factor.

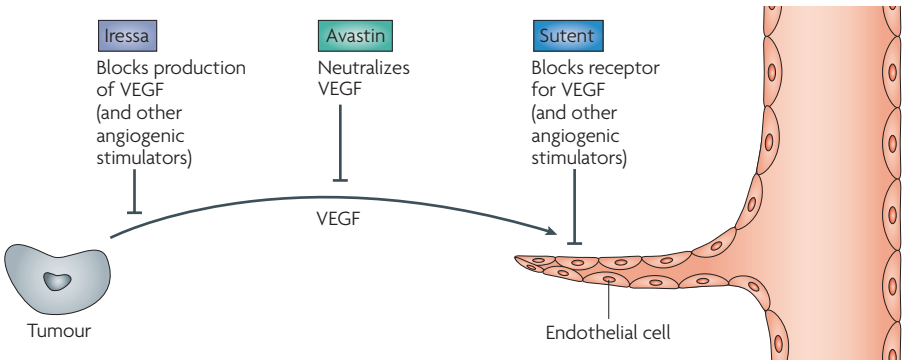

Figure 6 | **Three general mechanisms of angiogenesis inhibitors currently approved by the FDA.** Iressa blocks tumour expression of an angiogenic factor. Avastin blocks an angiogenic factor after its secretion from a tumour. Sutent blocks an endothelial cell receptor. VEGF, vascular endothelial growth factor.

in cases in which the intestine contains a tumour. Thalidomide has a slightly higher incidence of thromboembolic complications, as well as constipation and peripheral neuropathy — these are usually reversible upon discontinuation of thalidomide. Lenalidomide (Revlimid; Celgene), an FDA-approved derivative of thalidomide, has significantly reduced side effects. Side effects need to be carefully considered, especially when anti-angiogenic and cytotoxic medications are combined. So far, there are almost no data that allow a direct comparison of clotting risk for anti-angiogenic therapy alone, compared with cytotoxic therapy or combination therapy.

However, there can also be unexpected benefits from combining angiogenesis inhibitors, or drugs that have varying degrees of anti-angiogenic activity, with conventional chemotherapy. For example, Jain has shown that bevacizumab, by decreasing vascular leakage in a tumour, can lower intratumoral-tissue pressure and increase delivery of chemotherapy to a tumour[114]. In other words, anti-angiogenic therapy might 'normalize' tumour vessels[115]. Teicher *et al.* showed that anti-angiogenic therapy could decrease intratumoural pressure, which resulted temporarily in increased oxygenation to a tumour with subsequent increased sensitivity to ionizing radiation[116].

Biphasic dose efficacy of anti-angiogenic therapy. Dose efficacy is generally a linear function for chemotherapy. By contrast, several angiogenesis inhibitors have been reported to follow a biphasic, U-shaped dose-efficacy curve (known as hormesis[117]). For example, interferon-α (IFNα) is anti-angiogenic at low doses, but not at higher doses[118]. Similarly, rosiglitazone (Avandia; GlaxoSmithKline), a peroxisome proliferator-activated receptor-γ (PPARγ) ligand, as well as endostatin protein therapy[119] (FIG. 3b) and endostatin gene therapy[120] inhibit angiogenesis with a U-shaped dose-efficacy curve[121]. Before the U-shaped dose-efficacy response was recognized for anti-angiogenic gene therapy, my group had observed that gene therapy of endostatin could produce such high blood levels that all anti-angiogenic activity was lost[122]. It is now clear that blood levels of certain angiogenesis inhibitors (such as endostatin) that are too high or too low will be ineffective, and that the biphasic dose-efficacy curve offers the best explanation for why endostatin gene therapy of murine leukaemia failed[123,124].

Even the effect of endostatin on the gene expression (for example, hypoxia-inducible factor 1α; HIF1α) of fresh human endothelial cells *in vitro* reveals a U-shaped dose-efficacy pattern[28]. This is important information for drug discovery. For example, in the ranibizumab trial for age-related macular degeneration, a higher dose did not increase efficacy over a lower dose.

Anti-angiogenic therapy and drug resistance. Tumours might become refractory to anti-angiogenic therapy, especially if a mono-anti-angiogenic therapy targets only one angiogenic protein (for example, VEGF)[124]. Endothelial cells seem to have a lower probability for developing resistance to anti-angiogenic therapy, even though mouse endothelial cells in a tumour bed can become genetically unstable[80,125]. Although VEGF is expressed by up to 60% of human tumours, most tumours can also express five to eight other angiogenic proteins — for example, human breast cancers can express up to six angiogenic proteins (FIG. 5). High-grade brain tumours might express more angiogenic proteins than other tumours. When the expression of one angiogenic protein is suppressed for a long period, the expression of other angiogenic proteins might emerge[126]. The mechanism of this 'compensatory' response is unclear. Some angiogenesis inhibitors target up to three angiogenic proteins, whereas others target a broad range of angiogenic proteins (TABLE 4). Certain tumours, such as high-grade giant-cell tumours and angioblastomas, produce bFGF as their predominant angiogenic protein and do not seem to deviate from this. For this reason, low-dose daily IFNα therapy for 1–3 years is sufficient to return abnormally high levels of bFGF in the urine of these patients to normal. IFNα has been reported to suppress the production of bFGF by human cancer cells[118]. This treatment regimen has produced long term complete remissions (up to 10 years) without drug resistance (at the time of writing; see REFS 127–129 and L. Kaban, personal communication).

Currently, the majority of FDA-approved angiogenesis inhibitors, as well as those in Phase III clinical trials, neutralize VEGF, target its receptor or suppress its expression by tumour cells (FIG. 6). When drug resistance develops to some of these inhibitors, they are often perceived to represent the whole class of angiogenesis inhibitors. It remains to be seen if broad-spectrum angiogenesis inhibitors will develop less drug resistance than angiogenesis inhibitors that target against a single angiogenic protein. In experimental tumours, TNP-470, a synthetic analogue of fumagillin and caplostatin, its derivative[103,130], did not induce drug resistance when administered to mice for prolonged periods of time[104].

Anti-angiogenic chemotherapy (metronomic therapy). Browder *et al.* first reported that when murine tumours were made drug resistant to cyclophosphamide and then cyclophosphamide was administered on a conventional chemotherapy maximum-tolerated dose schedule, all mice died of large tumours[131]. However, if cyclophosphamide was administered more frequently at a lower dose, the tumours were potently inhibited because of endothelial apoptosis. If an angiogenesis inhibitor (TNP-470)[104] was added, which by itself could only inhibit the tumours by 50%, the drug-resistant tumours were eradicated[131]. This experiment demonstrated a new principle: a cytotoxic chemotherapeutic agent could be redirected to an endothelial target by changing its dose and frequency of

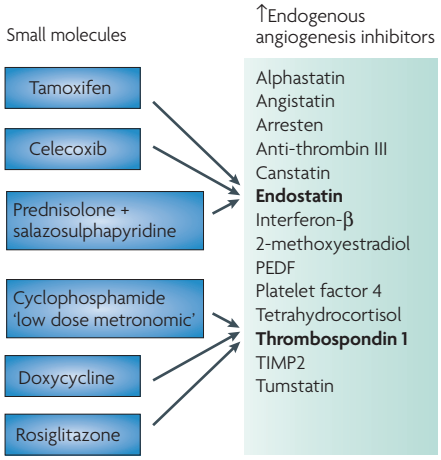

Figure 7| **Small molecules to increase endogenous angiogenesis inhibitors.** Examples of small molecules that are orally available and might induce increased levels of endogenous angiogenesis inhibitors in the blood or joint fluid. PEDF, pigment epithelium-derived factor; TIMP2, tissue inhibitor of matrix metalloproteinase 2 (REF. 124).

administration. Browder *et al.* called this regimen anti-angiogenic chemotherapy. Klement *et al.* confirmed this approach with a different chemotherapeutic agent[132]. Bocci *et al.*[133] further showed that anti-angiogenic chemotherapy increased circulating THBS1, and that deletion of the *THBS1* gene in mice completely abrogated the antitumour effect of this anti-angiogenic therapy. These results suggested that THBS1 acts as a mediator of anti-angiogenic chemotherapy[133]. The optimization of chemotherapy to treat vascular endothelium in the tumour bed is also called 'metronomic' therapy[134] (FIG. 3c) and has entered clinical trials for brain tumours and other tumours that were refractory to conventional chemotherapy. Kieran *et al.* recently studied 20 children with different types of brain tumours refractory to surgery, radiotherapy and chemotherapy, who were treated for 6 months with daily oral thalidomide and celecoxib (Celebrex; Pfizer), plus daily low-dose oral cyclophosphamide alternated every 21 days with daily low-dose oral etoposide[135]. Twenty-five percent of the patients were progression free more than 2.5 years from starting therapy. Forty percent of patients completed the 6 months of therapy, resulting in prolonged or persistent disease-free status. Sixteen percent of patients showed a radiographic partial response. Only elevated THBS1 levels in the blood correlated with prolonged response. This is consistent with the elevated circulating THBS1 levels observed in tumour-bearing mice treated with anti-angiogenic (metronomic) cyclophosphamide[133]. It is possible that angiogenesis inhibitors, such as bevacizumab, might be augmented by low dose anti-angiogenic (metronomic) chemotherapy with fewer side effects than conventional dosing of chemotherapy.

New pharmacology: oral drugs that increase endogenous angiogenesis inhibitors. The clinical finding that individuals with Down syndrome have an elevated circulating level of endostatin approximately 1.6-fold higher than normal individuals[91] is provocative. It suggests that small elevations of one or more endogenous angiogenesis inhibitors in the blood might protect against recurrent cancer, or might prevent the switch to the angiogenic phenotype in women at high risk for breast cancer. It is also possible that other genes on chromosome 21 have anti-angiogenic activity.

It has been found that certain orally available small molecules can upregulate expression of specific endogenous anti-angiogenic proteins, opening the way for a new field of pharmacology (FIG. 7). Endostatin is increased by tamoxifen[136], celecoxib[137] and (in joint fluid) by prednisolone plus salazosulphapyridine[138]. THBS1 is upregulated by low dose cyclophosphamide[133], doxycycline[139] and rosiglitazone[121]. This unifying concept points to future drug discovery in which the known endogenous angiogenesis inhibitors could be screened for small-molecule inducers that would increase the circulating level of one or more of them.

Outlook

Angiogenesis inhibitors are now being approved and introduced into medical practice throughout the world. At the same time, a need for molecular biomarkers is being met by an expanding worldwide research effort to develop gene-based and protein-based molecular signatures in blood, platelets and urine for very early diagnosis of recurrent cancer. One can speculate that if these two fields intersect, it might someday be possible to diagnose microscopic tumours at a millimetre size, at about the time of the angiogenic switch but perhaps years before they are symptomatic, or before they can be visualized by any conventional methods.

For example, today most individuals with the diagnosis of colon cancer are operated on. At least 50–60% of these patients are cured by the surgery. In the other patients, cancer will recur in approximately 4–6 years. Physicians are helpless to do anything until symptoms (such as pain and jaundice) occur, or until the recurrent cancer can be located by ultrasound, magnetic resonance imaging or CAT (computed axial tomography) scan. However, sensitive and specific molecular biomarkers that are being developed today could be used in the future to diagnose the presence of a microscopic recurrent tumour even before it could be anatomically located. Once these biomarkers are validated in clinical trials, then physicians could 'treat the rising biomarker' with non-toxic angiogenesis inhibitors until the biomarker returns to normal. A paradigm shift would be that recurrent cancer would be treated without waiting to see it, when it is still relatively harmless with low or no metastatic potential (that is, before the switch to the angiogenic phenotype). It might also be possible to use angiogenesis-based biomarkers to monitor the progression or regression of certain angiogenesis-dependent diseases that are non-neoplastic. These could include atherosclerosis, endometriosis, Crohn's disease and rheumatoid arthritis, among others.

There might be an analogy in the history of the treatment of infection. Before 1930, there were virtually no drugs for any infection, and most infections progressed to abscesses. Surgeons had to wait until the abscess was large enough to be located by X-rays so that the abscess could be surgically drained. The surgical textbooks of that era instructed surgeons how to locate an abscess: above the liver, behind the liver, in the mastoid, and so on. The term 'laudable' pus was commonly used to mean that if a surgeon could successfully drain an abscess the patient might live. After 1941, when antibiotics were introduced, it was no longer necessary to precisely locate an infection. Today the treatment of most infections is simply guided by blood tests (white-blood-cell count or blood cultures). As we continue to gain insight into angiogenesis and the role of angiogenic factors in seemingly unrelated diseases, the consequent potential of angiogenic modulators could see P. Carmeliet's prediction in the December 2005 issue of *Nature*[140] becoming prophetic: "Angiogenesis research will probably change the face of medicine in the next decades, with more than 500 million people worldwide predicted to benefit from pro- or anti-angiogenesis treatments"[140].

Judah Folkman is at the Children's Hospital and Harvard Medical School Boston, Massachusetts, USA.
e-mail: judah.folkman@childrens.harvard.edu
doi:10.1038/nrd2115

1. Sholley, M. M., Ferguson, G. P., Seibel, H. R., Montour, J. L., & Wilson, J. D. Mechanisms of neovascularization. Vascular sprouting can occur without proliferation of endothelial cells. *Lab. Invest.* **51**, 624–634 (1984).
2. Folkman, J. Angiogenesis. in *Harrison's Textbook of Internal Medicine* (eds Braunwald, E. *et al.*) (McGraw–Hill, New York, 2001).
3. Moulton, K. S. *et al.* Inhibition of plaque neovascularization reduces macrophage accumulation and progression of advanced atherosclerosis. *Proc. Natl Acad. Sci. USA* **100**, 4736–4741 (2003).
4. Folkman, J. Angiogenesis in psoriasis: therapeutic implications. *J. Invest. Dermatol.* **59**, 40–43 (1972).
5. Zeng, X., Chen, J., Miller, Y. I., Javaherian, K. & Moulton, K. S. Endostatin binds biglycan and LDL and interferes with LDL retention to the subendothelial matrix during atherosclerosis. *J. Lipid Res.* **46**, 1849–1859 (2005).
6. Ezekowitz, A., Mulliken, J. & Folkman, J. Interferon-α therapy of haemangiomas in newborns and infants. *Br. J. Haematol.* **79** (Suppl. 1), 67–68 (1991).
7. Szabo, S. *et al.* Accelerated healing of duodenal ulcers by oral administration of a mutein of basic fibroblast growth factor in rats. *Gastroenterology* **106**, 1106–1111 (1994).
8. Miller, J. W. *et al.* Vascular endothelial growth factor/vascular permeability factor is temporally and spatially correlated with ocular angiogenesis in a primate model. *Am. J. Pathol.* **145**, 574–584 (1994).
9. Folkman J. in *Targeted Therapies in Rheumatology* (eds Smolen, J. S. & Lipsky P. E.) 111–131 (Martin Dunitz, London, 2003).
10. Moulton, K. S. *et al.* Angiogenesis inhibitors endostatin or TNP-470 reduce intimal neovascularization and plaque growth in apolipoprotein E-deficient mice. *Circulation* **99**, 1726–1732 (1999).
11. Moulton, K. S. Angiogenesis in atherosclerosis: gathering evidence beyond speculation. *Curr. Opin. Lipidol.* **17**, 548–555 (2006).
12. Gimbrone, M. A., Jr., Cotran, R. S. & Folkman, J. Human vascular endothelial cells in culture. Growth and DNA synthesis. *J. Cell Biol.* **60**, 673–684 (1974).
13. Ausprunk, D. H., Knighton, D. R. & Folkman, J. Vascularization of normal and neoplastic tissues grafted to the chick chorioallantois. Role of host and preexisting graft blood vessels. *Am. J. Pathol.* **79**, 597–628 (1975).
14. Langer, R. & Folkman, J. Polymers for the sustained release of proteins and other macromolecules. *Nature* **263**, 797–800 (1976).
15. Gimbrone, M. A. Jr., Cotran, R. S., Leapman, S. B. & Folkman, J. Tumor growth and neovascularization: an experimental model using the rabbit cornea. *J. Natl Cancer Inst.* **52**, 413–427 (1974).
16. Auerbach, R., Arensman, R., Kubai, L. & Folkman, J. Tumor-induced angiogenesis: lack of inhibition by irradiation. *Int. J. Cancer* **15**, 241–245 (1975).
17. Taylor, S. & Folkman, J. Protamine is an inhibitor of angiogenesis. *Nature* **297**, 307–312 (1982).
18. Crum, R., Szabo, S. & Folkman, J. A new class of steroids inhibits angiogenesis in the presence of heparin or a heparin fragment. *Science* **230**, 1375–1378 (1985).
19. Folkman, J. Tumor angiogenesis: therapeutic implications. *N. Engl. J. Med.* **285**, 1182–1186 (1971).
20. Ausprunk, D. H., Falterman, K. & Folkman, J. The sequence of events in the regression of corneal capillaries. *Lab. Invest.* **38**, 284–294 (1978).
21. Maeshima, Y. *et al.* Tumstatin, an endothelial cell-specific inhibitor of protein synthesis. *Science* **295**, 140–143 (2002).
22. O'Reilly, M. S. *et al.* Angiostatin: a novel angiogenesis inhibitor that mediates the suppression of metastases by a Lewis lung carcinoma. *Cell* **79**, 315–328 (1994).
23. Frater-Schroder, M., Risau, W., Hallmann, R., Gautschi, P. & Bohlen, P. Tumor necrosis factor type α, a potent inhibitor of endothelial cell growth *in vitro*, is angiogenic *in vivo*. *Proc. Natl Acad. Sci. USA* **84**, 5277–5281 (1987).
24. Folkman, J. Endogenous angiogenesis inhibitors. *Acta Pathol. Microbiol. Immunol. Scand.* **112**, 496–507 (2004).
25. Nyberg, P., Xie, L. & Kalluri, R. Endogenous inhibitors of angiogenesis. *Cancer Res.* **65**, 3967–3979 (2005).
26. Folkman, J. in *Cancer Medicine* 7th Edn (eds Kufe, D. W. *et al*) (B.C. Decker, Hamilton, Ontario, 2006).
27. O'Reilly, M. S. *et al.* Endostatin: an endogenous inhibitor of angiogenesis and tumor growth. *Cell* **88**, 277–285 (1997).
28. Abdollahi, A. *et al.* Endostatin's antiangiogenic signaling network. *Mol. Cell* **13**, 649–663 (2004).
29. Inoue, K., Korenaga, H., Tanaka, N. G., Sakamoto, N. & Kadoya, S. The sulfated polysaccharide — peptidoglycan complex potently inhibits embryonic angiogenesis and tumor growth in the presence of cortisone acetate. *Carbohydr. Res.* **181**, 135–142 (1988).
30. Hurwitz, H. *et al.* Bevacizumab plus irinotecan, fluorouracil, and leucovorin for metastatic colorectal cancer. *N. Engl. J. Med.* **350**, 2335–2342 (2004).
31. Udagawa, T. *et al.* Analysis of tumor-associated stromal cells using SCID GFP transgenic mice: contribution of local and bone marrow-derived host cells. *FASEB J.* **20**, 95–102 (2006).
32. Higgins, K.J., Abdelrahim, M., Liu, S., Yoon, K. & Safe, S. Regulation of vascular endothelial growth factor receptor-2 expression in pancreatic cancer cells by Sp proteins. *Biochem. Biophys. Res. Commun.* **345**, 292–301 (2006).
33. Yasui, H., Hideshima, T., Richardson, P. G. & Anderson, K. C. Recent advances in the treatment of multiple myeloma. *Curr. Pharm. Biotechnol.* **7**, 381–393 (2006).
34. Ranieri, G. *et al.* Vascular endothelial growth factor (VEGF) as a target of bevacizumab in cancer: from the biology to the clinic. *Curr. Med. Chem.* **13**, 1845–1857 (2006).
35. Rosenfeld, P. J. Intravitreal bevacizumab: the low cost alternative to lucentis? *Am. J. Ophthalmol.* **142**, 141–143 (2006).
36. Rosenfeld, P. J., Heier, J. S., Hantsbarger, G. & Shams, N. Tolerability and efficacy of multiple escalating doses of ranibizumab (lucentis) for neovascular age-related macular degeneration. *Ophthalmology* **113**, 623–632 (2006).
37. Kim, I. K. *et al.* Effect of intravitreal injection of ranibizumab in combination with verteporfin PDT on normal primate retina and choroid. *Invest. Ophthalmol. Vis. Sci.* **47**, 357–363 (2006).
38. Husain, D. *et al.* Safety and efficacy of intravitreal injection of ranibizumab in combination with verteporfin PDT on experimental choroidal neovascularization in the monkey. *Arch. Ophthalmol.* **123**, 509–516 (2005).
39. Michels, S. & Rosenfeld, P. J. [Treatment of neovascular age-related macular degeneration with ranibizumab/lucentis]. *Klin. Monatsbl. Augenheilkd.* **222**, 480–484 (2005) (in German).
40. Pieramici, D. J. & Avery, R. L. Ranibizumab: treatment in patients with neovascular age-related macular degeneration. *Expert Opin. Biol. Ther.* **6**, 1237–1245 (2006).
41. Shima, D. T. *et al.* Hypoxic induction of endothelial cell growth factors in retinal cells: identification and characterization of vascular endothelial growth factor (VEGF) as the mitogen. *Mol. Med.* **1**, 182–193 (1995).
42. Ng, E. W. & Adamis, A. P. Targeting angiogenesis, the underlying disorder in neovascular age-related macular degeneration. *Can. J. Ophthalmol.* **40**, 352–368 (2005).
43. Lim, M. S. Re: Correlational of oral tongue cancer inversion with matrix metalloproteinases (MMPs) and vascular endothelial growth factor (VEGF) expression, by Kim S-H, Cho NH, Kim K, *et al. J. Surg. Oncol.* **93**, 253–254 (2006).
44. Des Guetz, G. *et al.* Microvessel density and VEGF expression are prognostic factors in colorectal cancer. Meta-analysis of the literature. *Br. J. Cancer* **94**, 1823–1832 (2006).
45. Kerbel, R. S., Viloria-Petit, A., Klement, G. & Rak, J. "Accidental" anti-angiogenic drugs. Anti-oncogene directed signal transduction inhibitors and conventional chemotherapeutic agents as examples. *Eur. J. Cancer* **36**, 1248–1257 (2000).
46. Morelli, M.P. *et al.* Anti-tumor activity of the combination of cetuximab, and anti-EGFR blocking monoclonal antibody and ZD6474, an inhibitor of BEGFR and EGFR tyrosine kinases. *J. Cell Physiol.* **208**, 344–353 (2006).
47. Pinedo, H.M. *et al.* Involvement of platelets in tumour angiogenesis? *Lancet* **352**, 1775–1777 (1998).
48. Greene, A. K. *et al.* Urinary matrix metalloproteinases and their endogenous inhibitors predict hepatic regeneration after murine partial hepatectomy. *Transplantation* **78**, 1139–1144 (2004).
49. Rupnick, M. A. *et al.* Adipose tissue mass can be regulated through the vasculature. *Proc. Natl Acad. Sci. USA* **99**, 10730–10735 (2002).
50. Giuriato, S. *et al.* Sustained regression of tumors upon MYC inactivation requires p53 or thrombospondin-1 to reverse the angiogenic switch. *Proc. Natl Acad. Sci. USA* **103**, 16266–16271 (2006).
51. Klagsbrun, M. & Eichmann, A. A role for axon guidance receptors and ligands in blood vessel development and tumor angiogenesis. *Cytokine Growth Factor Rev.* **16**, 535–548 (2005).
52. Yang, Q., Rasmussen, S. A. & Friedman, J. M. Mortality associated with Down's syndrome in the USA from 1983 to 1997: a population-based study. *Lancet* **359**, 1019–1025 (2002).
53. Soker, S., Takashima, S., Miao, H. Q., Neufeld, G. & Klagsbrun, M. Neuropilin-1 is expressed by endothelial and tumor cells as an isoform-specific receptor for vascular endothelial growth factor. *Cell* **92**, 735–745 (1998).
54. Vogel, G. Developmental biology. The unexpected brains behind blood vessel growth. *Science* **307**, 665–667 (2005).
55. Mukouyama, Y. S., Shin, D., Britsch, S., Taniguchi, M. & Anderson, D. J. Sensory nerves determine the pattern of arterial differentiation and blood vessel branching in the skin. *Cell* **109**, 693–705 (2002).
56. Kutcher, M. E., Klagsbrun, M. & Mamluk, R. VEGF is required for the maintenance of dorsal root ganglia blood vessels but not neurons during development. *FASEB J.* **18**, 1952–1954 (2004).
57. Folkman, J., Browder, T. & Palmblad, J. Angiogenesis research: guidelines for translation to clinical application. *Thromb. Haemost.* **86**, 23–33 (2001).
58. Klement, G. *et al.* Early tumor detection using platelet uptake of angiogenesis regulators. *Blood* **104** (ASH Annual Meeting Abstracts), 839 (2004).
59. Naumov, G. N. *et al.* A model of human tumor dormancy: an angiogenic switch from the nonangiogenic phenotype. *J. Natl Cancer Inst.* **98**, 316–325 (2006).
60. Almog, N. *et al.* Prolonged dormancy of human liposarcoma is associated with impaired tumor angiogenesis. *FASEB J.* **20**, 947–949 (2006).
61. Verheul, H. M. *et al.* Uptake of bevacizumab by platelets blocks the biological activity of platelet-derived vascular endothelial growth factor (VEGF). *Proc. Amer. Assoc. Cancer Res.* **47**, Abstract #5708 (2006).
62. Klement, G., Cervi, D., Yip, T. T., Folkman, J. & Italiano, J. Platelet PF-4 is an early marker of tumor angiogenesis. *Blood* **108** (ASH Annual Meeting Abstract), 1476 (2006).
63. Italiano, J., Richardson, J. L., Folkman, J. & Klement, G. Blood platelets organize pro- and anti-angiogenic factors into separate, distinct alpha granules: implications for the regulation of angiogenesis. *Blood* **108** (ASH Annual Meeting Abstracts), 393 (2006).
64. Volpert, O. V., Lawler, J. & Bouck, N. P. A human fibrosarcoma inhibits systemic angiogenesis and the growth of experimental metastases via thrombospondin-1. *Proc. Natl Acad. Sci USA* **95**, 6343–6348 (1998).
65. Rastinejad, F., Polverini, P. J. & Bouck, N. P. Regulation of the activity of a new inhibitor of angiogenesis by a cancer suppressor gene. *Cell* **56**, 345–355 (1989).
66. Dameron, K. M., Volpert, O. V., Tainsky, M. A. & Bouck, N. Control of angiogenesis in fibroblasts by p53 regulation of thrombospondin-1. *Science* **265**, 1582–1584 (1994).
67. Kang, S. -Y. *et al.* Repression of stromal thrombospondin-1 is a determinant for metastatic tissue specificity. *Proc. Amer. Assoc. Cancer Res.* **47**, Abstract #2798 (2006).
68. Iruela-Arispe, M. L., Porter, P., Bornstein, P. & Sage, E. H. Thrombospondin-1, an inhibitor of angiogenesis, is regulated by progesterone in the human endometrium. *J. Clin. Invest.* **97**, 403–412 (1996).
69. North, P. E. *et al.* A unique microvascular phenotype shared by juvenile hemangiomas and human placenta. *Arch. Dermatol.* **137**, 559–570 (2001).
70. Barnes, C. M. *et al.* Evidence by molecular profiling for a placental origin of infantile hemangioma. *Proc. Natl Acad. Sci USA* **102**, 19097–19102 (2005).
71. Greene, A. K. *et al.* Endothelial-directed hepatic regeneration after partial hepatectomy. *Ann. Surg.* **237**, 530–535 (2003).
72. Kolonin, M. G., Saha, P. K., Chan, L., Pasqualini, R. & Arap, W. Reversal of obesity by targeted ablation of adipose tissue. *Nature Med.* **10**, 625–632 (2004).

73. Folkman, J. Is tissue mass regulated by vascular endothelial cells? Prostate as the first evidence. *Endocrinology* **139**, 441–442 (1998).
74. Street, J. *et al*. Vascular endothelial growth factor stimulates bone repair by promoting angiogenesis and bone turnover. *Proc. Natl Acad. Sci. USA* **99**, 9656–9661 (2002).
75. Gerber, H. P., & Ferrara, N. The role of VEGF in normal and neoplastic hematopoiesis. *J. Mol. Med.* **81**, 20–31 (2003).
76. Kaplan, F. *et al*. Urinary basic fibroblast growth factor. A biochemical marker for preosseous fibroproliferative lesions in patients with fibrodysplasia ossificans progressiva. *Clin. Orthop.* **346**, 59–65 (1998).
77. Ferrara, N., LeCouter, J., Lin, R., & Peale, F. EG-VEGF and Bv8: a novel family of tissue-restricted angiogenic factors. *Biochim. Biophys. Acta* **1654**, 69–78 (2004).
78. Chin, L. & DePinho, R. A. Flipping the oncogene switch: illumination of tumor maintenance and regression. *Trends Genet.* **16**, 147–150 (2000).
79. Felsher, D. W. & Bishop, J. M. Reversible tumorigenesis by MYC in hematopoietic lineages. *Mol. Cell.* **4**, 199–207 (1999).
80. Felsher, D. W. & Bishop, J. M. Transient excess of MYC activity can elicit genomic instability and tumorigenesis. *Proc. Natl Acad. Sci. USA* **96**, 3940–3944 (1999).
81. Shachaf, C. M. *et al*. MYC inactivation uncovers pluripotent differentiation and tumour dormancy in hepatocellular cancer. *Nature* **431**, 1112–1117 (2004).
82. Jang, J. W., Boxer, R. B. & Chodosh, L. A. Isoform-specific ras activation and oncogene dependence during MYC- and Wnt-induced mammary tumorigenesis. *Mol. Cell. Biol.* **26**, 8109–8121 (2006).
83. Folkman, J. & Ryeom, S. Is oncogene addiction angiogenesis-dependent? *Cold Spring Harb. Symp. Quant. Biol.* **70**, 389–397 (2005).
84. Weinstein, I. B. & Joe, A. K. Mechanisms of disease: oncogene addiction — a rationale for molecular targeting in cancer therapy. *Nat. Clin. Pract. Oncol.* **3**, 448–457 (2006).
85. Demetri, G. D. Targeting *c-kit* mutations in solid tumors: scientific rationale and novel therapeutic options. *Semin. Oncol.* **28**, 19–26 (2001).
86. Duensing, A. *et al*. Mechanisms of oncogenic KIT signal transduction in primary gastrointestinal stromal tumors (GISTs). *Oncogene* **23**, 3999–4006 (2004).
87. Ritchie, E. & Nichols, G. Mechanisms of resistance to imatinib in CML patients: a paradigm for the advantages and pitfalls of molecularly targeted therapy. *Curr. Cancer Drug Targets* **6**, 645–657 (2006).
88. Rak, J. *et al*. Oncogenes and tumor angiogenesis: differential modes of vascular endothelial growth factor up-regulation in ras-transformed epithelial cells and fibroblasts. *Cancer Res.* **60**, 490–498 (2000).
89. Rak, J., Yu, J. L., Klement, G. & Kerbel, R. S. Oncogenes and angiogenesis: signaling three-dimensional tumor growth. *J. Investig. Dermatol. Symp. Proc.* **5**, 24–33 (2000).
90. Yoshioka, M. *et al*. Chondromodulin-1 maintains cardiac valvular function by preventing angiogenesis. *Nature Med.* **12**, 1151–1159 (2006).
91. Zorick, T. S. *et al*. High serum endostatin levels in Down syndrome: implications for improved treatment and prevention of solid tumours. *Eur. J. Hum. Genet.* **9**, 811–814 (2001).
92. Hesser, B. A. *et al*. Down syndrome critical region protein 1 (DSCR1), a novel VEGF target gene that regulates expression of inflammatory markers on activated endothelial cells. *Blood* **104**, 149–158 (2004).
93. Lourenco, G. J. *et al*. A high risk of occurrence of sporadic breast cancer in individuals with the 104NN polymorphism of the *COL18A1* gene. *Breast Cancer Res. Treat.* **100**, 335–338 (2006).
94. Sund, M. *et al*. Function of endogenous inhibitors of angiogenesis as endothelium-specific tumor suppressors. *Proc. Natl Acad. Sci. USA* **102**, 2934–2939 (2005).
95. Sommer, A. *et al*. Racial differences in the cause-specific prevalence of blindness in east Baltimore. *N. Engl. J. Med.* **325**, 1412–1417 (1991).
96. Rohan, R. M., Fernandez, A., Udagawa, T., Yuan, J. & D'Amato, R. J. Genetic heterogeneity of angiogenesis in mice. *FASEB J.* **14**, 871–876 (2000).
97. Rogers, M. S., Rohan, R. M., Birsner, A. E. & D'Amato, R. J. Genetic loci that control vascular endothelial growth factor-induced angiogenesis. *FASEB J.* **17**, 2112–2114 (2003).
98. Beecken, W. D. *et al*. Effect of antiangiogenic therapy on slowly growing, poorly vascularized tumors in mice. *J. Natl Cancer Inst.* **93**, 382–387 (2001).
99. Schuch, G., Kisker, O., Atala, A. & Soker, S. Pancreatic tumor growth is regulated by the balance between positive and negative modulators of angiogenesis. *Angiogenesis* **5**, 181–190 (2002).
100. Kisker, O. *et al*. Continuous administration of endostatin by intraperitoneally implanted osmotic pump improves the efficacy and potency of therapy in a mouse xenograft tumor model. *Cancer Res.* **61**, 7669–7674 (2001).
101. Roy, R., Wewer, U. M., Zurakowski, D., Pories, S. E. & Moses, M. A. ADAM 12 cleaves extracellular matrix proteins and correlates with cancer status and stage. *J. Biol. Chem.* **279**, 51323–51330 (2004).
102. In "Washington Post". (February 28, 2004).
103. Satchi-Fainaro, R. *et al*. Inhibition of vessel permeability by TNP-470 and its polymer conjugate, caplostatin. *Cancer Cell.* **7**, 251–261 (2005).
104. Satchi-Fainaro, R. *et al*. Targeting angiogenesis with a conjugate of HPMA copolymer and TNP-470. *Nature Med.* **10**, 255–261 (2004).
105. Pore, N. *et al*. EGFR tyrosine kinase inhibitors decrease VEGF expression by both hypoxia-inducible factor (HIF)-1-independent and HIF-1-dependent mechanisms. *Cancer Res.* **15**, 3197–3204 (2006).
106. Wood, J. *et al*. Novel antiangiogenic effects of the bisphosphonate compound zoledronic acid. *J. Pharmacol. Exp. Ther.* **302**, 1055–1061 (2002).
107. Giraudo, E., Inoue, M., and Hanahan, D. An amino-bisphosphonate targets MMP-9-expressing macrophages and angiogenesis to impair cervical carcinogenesis. *J. Clin. Invest.* **114**, 623–633 (2004).
108. Ferretti, G. *et al*. Zoledronic-acid-induced circulating level modifications of angiogenic factors, metalloproteinases and proinflammatory cytokines in metastatic breast cancer patients. *Oncology* **69**, 35–43 (2005).
109. Santini, D. *et al*. Zoledronic acid induces significant and long-lasting modifications of circulating angiogenic factors in cancer patients. *Clin. Cancer Res.* **9**, 2893–2897 (2003).
110. Boehm, T. *et al*. Antiangiogenic therapy of experimental cancer does not induce acquired drug resistance. *Nature* **390**, 404–407 (1997).
111. Kulke, M.H. *et al*. Phase II study of recombinant human endostatin in patients with advanced neuroendocrine tumors. *J. Clin. Oncol.* **24,** 3555–3561 (2006).
112. Mehta, P. Thalidomide and thrombosis. *Clin. Adv. Hematol. Oncol.* **1**, 464–465 (2003).
113. Fernandez, P. M. & Rickles, F. R. Tissue factor and angiogenesis in cancer. *Curr. Opin. Hematol.* **9**, 401–406 (2002).
114. Jain, R.K. Antiangiogenic therapy for cancer: current and emerging concepts. *Oncology* **9**, 7–16 (2005).
115. Jain, R.K. Normalization of tumor vasculature: an emerging concept in antiangiogenic therapy. *Science* **307**, 58–62 (2006).
116. Teicher, B.A. *et al*. Antiangiogenic agents can increase tumor oxygenation and response to radiation therapy. *Radiat. Oncol. Investig.* **2**, 269–176 (1995).
117. Calabrese, E. J., Staudenmayer, J. W. & Stanek, E. J. Drug development and hormesis: changing conceptual understanding of the dose response creates new challenges and opportunities for more effective drugs. *Curr. Opin. Drug Discov. Devel.* **9**, 117–123 (2006).
118. Slaton, J. W., Perrotte, P., Inoue, K., Dinney, C. P. & Fidler, I. J. Interferon-α-mediated down-regulation of angiogenesis-related genes and therapy of bladder cancer are dependent on optimization of biological dose and schedule. *Clin. Cancer Res.* **5**, 2726–2734 (1999).
119. Celik, I. *et al*. Therapeutic efficacy of endostatin exhibits a biphasic dose-response curve. *Cancer Res.* **65**, 11044–11050 (2005).
120. Tjin Tham Sjin, R. M. *et al*. Endostatin therapy reveals a U-shaped curve for antitumor activity. *Cancer Gene Ther.* (2006).
121. Panigrahy, D. *et al*. PPARγ ligands inhibit primary tumor growth and metastasis by inhibiting angiogenesis. *J. Clin. Invest.* **110**, 923–932 (2002).
122. Kuo, C. J. *et al*. Comparative evaluation of the antitumor activity of antiangiogenic proteins delivered by gene transfer. *Proc. Natl Acad. Sci USA* **98**, 4605–4610 (2001).
123. Marshall, E. Cancer therapy. Setbacks for endostatin. *Science* **295**, 2198–2199 (2002).
124. Folkman, J. Antiangiogenesis in cancer therapy — endostatin and its mechanisms of action. *Exp. Cell Res.* **312**, 594–607 (2006).
125. Hida, K. *et al*. Tumor-associated endothelial cells with cytogenetic abnormalities. *Cancer Res.* **64**, 8249–8255 (2004).
126. Dorrell, M.I., Aguilar, E., Scheppke, L. Barnett, F. H. & Friedlander, M. Combination angiostatic therapy completely inhibits ocular and tumor angiogenesis. *Proc. Natl Acad. Sci. USA* 8 Jan 2007 (doi:10.1073/pnas.0607542104).
127. Kaban, L. B. *et al*. Antiangiogenic therapy of a recurrent giant cell tumor of the mandible with interferon α-2a. *Pediatrics* **103**, 1145–1149 (1999).
128. Marler, J. J. *et al*. Successful antiangiogenic therapy of giant cell angioblastoma with interferon α 2b: report of 2 cases. *Pediatrics* **109**, e37 (2002).
129. Kaban, L. B. *et al*. Antiangiogenic therapy with interferon α for giant cell lesions of the jaws. *J. Oral Maxillofac. Surg.* **60**, 1103–1111 (2002).
130. Folkman, J. *The Harvey Lectures, Series 92, 1996–1997*. 65–82 (John Wiley & Sons, New York, 1998).
131. Browder, T. *et al*. Antiangiogenic scheduling of chemotherapy improves efficacy against experimental drug-resistant cancer. *Cancer Res.* **60**, 1878–1886 (2000).
132. Klement, G. *et al*. Continuous low-dose therapy with vinblastine and VEGF receptor-2 antibody induces sustained tumor regression without overt toxicity. *J. Clin. Invest.* **105**, R15–R24 (2000).
133. Bocci, G., Francia, G., Man, S., Lawler, J. & Kerbel, R. S. Thrombospondin 1, a mediator of the antiangiogenic effects of low-dose metronomic chemotherapy. *Proc. Natl Acad. Sci. USA* **100**, 12917–12922 (2003).
134. Hanahan, D., Bergers, G. & Bergsland, E. Less is more, regularly: metronomic dosing of cytotoxic drugs can target tumor angiogenesis in mice. *J. Clin. Invest.* **105**, 1045–1047 (2000).
135. Kieran, M. W. *et al*. A feasibility trial of antiangiogenic (metronomic) chemotherapy in pediatric patients with recurrent or progressive cancer. *J. Pediatr. Hematol. Oncol.* **27**, 573–581 (2005).
136. Nilsson, U. W. & Dabrosin, C. Estradiol and tamoxifen regulate endostatin generation via matrix metalloproteinase activity in breast cancer *in vivo*. *Cancer Res.* **66**, 4789–4794 (2006).
137. Ma, L., del Soldato, P. & Wallace, J. L. Divergent effects of new cyclooxygenase inhibitors on gastric ulcer healing: shifting the angiogenic balance. *Proc. Natl Acad. Sci. USA* **99**, 13243–13247 (2002).
138. Nagashima, M., Asano, G. & Yoshino, S. Imbalance in production between vascular endothelial growth factor and endostatin in patients with rheumatoid arthritis. *J. Rheumatol.* **27**, 2339–2342 (2000).
139. Kalas, W. *et al*. Restoration of thrombospondin 1 expression in tumor cells harbouring mutant *ras* oncogene by treatment with low doses of doxycycline. *Biochem. Biophys. Res. Commun.* **310**, 109–114 (2003).
140. Carmeliet, P. Angiogenesis in life, disease and medicine. *Nature* **438**, 932–936 (2005).
141. Marx, J. Angiogenesis. A boost for tumor starvation. *Science* **301**, 452–454 (2003).
142. Relf, M. *et al*. Expression of the angiogenic factors vascular endothelial cell growth factor, acidic and basic fibroblast growth factor, tumor growth factor β1 platelet-derived endothelail cell growth factor, placenta growth factor, and pleiotrophin in human primary breast cancer and its relation to angiogenesis. *Cancer Res.* **57(5)**, 963–969 (1997).

Acknowledgements

This work is supported in part by the Breast Cancer Research Foundation, a Department of Defense Innovator Award and a Department of Defense Congressional Award. I thank S. Connors and J. Grillo for help with the manuscript.

Competing interests statement

The author declares no competing financial interests.

DATABASES

The following terms in this article are linked online to:

Entrez Gene:
http://www.ncbi.nlm.nih.gov/entrez/query.fcgi?db=gene
EGFR | FGF2 | KDR | PF4 | PPRγ | PROK2 | TGFα | THBS1 | VEGFA

OMIM:
http://www.ncbi.nlm.nih.gov/entrez/query.fcgi?db=OMIM
Age-related macular degeneration | Alzheimer's disease | chronic myeloid leukaemia | colorectal cancer | Down syndrome | infantile haemangiomas | multiple myeloma | non-small-cell lung cancer | rheumatoid arthritis | testicular cancer

FURTHER INFORMATION

Judah Folkman's homepage: http://www.childrenshospital.org/cfapps/research/data_admin/Site105/mainpageS105P0.html

Access to this links box is available online.

blood

2007 110: 2786-2787
doi:10.1182/blood-2007-08-102178

Endostatin finds a new partner: nucleolin

Judah Folkman

Blood (print ISSN 0006-4971, online ISSN 1528-0020), is published semimonthly by the American Society of Hematology, 1900 M St, NW, Suite 200, Washington DC 20036.

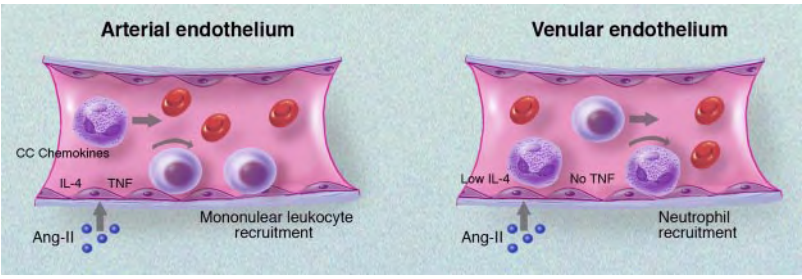

Comparison of angiotensin-II (Ang-II)–mediated leukocyte recruitment in arterioles and venules. In arterioles, high constitutive expression of IL-4 and Ang-II–induced TNF induces expression of CC chemokines such as MCP-1 and RANTES over a time course of several hours. These chemokines mediate selective arrest of mononuclear leukocytes in arterioles. In contrast, in postcapillary venules, Ang-II induces rolling and arrest within 60 minutes, predominantly recruiting neutrophils to the endothelial surface. This process does not require either IL-4 or TNF.

Conflict-of-interest disclosure: The authors declare no competing financial interests. ■

REFERENCES

1. Kunkel EJ, Jung U, Ley K. TNF-alpha induces selectin-mediated leukocyte rolling in mouse cremaster muscle arterioles. Am J Physiol. 1997;272:H1391-H1400.

2. Hickey MJ, Sharkey KA, Sihota EG, et al. Inducible nitric oxide synthase (iNOS)-deficient mice have enhanced leukocyte-endothelium interactions in endotoxemia. FASEB J. 1997;11:955-964.

3. Eriksson EE, Kie X, Werr J, Thoren P, Lindbom L. Direct viewing of atherosclerosis in vivo: plaque invasion by leukocytes is initiated by endothelial selectins. FASEB J. 2001;15:1149-1157.

4. Alvarez A, Cerda-Nicolas M, Naim Abu Nabah Y, et al. Direct evidence of leukocyte adhesion in arterioles by angiotensin II. Blood. 2004;104:402-408.

5. Hickey MJ, Granger DN, Kubes P. Molecular mechanisms underlying IL-4–induced leukocyte recruitment *in vivo*: a critical role for the α_4-integrin. J Immunol. 1999;163:3441-3448.

6. Bernhagen J, Krohn R, Lue H, et al. MIF is a noncognate ligand of CXC chemokine receptors in inflammatory and atherogenic cell recruitment. Nat Med. 2007;13:587-596.

7. Langheinrich AC, Kampschulte M, Buch T, Bohle RM. Vasa vasorum and atherosclerosis - Quid novi? Thromb Haemost. 2007;97:873-879.

8. Mullick AE, Tobias PS, Curtiss LK. Toll-like receptors and atherosclerosis: key contributors in disease and health? Immunol Res. 2006;34:193-209.

HEMOSTASIS

Comment on Shi et al, page 2899

Endostatin finds a new partner: nucleolin

Judah Folkman CHILDREN'S HOSPITAL AT HARVARD MEDICAL SCHOOL

In this issue of *Blood*, Shi and colleagues examine the endostatin binding of nucleolin on angiogenic endothelial cells, as well as the transport of nucleolin to the nucleus, where it prevents proliferation—thus revealing a novel mechanism for endostatin's antiangiogenic activity.

During the past 3 years, 8 new drugs with antiangiogenic activity have received approval from the Food and Drug Administration of the United States for the treatment of cancer and age-related macular degeneration, and have also been approved in more than 30 other countries. These are mainly antibodies, aptamers, or synthetic molecules. They block at least 1 to 3 proangiogenic proteins or their receptors.[1] This new class of drugs has been prescribed for more than 1.2 million patients. More than 50 drugs with antiangiogenic activity are in phase 2 or 3 clinical trials.[2] Since 1980, 28 endogenous angiogenesis inhibitors, including platelet factor 4, angiostatin, endostatin, thrombospondin-1, tumstatin, and canstatin, have been discovered in blood or tissues.[3,4] At this writing, more than 1000 reports on endostatin have been published since its discovery in 1997, and reveal that endostatin has the broadest antitumor spectrum of the endogenous angiogenesis inhibitors. It is also the first endogenous inhibitor to receive approval for anticancer therapy, under the trade name "Endostar" in China.

The integrin $\alpha_5\beta_1$ has been proposed as a receptor for endostatin, and endostatin has been shown to regulate an entire program of antiangiogenic gene expression in human microvascular endothelial cells stimulated by VEGF or bFGF.[5] Nevertheless, certain antiangiogenic actions of endostatin have no molecular explanation and remain as open questions. In this issue of *Blood*, Shi and colleagues address 3 of these questions. Why does endostatin specifically target angiogenic blood vessels, but not quiescent blood vessels? Why does endostatin inhibit tumor angiogenesis with virtually no toxicity in animal studies and clinical trials? Why has the antiangiogenic activity of endostatin appeared to be heparin-dependent in previous studies? These questions are answered by a novel and important finding: that nucleolin is expressed on the surface of proliferating angiogenic human microvascular endothelial cells, but not on the surface of quiescent endothelium. In angiogenic endothelial cells, the cell-surface nucleolin binds endostatin and transports it to the nucleus, where endostatin inhibits phosphorylation of nucleolin. Phosphorylation of nucleolin induced by VEGF or bFGF has been reported to be essential for cell proliferation. Furthermore, endostatin does not inhibit proliferation of many types of tumor cells per se, possibly because while they express nucleolin on their surfaces, they do not internalize it in the presence of endostatin. The heparin binding sites on nucleolin were found to be critical for endostatin. Increasing concentrations of exogenous heparin dissociated the binding of endostatin to nucleolin.

The article by Shi and colleagues is also thought-provoking because the endostatin-nucleolin connection is now fertile soil for future studies. For example, it will be interesting to learn how specific the binding of endostatin is to nucleolin compared with other proteins that also bind to endostatin, as reported by the authors. Furthermore, it will be helpful if the relationship of nucleolin to other cell-surface endostatin-binding proteins can be uncovered, particularly $\alpha_5\beta_1$. Will this endostatin-nucleolin connection lead to the uncovering of a mechanism

for the biphasic, ∪-shaped anticancer dose-response curve recently reported for endostatin,[6] and originally shown for the antiendothelial activity of interferon α?[7] This biphasic dose response is common to other angiogenesis inhibitors. Endostatin increases nucleolin expression in human microvascular endothelial cells in vitro by approximately 20%.[5] Is p53-mediated inhibition of angiogenesis, in part through increased expression of endostatin,[8,9] also regulated by nucleolin? Because the endothelial-cell expression of another endogenous angiogenesis inhibitor, thrombospondin-1, is up-regulated by endostatin, is thrombospondin-1 indirectly nucleolin-dependent? Are any other endogenous angiogenesis inhibitors regulated by binding to nucleolin? Angiogenesis in wound healing and pregnancy is not delayed by high endostatin levels, as for example in individuals with Down syndrome, or in animals receiving endostatin therapy.[10] Is this because proliferating endothelial cells in reproduction and repair do not express nucleolin on their cell surface, or do not internalize it?

The novel role for nucleolin, as a regulator of the antiangiogenic activities of endostatin, has fundamental implications for understanding the biology of endostatin and for its clinical application.

Acknowledgment: I thank Sandra Ryeom and Kashi Javaherian for helpful discussions.

Conflict-of-interest disclosure: The author declares no competing financial interests. ■

REFERENCES

1. Folkman J. Angiogenesis: an organizing principle for drug discovery? Nat Rev Drug Discov. 2007;6:273-286.
2. Davis DW, Herbst RS, Abbruzzese JL, eds. Antiangiogenic Cancer Therapy. Boca Raton, FL: CRC; 2008.
3. Folkman J. Endogenous angiogenesis inhibitors. Acta Pathologica, Microbiologica, et Immunologica Scandinavica. 2004;112:496-507.
4. Nyberg P, Xie L, Kalluri R. Endogenous inhibitors of angiogenesis. Cancer Res. 2005;10:3967-3979.
5. Abdollahi A, Hahnfeldt P, Maercker C, et al. Endostatin's antiangiogenic signaling network. Mol Cell. 2004;13:649-663.
6. Celik I, Surucu O, Dietz C, et al. Therapeutic efficacy of endostatin exhibits a biphasic dose-response curve. Cancer Res. 2005;65:11044-11050.
7. Slaton JW, Perrotte P, Inoue K, Dinney CP, Fidler IJ. Interferon-alpha-mediated down-regulation of angiogenesis-related genes and therapy of bladder cancer are dependent on optimization of biological dose and schedule. Clin Cancer Res. 1999;5:2726-2734.
8. Teodoro JG, Parker AE, Zhu X, Green MR. p53-mediated inhibition of angiogenesis through up-regulation of a collagen prolyl hydroxylase. Science. 2006;313:968-971.
9. Folkman J. Tumor suppression by p53 is mediated in part by the antiangiogenic activity of endostatin and tumstatin. Sci STKE. 2006;354:pe35.
10. Becker CM, Sampson DA, Rupnick MA, et al. Endostatin inhibits the growth of endometriotic lesions but does not affect fertility. Fertil Steril. 2005;84:1144-1155.

HEMATOPOIESIS

Comment on Chen et al, page 2889

Cited2: master regulator of HSC function?

Hal E. Broxmeyer INDIANA UNIVERSITY SCHOOL OF MEDICINE

Defining intracellular molecules involved in hematopoietic stem cell (HSC) function is important for future efforts to enhance transplantation. Toward this aim, Chen and colleagues report that Cited2, a transcriptional modifier, is necessary for mouse fetal liver hematopoiesis.

Understanding intracellular events that mediate functions of hematopoietic stem cells (HSCs) is important for realizing improved efficacy of HSC transplantation. In this issue of *Blood*, Chen and colleagues have advanced this area by demonstrating a new role for Cited2 (cAMP-responsive element–binding protein [CBP]/p300-interacting transactivators with glutamic acid [E] and aspartic acid [D]–rich tail 2)[1] in steady-state embryogenesis.

Gene-expression profiling linked Cited2 expression with long-term marrow HSC activity.[2] However, the current authors had to study Cited2$^{-/-}$ fetal liver hematopoiesis, since functional deletion of Cited2, a member of a new family of transcriptional modulators, results in embryonic lethality.[3] A role for Cited2 in hematopoiesis was shown by the authors in elegant studies demonstrating that Cited2$^{-/-}$ fetal liver was greatly reduced in phenotyped hematopoietic progenitors (HPCs); compromised reconstitution of T- and B-lymphocyte and myeloid cells was apparent after both primary and secondary transplantation of Cited2$^{-/-}$ fetal liver cells, and the competitive repopulating capacity of these HSCs was decreased.

Exactly how Cited2 acts, alone or in combination with other mediators, to regulate normal hematopoiesis is not known. A number of receptor and intracellular signals are reported to modulate HSC and HPC functions.[4] These include Notch and Notch ligands, Wnt signaling, HoxB4/PBX1, Bmi-1, C/EBPα, Gfi-1, p21$^{cip1/waf1}$, p27^{kip1}, PTEN, Nov/CLN3, glycogen synthase kinase-3, ERK1/2- and p38-MAP kinase, ME/ELK4, RAR-γ, Stat3, Stat5, and Mad2. Microarray analysis by Chen and colleagues showed decreased expression of Wnt5a and a panel of myeloid markers in Cited2$^{-/-}$ fetal livers, as well as decreased expression of Bmi-1, Notch, LEF-1, Mcl-1, and GATA-2 in Cited2$^{-/-}$ c-kit^{+} lineage^{-} fetal liver cells. Placing these molecules into correct positions within interacting networks required to properly mediate self-renewal, proliferation, survival, differentiation, and migration of HSCs—and determining where Cited2 fits into this schema—are vital missing pieces of information. For example, which signals are in linear, branching, or completely separate pipelines, and which occupy key regulatory positions in the cascading sequence of events? Do any of these molecules act as a master switch, and is Cited2 a master regulator? What other roles, if any, does Cited2 play in HSC/HPC function and hematopoiesis? The authors propose future studies involving overexpression of genes identified from the current study in Cited2$^{-/-}$ HSCs, and generation of conditional Cited2 knockout mice at specific development stages and in specific hematopoietic lineages. This should bring us closer to knowing what Cited2 does and does not do.

How HSCs renew themselves is still essentially unknown. While investigators continue to dig away, little by little, at this crucial HSC function, it may be that the field needs to be more creative and think out of the box to get a true picture of the renewal of HSCs, which may not occur as we currently envision it. Whatever model or models are eventually identified for renewal of HSCs, it may be that Cited2 will be an important player in these events. We look forward to finding out.

Conflict-of-interest disclosure: The author declares no competing financial interests. ■

In vivo vasculogenic potential of human blood-derived endothelial progenitor cells

Juan M. Melero-Martin,[1] Zia A. Khan,[1] Arnaud Picard,[1] Xiao Wu,[1] Sailaja Paruchuri,[1] and Joyce Bischoff[1]

[1]Vascular Biology Program and Department of Surgery, Children's Hospital, Boston, Harvard Medical School, Boston, MA

Vascularization of tissues is a major challenge of tissue engineering (TE). We hypothesize that blood-derived endothelial progenitor cells (EPCs) have the required proliferative and vasculogenic activity to create vascular networks in vivo. To test this, EPCs isolated from human umbilical cord blood or from adult peripheral blood, and human saphenous vein smooth muscle cells (HSVSMCs) as a source of perivascular cells, were combined in Matrigel and implanted subcutaneously into immunodeficient mice. Evaluation of implants at one week revealed an extensive network of human-specific lumenal structures containing erythrocytes, indicating formation of functional anastomoses with the host vasculature. Quantitative analyses showed the microvessel density was significantly superior to that generated by human dermal microvascular endothelial cells (HDMECs) but similar to that generated by human umbilical vein endothelial cells (HUVECs). We also found that as EPCs were expanded in culture, their morphology, growth kinetics, and proliferative responses toward angiogenic factors progressively resembled those of HDMECs, indicating a process of in vitro maturation. This maturation correlated with a decrease in the degree of vascularization in vivo, which could be compensated for by increasing the number of EPCs seeded into the implants. Our findings strongly support the use of human EPCs to form vascular networks in engineered organs and tissues. (Blood. 2007; 109:4761-4768)

Introduction

Tissue engineering (TE) holds promise as a new approach for creating replacement tissue to repair congenital defects or diseased tissue.[1] One strategy is to seed the appropriate cells on a biodegradable scaffold engineered with the desired mechanical properties, followed by stimulation of cell growth and differentiation in vitro, such that, on implantation in vivo, the engineered construct undergoes remodeling and maturation into functional tissue.[2] Examples of this approach include blood vessels and cardiovascular substitutes, where autologous vascular cells have been used for this purpose without immune rejection.[3-5] Despite advances in this field, TE still faces important constraints. There are no TE constructs presently available that have an inherent microvascular bed ready to be connected to the host vascular system. Consequently, tissues implanted with a volume more than 2 to 3 mm^3 cannot obtain appropriate provision of nutrients, gas exchange, and elimination of waste products since all these mechanisms are limited by the diffusion distance.[6] To overcome the problem of vascularization, strategies such as embedding angiogenic factors into the scaffold to promote ingrowth of microvessels, fabrication technologies to create polymers containing vessel-like networks, and prevascularization of matrices prior to cell seeding have been proposed.[7-11]

The need for prefabricated channels or growth factor–induced angiogenesis could be avoided by exploiting the inherent vasculogenic ability of endothelial cells (ECs). Using human umbilical vein ECs (HUVECs), microvascular networks in collagen/fibronectin gels were formed within 31 days of implantation into immunodeficient mice.[12] Similar results have been reported with human microvascular ECs (HDMECs) seeded on biopolymer matrices, where functional microvessels were evident 7 to 10 days after implantation into mice.[13] Nevertheless, the clinical use of mature ECs derived from autologous vascular tissue presents some important limitations: (1) the isolation relies on an invasive procedure, (2) mature ECs show relatively low proliferative potential, and (3) it is difficult to obtain a sufficient number of cells from a small biopsy of autologous tissue. These limitations have instigated the search for other sources of ECs with more proliferative and vasculogenic activities such as those derived from both embryonic and adult stem and progenitor cells.[14] One recent example showed how seeding of endothelial cells derived from embryonic stem cells along with myoblast and embryonic fibroblasts resulted in the formation of skeletal muscle tissue.[15] However, ethical considerations along with a poor understanding of the mechanisms controlling the differentiation of embryonic stem cells are hurdles that need to be overcome before these cells can be used in a clinical setting.

For clinical applications, the presence of endothelial progenitor cells (EPCs) in circulation represents a promising opportunity to noninvasively obtain the required endothelial population.[16] In previous work, we showed the creation of microvascular networks in vitro using biodegradable scaffolds seeded with EPCs that had been isolated from human umbilical cord blood and expanded in vitro as mature ECs.[17] Using a sheep model, we also showed that blood-derived EPCs could endothelialize small-diameter blood vessels.[5] We now propose that human blood-derived EPCs constitute a robust source of ECs with the potential to form functional

Submitted December 15, 2006; accepted February 5, 2007. Prepublished online as *Blood* First Edition Paper, February 27, 2007; DOI 10.1182/blood-2006-12-062471.

The online version of this article contains a data supplement.

The publication costs of this article were defrayed in part by page charge payment. Therefore, and solely to indicate this fact, this article is hereby marked "advertisement" in accordance with 18 USC section 1734.

capillary networks in vivo. To test this, we used a xenograft model where human cells were mixed in Matrigel and implanted subcutaneously into immunodeficient mice. Our goal was to advance feasibility studies by evaluating the ease with which highly purified and phenotypically defined human EPCs can create microvascular structures that form functional anastomoses with the host vasculature.

Material and methods

Isolation and culture of blood-derived EPCs

Human umbilical cord blood was obtained from the Brigham and Women's Hospital in accordance with an institutional review board–approved protocol. Adult peripheral blood was collected from volunteer donors in accordance with a protocol approved by Children's Hospital Boston Committee on Clinical Investigation and was obtained with informed consent according to the Declaration of Helsinki and under a protocol approved by the Committee on Clinical Investigation. Both cord blood–derived EPCs (cbEPCs) and adult peripheral blood–derived EPCs were obtained from the mononuclear cell (MNC) fractions, in a similar manner as used in previous studies.[18-20] MNCs were seeded on 1% gelatin-coated tissue culture plates using endothelial basal medium (EBM-2) supplemented with SingleQuots (except for hydrocortisone) (Cambrex Bio-Science, Walkersville, MD), 20% FBS (Hyclone, Logan, UT), 1 × glutamine-penicillin-streptomycin (GPS; Invitrogen, Carlsbad, CA), and 15% autologous plasma.[17] Unbound cells were removed at 48 hours for cord blood and at 4 days for adult blood. In both cases, the bound cell fraction was then maintained in culture using EBM-2 supplemented with 20% FBS, SingleQuots (except for hydrocortisone), and 1 × GPS (this medium is referred to as EBM-2/20%). Colonies of endothelial-like cells were allowed to grow until confluence, trypsinized, and purified using CD31-coated magnetic beads (Dynal Biotech, Brown Deer, WI) (Figures S1 and S5, available on the *Blood* website; see the Supplemental Materials link at the top of the online article). CD31-selected EPCs were serially passaged and cultured on fibronectin (FN)–coated (1 μg/cm^2; Chemicon International, Temecula, CA) plates at 5×10^3 cell/cm^2 in EBM-2/20%. HDMECs from newborn foreskin cultured in the same condition as cbEPCs were used as positive controls.[21] Human saphenous vein smooth muscle cells (HSVSMCs) grown in DMEM (Invitrogen), 10% FBS, 1 × GPS, and 1 × nonessential amino acids (Sigma-Aldrich, St Louis, MO) were used as negative controls for endothelial phenotype.

Phenotypic characterization of cbEPCs

Methods for flow cytometry, indirect immunofluorescence, and reverse-transcription–polymerase chain reaction (RT-PCR) are described in Document S1.

In vitro maturation of cbEPCs

Expansion potential of cbEPCs. cbEPCs and adult EPCs, isolated as described in "Isolation and culture of blood-derived EPCs," were expanded for 112 and 60 days, respectively. All passages were performed by plating the cells onto 1 μg/cm^2 FN-coated tissue culture plates at 5×10^3 cell/cm^2 using EBM-2/20%. Medium was refreshed every 2 to 3 days and cells were harvested by trypsinization and replated in the same culture conditions for the next passage. Cumulative values of total cell number were calculated by counting the cells at the end of each passage using a hemocytometer.

Growth kinetics assay. Growth curves of cbEPCs were evaluated at different passages. Cells were plated in triplicates onto 1 μg/cm^2 FN-coated 24-well tissue culture plates at 5×10^3 cell/cm^2 in 0.5 mL EBM-2/20%. Medium was refreshed every 2 days and cell numbers were evaluated at 24-hour intervals for 7 days by counting the cells after trypsinization using a hemocytometer. Doubling time profiles were calculated from the mean values obtained from each growth curve at different passages.[22]

Cell size measurements. Morphologic differences of cbEPCs were evaluated at different passages. Confluent cell monolayers were immunostained with VE-cadherin antibody for cell surface and DAPI for nuclear visualization as described in Document S1. The areas occupied by cell bodies and cell nuclei were measured by analysis (ImageJ software; NIH, Bethesda, MD) of the images obtained from randomly selected fields from 3 separate cultures after immunostaining. All values were normalized to the value of total cell area.

Proliferation assay. Cells were seeded in triplicates onto 1 μg/cm^2 FN-coated 24-well plates at 5×10^3 cell/cm^2 using EMB-2 supplemented with 5% FBS and 1 × GPS (control medium); plating efficiency was determined at 24 hours, then cells were treated for 48 hours using control medium in the presence or absence of either 10 ng/mL VEGF-A (R&D Systems, Minneapolis, MN) or 1 ng/mL bFGF (Roche Applied Science, Indianapolis, IN). Cells were trypsinized and counted using a hemocytometer. Values were normalized to the cell numbers determined at 24 hours.

In vivo vasculogenesis experiments

Matrigel implantations. Unless otherwise indicated, 1.5×10^6 EPCs were mixed with 0.375×10^6 HSVSMCs (4:1 ratio) and resuspended in 200 μL phenol red–free Matrigel (BD Bioscience, San Jose, CA) on ice. The mixture was implanted on the back of a 6-week-old male athymic nu/nu mouse (Charles River Laboratories, Boston, MA) by subcutaneous injection using a 25-gauge needle. One implant was injected per mouse. Each experimental condition was performed with 4 mice.

Histology and immunohistochemistry. Matrigel implants were removed at one week after xenografting, fixed in 10% buffered formalin overnight, embedded in paraffin, and sectioned. Hematoxylin and eosin (H&E)–stained 7-μm–thick sections were examined for the presence of lumenal structures containing red blood cells. For immunohistochemistry, 7-μm–thick sections were deparaffinized, blocked for 30 minutes in 5% horse serum, and incubated with human-specific CD31 monoclonal antibody (1:50; DakoCytomation, Carpinteria, CA), anti–human α-SMA (1:750; Sigma-Aldrich), or mouse IgG (DakoCytomation) for 1 hour at room temperature. Horseradish peroxidase–conjugated secondary antibody and 3,3′-diaminobenzidine (DAB) were used for detection. The sections were counterstained with hematoxylin and mounted using Permount (Fisher Scientific, Hampton, NH). Images were taken with a Nikon Eclipse TE300 (Nikon, Melville, NY) using Spot Advance 3.5.9 software (Diagnostic Instruments, Sterling Heights, MI) and a 10×/0.45 objective lens. Images were assembled into multipanel figures using Adobe Illustrator CS 11.0.0 (Adobe Systems, San Jose, CA).

Microvessel density analysis. Microvessels were detected by the evaluation of H&E-stained sections taken from the middle part of the implants. The full area of each individual section was evaluated. Microvessels were identified and counted as lumenal structures containing red blood cells. The area of each section was estimated by image analysis. Microvessel density was calculated by dividing the total number of red blood cell–filled microvessels by the area of each section (expressed as vessels/mm^2). Values reported for each experimental condition correspond to the average values obtained from 4 individual animals.

Statistical analysis

The data were expressed as means ± SD. Where appropriate, data were analyzed by analysis of variance (ANOVA) followed by 2-tailed Student unpaired *t* tests. *P* values below .05 were considered to indicate a statistically significant difference.

Results

Phenotypic characterization of cbEPCs

We isolated EPCs from the MNC fraction of human umbilical cord blood samples (n = 19) in a similar manner as used in previous studies.[18,19] Cord blood–derived endothelial colonies (identified by typical cobblestone morphology) emerged in culture after one

week (Figure S1). The size, frequency, and time of appearance of these colonies varied as already reported[18] (data not shown). Endothelial colonies were left to grow in the original culture plates until confluence and purified thereafter (at passage 1) by selection of $CD31^+$ cells (Figure S1). This procedure resulted in superior cell yields compared with our previous isolation protocol based on double selection of $CD34^+/CD133^+$ cells from the MNC fraction.[17] However, since CD31 is not a specific marker of EPCs and due to the heterogeneity of blood preparations, both phenotypical and functional characterization were performed. This was especially important considering that earlier studies have shown that some EPC colonies isolated from MNCs contain cells that express the hematopoietic-specific cell-surface antigen CD45,[14,23,24] raising questions about the cellular origin of circulating EPCs.

The endothelial phenotype of the isolated cbEPCs was confirmed by different methods. Flow cytometric analysis of cbEPCs showed remarkably uniform expression of EC markers CD34, VEGF-R2, CD146, CD31, VWF, and CD105 (Figure 1A). In addition, cells were negative for mesenchymal marker CD90 and hematopoietic markers CD45 and CD14, confirming that the cells were not contaminated with either mesenchymal or hematopoietic cells. Additionally, RT-PCR analyses showed the expression of EC markers CD34, VEGF-R2, CD31, VE-cadherin, VWF, and eNOS at the mRNA level (Figure 1B). Indirect immunofluorescent staining was performed to further examine the expression of EC markers. The results showed that cbEPCs expressed CD31, VE-cadherin, and VWF (Figure 1C). Of importance, the localization of CD31 and VE-cadherin at the cell-cell borders and VWF in a punctuate pattern in the cytoplasm showed clear indications of EC properties.

In addition, we tested whether cbEPCs were able to up-regulate leukocyte adhesion molecules in response to the inflammatory cytokine TNF-α. The low-to-undetectable levels of E-selectin, ICAM-1, and VCAM-1 in the untreated cbEPC cultures were up-regulated upon 5 hours of incubation with TNF-α (Figure 1D). This response to an inflammatory cytokine is characteristic of ECs and suggests that the use of cbEPC in the formation of microvascular vessels could also provide physiologic proinflammatory properties.

In summary, this combination of analyses provides a definitive demonstration that the cells isolated from umbilical cord blood were ECs and discards the possibility of hematopoietic/monocytic cells in the culture.[20] Based on the isolation methodology and the phenotypical characteristics, our isolated cells are similar to those referred to by other authors as late EPCs or endothelial outgrowth cells.[19,24] The characterization depicted in Figure 1 corresponded to cbEPCs at passage 6. However, a detailed characterization was performed at passages 4, 9, 12, and 15 with similar results (Figure

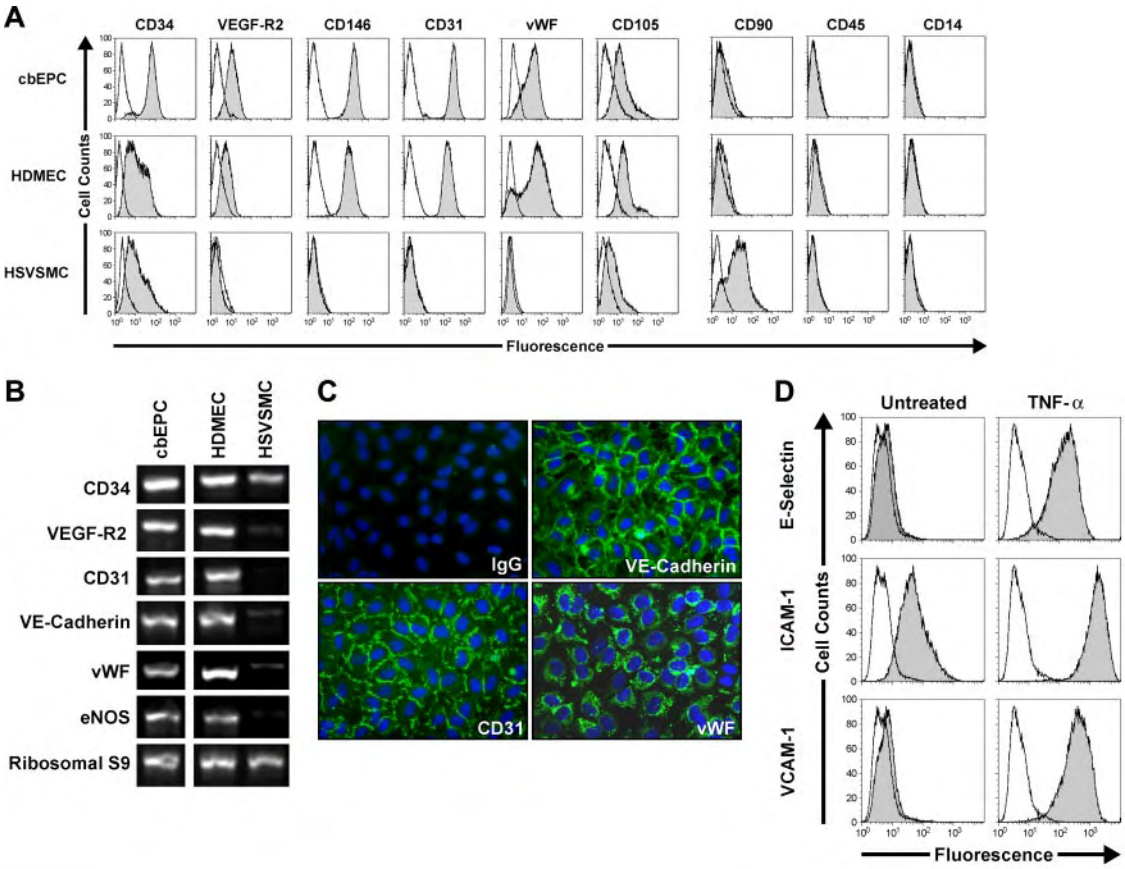

Figure 1. Phenotypic characterization of EPCs. CD31-selected cbEPCs were evaluated at passage 6. HDMECs and HSVSMCs served as positive and negative controls, respectively. (A) Cytometric analysis of cultured cbEPCs for endothelial markers CD34, VEGF-R2, CD146, CD31, VWF, and CD105, the mesenchymal marker CD90, and hematopoietic/monocytic markers CD45 and CD14. Solid gray histograms represent cells stained with fluorescent antibodies. Isotype-matched controls are overlaid in a black line on each histogram. (B) RT-PCR analysis of cbEPCs for endothelial markers CD34, VEGF-R2, CD31, VE-cadherin, VWF, and eNOS (the lanes were rearranged from the same picture to match panel A). (C) Indirect immunofluorescence of cultured cbEPCs grown in confluent monolayer showing positive staining for CD31, VE-cadherin, and VWF. VECTASHIELD mounting medium with 4,6 diamidino-2-phenylindole (DAPI; Vector Laboratories) was used. Images were taken with a Nikon Eclipse TE300 (Nikon, Melville, NY) using Spot Advance 3.5.9 software (Diagnostic Instruments) and a 20×/0.45 objective lens. Images were assembled into multipanel figures using Adobe Illustrator CS 11.0.0. (D) Up-regulation of E-selectin, ICAM-1, and VCAM-1 in cultured cbEPCs in response to TNF-α. Solid gray histograms represent cells stained with fluorescent antibodies, while black lines correspond to the isotype-matched control fluorescent antibodies.

S2A-D), indicating a stable endothelial phenotype through long-term culture. Furthermore, we provide additional characterization of the cbEPCs at passage 6 (Figure S3) to show that cbEPCs express 2 other VEGF receptors, neuropilin-1 and Flt-1 (panel A), and that the cbEPCs do not express the smooth muscle/mesenchymal cell markers PDGF-Rβ (panel B), α-SMA, or calponin (panel C).

In vivo vasculogenic potential of cbEPCs

Our previous work showed the creation of microvascular network in vitro by culturing cbEPCs and HSVSMCs on biodegradable scaffolds.[17] To answer the question of whether cbEPCs were capable of forming functional capillary networks in vivo, we implanted cbEPCs in Matrigel subcutaneously into nude mice for one week. For this experiment, 1.5×10^6 cbEPCs (passage 6) were combined with 0.375×10^6 HSVSMCs in 200 μL Matrigel, resulting in a ratio of cbEPCs to HSVSMCs of 4 to 1, and injected subcutaneously. This ratio of cbEPCs to HSVSMCs was less than the 1:1 ratio previously used,[17] with the intention to minimize the contribution of smooth muscle cells. After harvesting the Matrigel implants, H&E staining revealed the presence of lumenal structures containing murine erythrocytes throughout the implants (Figure 2A). Similar results were obtained with cbEPCs isolated from 3 different cord blood samples, yielding an average of 47.5 ± 8 microvessels/mm^2 (data not shown). Of importance, implants with either cbEPCs or HSVSMCs alone failed to form any detectable microvessels after one week (Figure 2B-C). Injections of Matrigel alone resulted in the appearance of few host cells infiltrated into the borders of the implants (Figure 2D), indicating that Matrigel itself was not responsible for the presence of vascular structures within the implants.

To further characterize the microvascular structures detected, sections of the implant were immunohistochemically stained using a human-specific CD31 antibody. As depicted in Figure 2K, nearly all of the lumenal structures stained positive for human CD31, confirming that those lumens were formed by the implanted human cbEPCs and not by the host cells. This result was important because it demonstrated that the formation of microvascular vessels within the implant is the result of a process of in vivo vasculogenesis carried out by the implanted cells and it is not due to blood vessel invasion and sprouting (ie, an angiogenic response from nearby host vasculature). The specificity of the anti–human CD31 antibody[25,26] was confirmed by the negative reaction obtained when mouse lung tissue sections were stained in parallel (Figure S4). Taken together, the human endothelial identity of the lumenal structures (Figure 2K) and the presence of murine erythrocytes within those structures (Figure 2A,H,J), it was evident that vasculogenesis occurred and, in addition, the newly created microvessels formed functional anastomoses with the host circulatory system. Next, the time course of vasculogenesis in the Matrigel was analyzed by harvesting implants at 2, 4, and 7 days after xenografting. At 2 days, a low degree of cellular organization was seen (Figure 2E). At 4 days, a high degree of organization with clear alignment of cells throughout the implant was observed, suggesting formation of cellular cords (Figure 2F). The presence of functional microvascular vessels, defined by the presence of red blood cells within the lumen, was appreciable one week after implantation (Figure 2G-H,J).

The location of the HSVSMCs was also examined by immunohistochemical staining using anti–α-SMA. Smooth muscle cells were detected both around the lumenal structures and throughout the Matrigel implants (Figure 2L), suggesting an ongoing process of vessel maturation and stabilization.[27-29] However, the α-SMA antibody is not human specific, as shown by the positive staining of control tissue sections obtained from mouse lung (Figure S4). Therefore, the observed α-SMA–positive cells could have corresponded to the implanted HSVSMCs or murine cells recruited from the host, or a combination of these.

Maturation of cbEPCs during in vitro expansion

cbEPCs were serially passaged to determine their expansion potential. Remarkably, 10^{14} cells could theoretically be obtained after only 40 days in culture, and thereafter cells were expanded up to 70 population doublings (Figure 3A), which is consistent with previous studies.[18] Significant expansion of adult blood EPCs (10^8 cells) was also achieved under the same conditions using 50 mL adult peripheral blood (Figure 3A). In addition to this enormous proliferative capacity, cbEPCs expressed and maintained a definitive endothelial phenotype in vitro as shown in Figure 1. However, neither the expansion potential nor the phenotypical stability rules out the possibility of cbEPCs undergoing cellular changes during their expansion in vitro. To investigate potential changes, the growth kinetics of cbEPCs at different passages were examined by the generation of growth curves (Figure 3B). We found that cells from earlier passages presented superior growth kinetics and reached higher cell densities at confluence. The former was

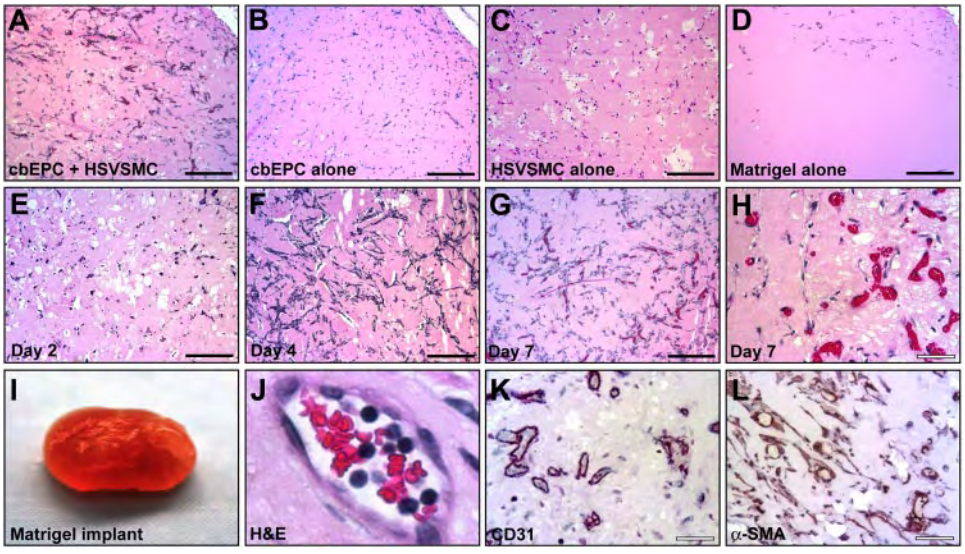

Figure 2. In vivo vasculogenic potential of EPCs. Matrigel implants containing cbEPCs and/or HSVSMCs evaluated after one week. (A) H&E staining of implants (×100) containing a combination of cbEPCs (passage 6) and HSVSMCs, (B) only cbEPCs, (C) only HSVSMCs, (D) and Matrigel alone. H&E staining of implants containing both cbEPCs and HSVSMCs evaluated at day 2 (E), day 4 (F), and day 7 (G, ×100; H, ×400) after xenografting. (I-L) Matrigel plug containing cbEPCs and HSVSMCs harvested one week after implantation. (I) Macroscopic view of explanted Matrigel plug. (J) H&E staining showing high-power view of one microvessel containing hematopoietic cells. (K) Immunohistochemical staining at one week with human-specific CD31 antibody (×400) and with (L) α-SMA antibody. All images are representative of implants harvested from 4 different animals. (Black scale bar represents 250 μm; white scale bar, 50 μm.)

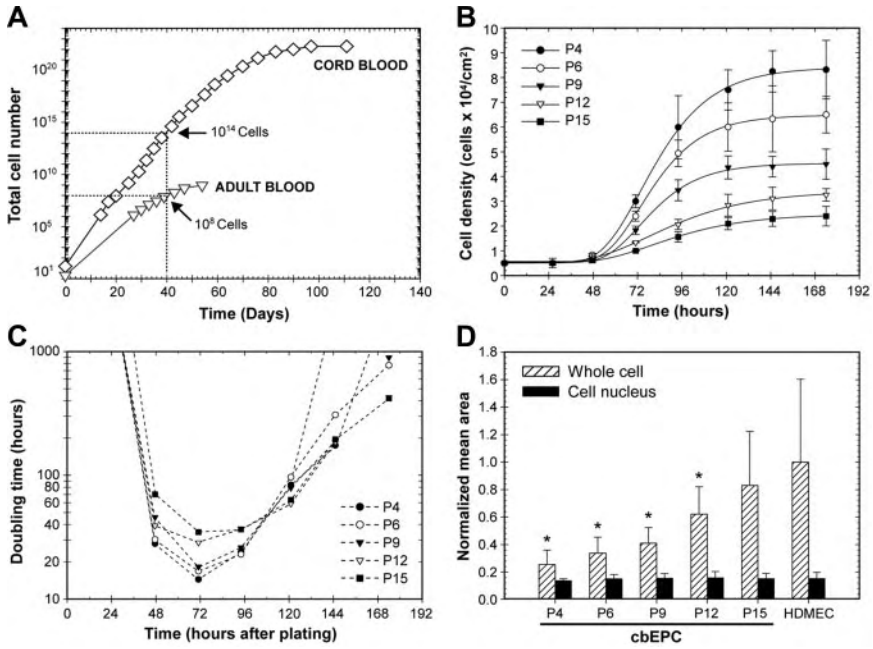

Figure 3. Growth kinetics and in vitro expansion of EPCs. (A) In vitro expansion of cbEPCs and adult blood EPCs isolated from mononuclear cells and purified by $CD31^+$ selection. (B) Growth curves of cbEPCs at different passage numbers (P4, P6, P9, P12, and P15). Each data point represents the mean of 3 separate cultures ± SD. (C) Doubling time profiles of cbEPCs at different passage numbers. Values were calculated from the mean values of cell number obtained at specific time points after plating. (D) Morphologic differences of cbEPCs at increasing passage. Each bar represents the mean area ± SD obtained from randomly selected fields. All values were normalized to the total cell area occupied by HDMECs. *$P < .05$ compared with HDMECs.

confirmed by the generation of the doubling time profiles (Figure 3C), where lower passage number corresponded with shorter doubling times. The u shape of these profiles is the result of mechanisms controlling cell growth in vitro: longer doubling times were found during both the early and late stages of the culture corresponding to the initial lag phase and the inhibition of cell growth by cell-cell contacts, respectively. Taking the minimum values as representative of the dividing capacity, cbEPCs presented minimum doubling times of 14, 17, 18, 29, and 35 hours at passages 4, 6, 9, 12, and 15, respectively. These results illustrated the remarkable dividing capacity of cbEPCs at low passage numbers, and showed that as cbEPCs were expanded in vitro, their growth kinetics progressively slowed.

Serially passaging of cbEPCs also resulted in evident morphologic differences. As they were expanded, cells progressively occupied larger areas in culture (Figure 3D). While the areas occupied by the cell nuclei remained constant at each passage, cbEPCs were found to be significantly ($P < .05$) smaller than the control HDMECs, with the exception of passage 15. As cbEPCs were expanded in vitro, the average area occupied by the cells increased toward that of HDMECs. The mean area of cbEPCs ranged from values 75% smaller than HDMECs at passage 4 to 17% smaller at passage 15. These results were consistent with the differences found in cell density at confluence (Figure 3B).

We next compared the proliferative response of cbEPCs at different passages with stimulation by angiogenic factors VEGF or bFGF (Figure 4). We found that both angiogenic factors produced a proliferative response in all the cases evaluated compared with basal proliferation in the presence of 5% serum (control). The response was statistically significant ($P < .05$) in all the groups treated with bFGF. Of interest, the proliferative response to bFGF was progressively reduced as passage number increased, and ranged from 5.4-fold at passage 4 to 2-fold at passage 15. When compared with HDMECs, the response toward bFGF was found to be significantly higher in cbEPCs at passages 4, 6, and 9, but not in the later passages. In the case of VEGF treatment, the response was statistically significant ($P < .05$) at passages 4 and 6 compared with basal proliferation. Again, the proliferative response was progressively reduced as passage number increased, and varied from 3.1-fold in the earliest passage to 1.3-fold in the latest passage group. Collectively, these in vitro experiments demonstrate that despite the consistent and stable expression of endothelial markers, cbEPCs undergo cellular and functional changes as they are expanded in culture. Their morphology, growth kinetics, and proliferative responses toward angiogenic growth factors progressively resembled those of HDMECs, indicating a process of in vitro cell maturation over time. We showed previously that proliferative responses of HDMECs isolated in our laboratory do not change from passage 3 to 12.[21]

Effect of in vitro expansion of cbEPCs on in vivo vasculogenesis

We next tested whether the maturation of cbEPCs observed during their expansion in vitro has any effect on their vasculogenic ability in vivo. To answer this question, cbEPCs at different passages (3, 6, and 12) were implanted subcutaneously into nude mice in the presence of HSVSMCs. Examination after one week of the

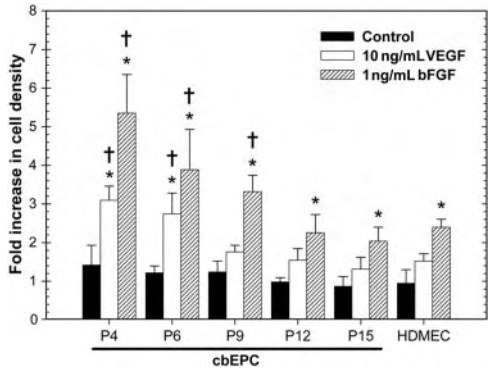

Figure 4. Proliferative response toward angiogenic factors of EPCs. cbEPCs at different passage numbers (P4, P6, P9, P12, and P15) were seeded on FN-coated plates in EMB-2 supplemented with 5% FBS (control medium). After the initial 24-hour period, cells were treated with control medium in the presence or absence of either 10 ng/mL VEGF or 1 ng/mL bFGF and assayed for cell number after 48 hours. Each bar represents the mean of 3 separate cultures ± SD, with values normalized to the values of cell density obtained at 24 hours when treatment began. *$P < .05$ compared with control. †$P < .05$ compared with equivalent treatment on HDMECs.

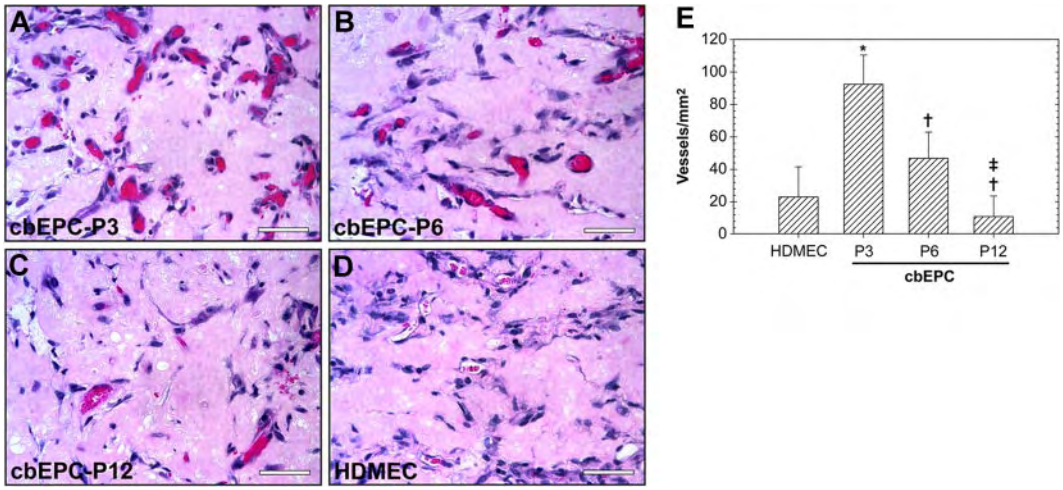

Figure 5. Effect of in vitro expansion of EPCs on in vivo vasculogenesis. Matrigel implants containing cbEPCs and HSVSMCs (4:1 ratio) were evaluated after one week. (A-C) H&E staining of Matrigel implants (× 400) containing cbEPCs at passages 3 (A), 6 (B), and 12 (C). HDMECs implants (with HSVSMCs; 4:1 ratio) were used as control for mature ECs (D; × 400). All images are representative of implants harvested from 4 different animals (scale bar represents 50 μm). (E) Microvessel density in Matrigel implants was quantified by counting lumenal structures containing red blood cells. Each bar represents the mean microvessel density value determined from 4 separated implants and animals ± SD. *$P < .05$ compared with HDMEC. †$P < .05$ compared with cbEPC-P3. ‡$P < .05$ compared with cbEPC-P6.

H&E-stained implants (Figure 5A-D) revealed a difference in the level of in vivo vascularization. Quantification of the red blood cell–containing microvessels (Figure 5E) showed that the differences among the groups were statistically significant ($P < .05$) in all the cases, with values ranging from 93 ± 18 vessels/mm^2 when using cbEPCs at passage 3 to 11 ± 13 vessels/mm^2 with passage 12. These results show that expansion of the cell population in vitro has indeed a significant impact in the subsequent performance in vivo. Parallel evaluation using mature HDMECs also revealed the presence of 23 ± 19 vessels/mm^2. This number of microvessels was inferior to those generated by the earliest passages of cbEPCs (passages 3 and 6), with values significantly higher in the case of cbEPCs at passage 3. In contrast, HUVECs combined with HSVSMCs formed 52 ± 9 vessels/mm^2 (data not shown), indicating a robust vasculogenic potential from this source of ECs.

We tested whether the lower vasculogenic ability observed in expanded cbEPCs could be compensated for by increasing the initial number of EPCs seeded into the implants. To evaluate this, we implanted either 0.5 × 10^6 (referred to as × 1/3), 1.5 × 10^6 (× 1), or 4.5 × 10^6 (× 3) cbEPCs at passages 6 and 12 (Figure 6) in the presence of HSVSMCs at a constant 4:1 ratio. One week after xenografting, examination of the H&E-stained implants (Figure 6A-F) revealed that an increase in the number of cbEPCs resulted in a higher degree of in vivo vascularization. Quantification of the microvessel densities (Figure 6J) showed that the differences among the groups of cbEPCs at passage 6 were statistically

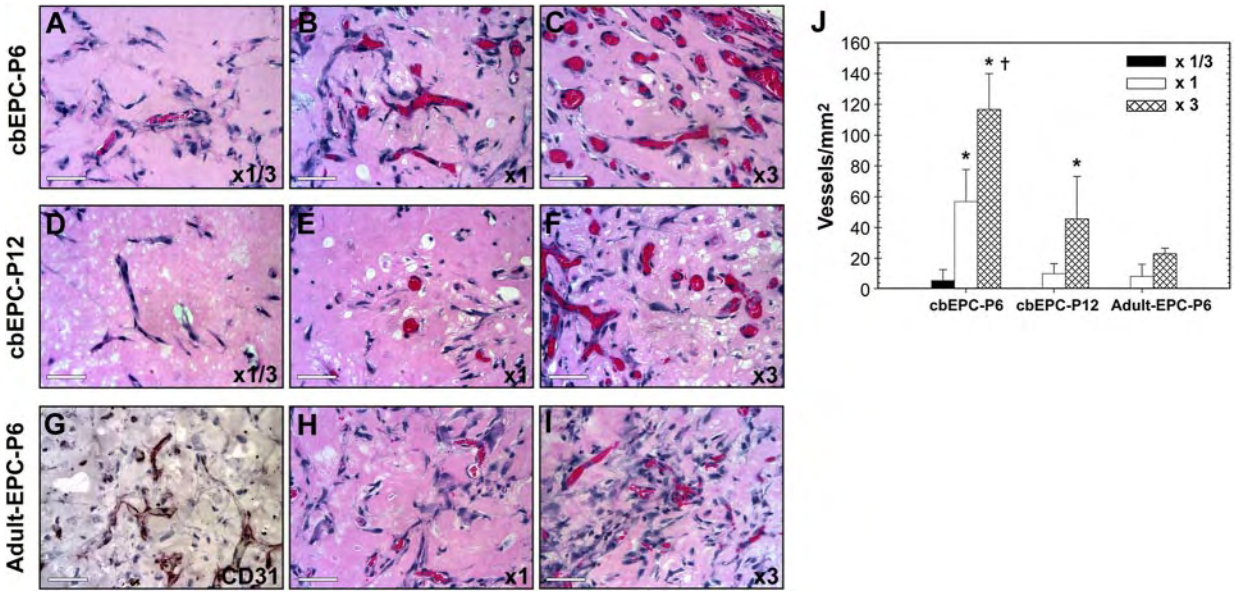

Figure 6. Effect of implanted cell number on vasculogenic performance of EPCs. Matrigel implants containing either 0.5 × 10^6 (× 1/3) (A,D), 1.5 × 10^6 (× 1) (B,E,H), or 4.5 × 10^6 (× 3) (C,F,I) EPCs in the presence of HSVSMCs (4:1 EPCs/HSVSMCs ratio) were evaluated after one week. (A-C) H&E staining of Matrigel implants containing cbEPCs at passage 6 (× 400); (D-F) cbEPCs at passage 12 (× 400); and (G-I) adult EPCs at passage 6 (× 400). (G) Anti–human CD31 immunostained section of adult EPCs at passage 6 seeded at × 3. All images are representative of implants harvested from 4 different animals (scale bar represents 50 μm). (J) Microvessel density was quantified by counting lumenal structures containing red blood cells. Each bar represents the mean microvessel density value determined from 4 separated implants and animals ± SD. *$P < .05$ compared with × 1/3. †$P < .05$ compared with × 1.

significant ($P < .05$), with values ranging from 6 ± 7 vessels/mm^2 to 117 ± 23 vessels/mm^2 when using $\times$ 1/3 or $\times$ 3, respectively. Consistent with the previous results (Figure 5), the values of microvessel density in implants of cbEPCs at passage 6 were always higher than those at passage 12 when the same numbers of cbEPCs were used; indeed no microvessels were detected with $\times$ 1/3 passage 12 cells. Nevertheless, at passage 12, the partial loss of vasculogenic potential was compensated by increasing the number of seeded cells. As seen in Figure 6D-F,J, by simply seeding the implants with 3 times higher density of cbEPCs at passage 12, microvessel density was raised from 10 ± 6 vessels/mm^2 ($\times$ 1) to 46 ± 28 vessels/mm^2 ($\times$ 3). Furthermore, the microvessel level achieved with $\times$ 3 passage 12 cells was similar to the level achieved with passage 6 cells at $\times$ 1 ($P = .56$).

We evaluated whether a similar approach (ie, increasing the number of EPCs seeded) would result in increased vasculogenesis when using EPCs isolated from blood of adult volunteers (Figure S5). To test this, we implanted either 1.5×10^6 ($\times$ 1) or 4.5×10^6 ($\times$ 3) adult EPCs at passage 6 in the presence of HSVSMCs (4:1 ratio). One week after xenografting, examination of the H&E-stained sections (Figure 6H-I) and human CD31-specific immunostaining (Figure 6G) revealed the presence of human microvessels containing red blood cells in both cases. As occurred with cbEPCs, we found that an increase in the number of adult EPCs resulted in a higher degree of in vivo vascularization with values ranging from 8 ± 8 lumens/mm^2 to 23 ± 4 lumens/mm^2 when using $\times$ 1 or $\times$ 3 adult EPCs, respectively. Quantification of the microvessel densities (Figure 6J) showed that adult EPCs at $\times$ 3 was similar to cbEPC-P6 $\times$ 1 ($P = .10$) and cbEPC-P12 $\times$ 3 ($P = .2$). In summary, these in vivo experiments clearly show that in addition to the cellular and functional changes observed in vitro, the vasculogenic ability of expanded EPCs progressively diminished but that this effect can be compensated for by increasing the number of EPCs initially seeded in Matrigel.

Discussion

Tissue vascularization is one of the major challenges to be addressed for the therapeutic success of TE applications. Here, we show that blood-derived EPCs have an inherent vasculogenic ability that can be exploited to create functional microvascular networks in vivo. Implantation of EPCs with HSVSMCs resulted in the formation of an extensive blood vessel network after one week. The presence of human EC-lined lumens containing murine erythrocytes throughout the implants indicated not only a process of vasculogenesis by the implanted cells, but also the formation of functional anastomoses with the host circulatory system. Our results are the first to demonstrate the in vivo vasculogenic potential of blood-derived EPCs in a TE setting. Based on our results, we speculate that microvascular networks could be formed in many types of TE constructs with use of blood-derived EPCs.

Previous investigators have suggested the possibility of creating microvascular networks using mature ECs derived from vascular tissue. Both HUVECs and HDMECs, seeded into collagen/fibronectin gels and biopolymer matrices, respectively, were shown to form complex vascular structures perfused by the host circulation after implantation into immunodeficient mice.[12,13] Alternatively, the use of fat-derived vessel fragments embedded into collagen gels was shown to generate perfused microvessels in immunodeficient mice.[30] Nevertheless, the necessity of invasive procedures together with their limited proliferative and vasculogenic ability represents important constraints for the clinical use of mature ECs derived from autologous vascular tissue.

For therapeutic applications, one critical requisite will be to isolate defined populations of cells so that growth and differentiation can be controlled and regulated during tissue development. Since first identified,[16] EPCs have been isolated from the MNC fraction of blood in numerous studies.[5,18-20,24,31,32] However, their phenotypical characterization has been often controversial.[20] In our study, we show that 10^{11} homogeneous EPCs can be obtained from 25 to 50 mL cord blood after 30 days in culture and 10^8 EPCs from 50 mL adult peripheral blood. These cell numbers are likely to exceed, in the case of cord blood, and be sufficient, in the case of adult blood, what would be needed for most TE applications. Hence, we foresee that adult blood will also be a feasible source of EPCs for autologous TE and regenerative therapies. In summary, this remarkable yield confirms peripheral blood as a robust source of ECs for autologous TE. Furthermore, our data demonstrate that these cells maintain both the expression of endothelial markers and functions through prolonged periods in culture.

As we previously demonstrated in vitro,[17] the presence of vascular smooth muscle cells in the implants was found to be critical. Seeding cbEPCs with HSVSMCs dramatically enhanced the assembly of CD31$^+$ cells into microvessel structures. Although the mechanisms by which the implanted smooth muscle cells facilitate the formation of vascular structures need to be further investigated, this finding is consistent with the extensive literature on endothelium–smooth muscle cell interactions in vascular development.[27-29] In our implants, α-SMA–positive cells were detected both around the lumenal structures and throughout the Matrigel, suggesting an ongoing process of vessel assembly, maturation, and stabilization.[27,28] We are currently investigating alternative sources that could provide autologous smooth muscle cells without the necessity of invasive procedures.

For TE applications, it is of most interest to determine the time course and the sequence of events that leads to the formation of functional microvessels. Time course analyses of the implants revealed that cells appeared dispersed throughout the implant by day 2. Thereafter, cells became organized into tubular structures without red blood cells by day 4, and formed functional erythrocyte-filled microvessels by day 7. Hence, our in vivo model of tissue vascularization is well suited for the study of the physiology of microvessel development and for the investigation of strategies to accelerate neovascularization. We speculate that, in Matrigel, these vessels would regress after some period of time due to the lack of metabolic demand. In future studies, the usefulness of this approach for tissue vascularization will be tested by incorporating EPCs into tissue or organ constructs that require a blood supply.

Another important finding of our study is related to the consequences the in vitro expansion had on vasculogenic ability. In previous work, we reported that far from remaining constant, the migratory capacity of EPCs in vitro decreased over time in culture.[33] Consistent with this concept, we have now shown that as cbEPCs were expanded in culture, their morphology, growth kinetics, and proliferative responses toward angiogenic growth factors progressively resembled those of HDMECs, indicating a process of in vitro cell maturation over time. In addition, this maturation correlated with a decrease in the degree of vascularization in vivo (Figure 5). Even though at first examination this finding may seem to impose a limitation on the extent to which cbEPCs could be expanded in vitro prior to implantation, we showed that the partial loss of vasculogenic ability can be compensated for by increasing the number of EPCs seeded into the implants (Figure 6). The number of EPCs in adult blood is known to be significantly lower than in cord blood,[34] which implies a more extensive expansion in vitro or greater

starting volume will be needed to obtain a sufficient number. In addition, adult EPCs are also known to have an inherently lower proliferative capacity in vitro,[18] which agrees with their lower vasculogenic ability in vivo reported here. Nevertheless, as occurred with cbEPCs after extensive expansion, these apparent limitations were overcome by increasing the number of adult EPCs seeded into the implants (Figure 6). Therefore, we speculate that the in vivo vasculogenic ability of EPCs from cord blood or adult peripheral blood can be modulated to the desired degree of vascularization.

In summary, our results strongly support the therapeutic potential of using human EPCs to form vascular networks that will allow sufficient vascularization of engineered organs and tissues. For infants, other sources such as HUVECs may also be isolated and used for this purpose. Further efforts are required to implement strategies for controlled vasculogenesis in tissue-engineered constructs using both autologous vascular endothelial and smooth muscle cells obtained from adult blood.

Acknowledgments

This work was supported by funding from the US Army Medical Research and Materiel Command (W81XWH-05-1-0115).

We thank Dr M. Aikawa for providing HSVSMCs (Brigham and Women's Hospital) and thank J. Wylie-Sears and T. Bartch for technical assistance.

Authorship

Contribution: J.M.M.-M. designed, executed, and interpreted all experiments and wrote the first draft of the paper; Z.A.K. performed RT-PCR analyses and provided intellectual advice and assistance with all aspects of the animal studies; A.P. contributed intellectual advice and technical assistance with mouse studies; X.W. provided invaluable expertise in the early stages of isolating cord blood cells; S.P. performed analyses of adhesion molecule expression; J.B. was involved in conceptual design of this project, interpretation of experimental results, and writing and editing drafts of the paper and figures.

Conflict-of-interest disclosure: The authors declare no competing financial interests.

Correspondence: Joyce Bischoff, Vascular Biology Research Program and Department of Surgery, Children's Hospital Boston, Harvard Medical School, Boston, MA 02115; e-mail: joyce.bischoff@childrens.harvard.edu.

References

1. Vacanti JP, Langer R. Tissue engineering: the design and fabrication of living replacement devices for surgical reconstruction and transplantation. Lancet. 1999;354(suppl 1):SI32-S134.
2. Langer R, Vacanti JP. Tissue engineering. Science. 1993;260:920-926.
3. Stock UA, Sakamoto T, Hatsuoka S, et al. Patch augmentation of the pulmonary artery with bioabsorbable polymers and autologous cell seeding. J Thorac Cardiovasc Surg. 2000;120:1158-1167; discussion 1168.
4. Hoerstrup SP, Sodian R, Daebritz S, et al. Functional living trileaflet heart valves grown in vitro. Circulation. 2000;102(19 Suppl 3):III44-III49.
5. Kaushal S, Amiel GE, Guleserian KJ, et al. Functional small-diameter neovessels created using endothelial progenitor cells expanded ex vivo. Nat Med. 2001;7:1035-1040.
6. Shieh SJ, Vacanti JP. State-of-the-art tissue engineering: from tissue engineering to organ building. Surgery. 2005;137:1-7.
7. Chrobak KM, Potter DR, Tien J. Formation of perfused, functional microvascular tubes in vitro. Microvasc Res. 2006;71:185-196.
8. Nomi M, Atala A, Coppi PD, Soker S. Principals of neovascularization for tissue engineering. Mol Aspects Med. 2002;23:463-483.
9. Lee H, Cusick RA, Browne F, et al. Local delivery of basic fibroblast growth factor increases both angiogenesis and engraftment of hepatocytes in tissue-engineered polymer devices. Transplantation. 2002;73:1589-1593.
10. Ochoa ER, Vacanti JP. An overview of the pathology and approaches to tissue engineering. Ann N Y Acad Sci. 2002;979:10-26; discussion 35-38.
11. Peters MC, Polverini PJ, Mooney DJ. Engineering vascular networks in porous polymer matrices. J Biomed Mater Res. 2002;60:668-678.
12. Schechner JS, Nath AK, Zheng L, et al. In vivo formation of complex microvessels lined by human endothelial cells in an immunodeficient mouse. Proc Natl Acad Sci U S A. 2000;97:9191-9196.
13. Nor JE, Peters MC, Christensen JB, et al. Engineering and characterization of functional human microvessels in immunodeficient mice. Lab Invest. 2001;81:453-463.
14. Rafii S, Lyden D. Therapeutic stem and progenitor cell transplantation for organ vascularization and regeneration. Nat Med. 2003;9:702-712.
15. Levenberg S, Rouwkema J, Macdonald M, et al. Engineering vascularized skeletal muscle tissue. Nat Biotechnol. 2005;23:879-884.
16. Asahara T, Murohara T, Sullivan A, et al. Isolation of putative progenitor endothelial cells for angiogenesis. Science. 1997;275:964-967.
17. Wu X, Rabkin-Aikawa E, Guleserian KJ, et al. Tissue-engineered microvessels on three-dimensional biodegradable scaffolds using human endothelial progenitor cells. Am J Physiol Heart Circ Physiol. 2004;287:H480-H487.
18. Ingram DA, Mead LE, Tanaka H, et al. Identification of a novel hierarchy of endothelial progenitor cells using human peripheral and umbilical cord blood. Blood. 2004;104:2752-2760.
19. Lin Y, Weisdorf DJ, Solovey A, Hebbel RP. Origins of circulating endothelial cells and endothelial outgrowth from blood. J Clin Invest. 2000;105:71-77.
20. Yoder MC, Mead LE, Prater D, et al. Redefining endothelial progenitor cells via clonal analysis and hematopoietic stem/progenitor cell principals. Prepublished on October 19, 2006, as DOI 10.1182/blood-2006-08-043471. (Now available as Blood. 2007;109:1801-1809.)
21. Kraling BM, Bischoff J. A simplified method for growth of human microvascular endothelial cells results in decreased senescence and continued responsiveness to cytokines and growth factors. In Vitro Cell Dev Biol Anim. 1998;34:308-315.
22. Melero-Martin JM, Dowling MA, Smith M, Al-Rubeai M. Optimal in-vitro expansion of chondroprogenitor cells in monolayer culture. Biotechnol Bioeng. 2006;93:519-533.
23. Rehman J, Li J, Orschell CM, March KL. Peripheral blood "endothelial progenitor cells" are derived from monocyte/macrophages and secrete angiogenic growth factors. Circulation. 2003;107:1164-1169.
24. Gulati R, Jevremovic D, Peterson TE, et al. Diverse origin and function of cells with endothelial phenotype obtained from adult human blood. Circ Res. 2003;93:1023-1025.
25. Parums DV, Cordell JL, Micklem K, Heryet AR, Gatter KC, Mason DY. JC70: a new monoclonal antibody that detects vascular endothelium associated antigen on routinely processed tissue sections. J Clin Pathol. 1990;43:752-757.
26. Levenberg S, Huang NF, Lavik E, Rogers AB, Itskovitz-Eldor J, Langer R. Differentiation of human embryonic stem cells on three-dimensional polymer scaffolds. Proc Natl Acad Sci U S A. 2003;100:12741-12746.
27. Folkman J, D'Amore PA. Blood vessel formation: what is its molecular basis? Cell. 1996;87:1153-1155.
28. Darland DC, D'Amore PA. Blood vessel maturation: vascular development comes of age. J Clin Invest. 1999;103:157-158.
29. Darland DC, D'Amore PA. Cell-cell interactions in vascular development. Curr Top Dev Biol. 2001;52:107-149.
30. Shepherd BR, Chen HY, Smith CM, Gruionu G, Williams SK, Hoying JB. Rapid perfusion and network remodeling in a microvascular construct after implantation. Arterioscler Thromb Vasc Biol. 2004;24:898-904.
31. Shi Q, Rafii S, Wu MH, et al. Evidence for circulating bone marrow-derived endothelial cells. Blood. 1998;92:362-367.
32. Hristov M, Erl W, Weber PC. Endothelial progenitor cells: isolation and characterization. Trends Cardiovasc Med. 2003;13:201-206.
33. Khan ZA, Melero-Martin JM, Wu X, et al. Endothelial progenitor cells from infantile hemangioma and umbilical cord blood display unique cellular responses to endostatin. Blood. 2006;108:915-921.
34. Peichev M, Naiyer AJ, Pereira D, et al. Expression of VEGFR-2 and AC133 by circulating human CD34(+) cells identifies a population of functional endothelial precursors. Blood. 2000;95:952-958.

Engineering vascular networks *in vivo* with human postnatal progenitor cells isolated from blood and bone marrow

Juan M. Melero-Martin [1], Maria E. De Obaldia [1], Soo-Young Kang [1], Zia A. Khan [1], Lei Yuan [2], Peter Oettgen [2], and Joyce Bischoff [1]

[1] Vascular Biology Program and Department of Surgery, Children's Hospital Boston, Harvard Medical School, Boston MA, USA

[2] Division of Cardiology, Beth Israel Deaconess Medical Center, Harvard Medical School, Boston MA, USA

Keywords: Vascular networks; blood vessels; endothelial progenitor cells; mesenchymal stem cells; mesenchymal progenitor cells; tissue engineering; regenerative medicine; vasculogenesis; angiogenesis.

Corresponding Author:
Dr. Joyce Bischoff
Vascular Biology Research Program and Department of Surgery
Children's Hospital Boston
Harvard Medical School
Boston, MA 02115
Tel.: (617) 919-2192
Fax: (617) 730-0231
Email: joyce.bischoff@childrens.harvard.edu

Abstract

The success of therapeutic vascularization and tissue engineering will rely heavily on our ability to create vascular networks *in vivo*, and therefore the search for clinically relevant sources of vasculogenic cells is of utmost importance. Here we describe the formation of functional microvascular beds in immunodeficient mice by co-implantation of human endothelial and mesenchymal progenitor cells (EPCs and MPCs) isolated from blood and bone marrow. Evaluation of implants after one week revealed an extensive network of human blood vessels containing erythrocytes, indicating the rapid formation of functional anastomoses within the host vasculature. The implanted EPCs were restricted to the luminal aspect of the vessels; MPCs were adjacent to lumens, confirming their role as perivascular cells. Importantly, the engineered vascular networks remained patent at 4 weeks *in vivo*. This rapid formation of long-lasting microvascular networks by postnatal progenitor cells obtained from non-invasive sources constitutes an important step forward in the development of clinical strategies for tissue vascularization.

Engineered tissues must have the capacity to generate a vascular network which rapidly anastomoses with the host vasculature in order to guarantee adequate nutrients provision, gas exchange, and elimination of waste products [1]. Currently, there are no tissue-engineered (TE) constructs clinically available with an inherent microvascular bed, and therefore successes have been restricted to the replacement of relatively thin (skin) or avascular (cartilage) tissues, where post-implantation vascularization from the host is sufficient.

To overcome the problem of vascularization, strategies to promote ingrowth of microvessels by delivery of angiogenic molecules have been proposed [2-5]. However, rapid and complete vascularization of thick engineered tissues is likely to require an additional process of vasculogenesis [1, 6]. Towards this goal, the feasibility of engineering microvascular networks *in vivo* have been shown by studies using human umbilical vein ECs (HUVECs) and human microvascular ECs (HDMECs) [7-9]; however, such autologous tissue-derived ECs present problems for wide clinical use, since they are difficult to obtain in sufficient quantities with minimal donor site morbidity. These limitations have instigated the search for other sources of ECs, such as those derived from embryonic and adult stem and progenitor cells [6]. For instance, endothelial cells derived from embryonic stem cells (ESCs) have been used to form blood vessels and to enhance the vascularization of engineered skeletal muscle constructs *in vivo* [10, 11]. However, the mechanisms controlling ESCs differentiation must be

understood, and ethical issues surrounding their use must be resolved prior to their implementation in therapeutic strategies.

The identification of endothelial progenitor cells (EPCs) in blood presented an opportunity to non-invasively obtain ECs [12-14]. We and other authors have shown that adult and cord blood-derived EPCs have the required vasculogenic capacity to form functional vascular networks *in vivo* [15-17]. Importantly, these studies have also shown that in order to obtain stable and durable vascular networks, EPCs require co-implantation with perivascular cells. In our previous work, the role of perivascular cells was undertaken by smooth muscle cells (SMCs) isolated from human saphenous veins [15]. In the work by Au *et al*, the mouse embryonic cell line 10T1/2 served as the perivascular component of the vascular networks [16]. However, neither source is suitable for clinical utilization: harvesting SMCs from healthy vasculature would impose serious morbidity in patients and murine-derived cell lines will not be used in humans. Therefore, to exploit the full vasculogenic potential of EPCs, we set out to establish clinically viable sources of perivascular cells. The ideal perivascular cells must present several key properties: 1) isolation with minimal donor site morbidity; 2) availability in sufficient quantities; and 3) immunological compatibility with the recipients [1]. Mesenchymal stem/progenitor cells (herein referred to as MPCs) [18] meet these requirements. MPCs can be isolated by minimally invasive procedures from a diversity of human tissues, including bone marrow [18], adult blood [19], umbilical cord blood [20-22], and adipose tissue [23]. Furthermore, MPCs undergo self-renewal,

and therefore can potentially be expanded to sufficient quantities for tissue and organ regeneration [24].

Here we demonstrate that MPCs obtained from both human adult bone marrow and human cord blood can serve as perivascular cells for *in vivo* vasculogenesis. Subcutaneous co-implantation of EPCs and MPCs, suspended as single cells in Matrigel, into immunodeficient mice resulted in the creation of extensive microvascular beds that rapidly formed anastomoses with the host vasculature. This study constitutes a step forward in the clinical development of therapeutic vasculogenesis by showing the feasibility of using human postnatal progenitor cells as the basic cellular building blocks to create functional vascular networks *in vivo*.

RESULTS

Isolation of EPCs and MPCs

Cord blood-derived EPCs (cbEPCs) (Fig. 1a) were isolated from the mononuclear cell (MNC) fraction of human umbilical cord blood samples and purified by CD31-selection as previously described (see Supplementary Fig. 1 online for morphology of cbEPCs) [15]. MPCs were isolated from the MNC fractions of both human bone marrow samples (bmMPCs) and human cord blood samples (cbMPCs). bmMPCs adhered rapidly to the culture plates and proliferated until confluent while cbMPCs emerged more slowly, forming mesenchymal-like colonies after one week (Supplementary Fig. 1 online). cbMPC colonies were

selected with cloning rings and expanded. Both bmMPCs (Fig. 1b) and cbMPCs (Fig. 1c) presented spindle morphology characteristic of mesenchymal cells in culture [18].

cbEPCs and MPCs were grown in EPC-medium and MPC-medium respectively and their expansion potentials estimated by the cumulative cell numbers obtained from 25 mL of either cord blood or bone marrow samples after 25, 40 and 60 days in culture (Fig. 1d). Remarkably, up to 10^{13} cbEPCs and 10^{11} bmMPCs were obtained after only 40 days, which is consistent with previous studies [13, 15]. The number of cells continued to increase so that at 60 days there were an estimated 10^{18} cbEPCs and 10^{14} bmMPCs respectively. In the case of cbMPCs, a longer culture period was necessary to obtain a significant cell number. The apparent decreased number of cbMPCs was likely due to the smaller number of MPCs in cord blood samples (typically 1-2 colonies/25 mL; data not shown) as compared to bone marrow samples, where the majority of the adherent cells contributed to the final bmMPC population (Supplementary Fig. 1 online).

The phenotypes of the MPCs were confirmed by three methods. Flow cytometry (Fig. 1e) showed that bmMPCs and cbMPCs uniformly expressed the mesenchymal marker CD90 and were negative for the endothelial marker CD31 and the hematopoietic marker CD45 (see further flow cytometric evaluations in Supplementary Fig. 2 online). As expected, cbEPCs expressed CD31, but not

the mesenchymal and hematopoietic markers. Western blot analyses (Fig. 1f, g) confirmed the endothelial phenotype of cbEPCs (expression of CD31 and VE-cadherin) and the mesenchymal phenotype of bmMPCs and cbMPCs (expression of α-SMA and calponin). These data were extended by indirect immunofluorescent staining (Supplementary Fig. 3 online): bmMPCs and cbMPCs were shown to express the mesenchymal markers α-SMA, calponin, and NG_2 but not the EC markers CD31, VE-cadherin and vWF. Importantly, smooth muscle myosin heavy chain (smMHC), a specific marker of differentiated smooth muscle cells [25, 26], was found in mature SMCs but not in any of the MPCs.

The ability of MPCs to differentiate into multiple mesenchymal lineages was evaluated *in vitro* using well-established protocols [18]. Both bmMPCs and cbMPCs differentiated into osteocytes and chondrocytes as shown by the expression of alkaline phosphatase (osteogenesis; Fig. 2a, b) and glycosaminoglycan deposition in pellet cultures (chondrogenesis; Fig. 2c, d) respectively (see also Supplementary Fig. 4). Adipogenesis was only evident with bmMPCs (Fig. 2e), and not in cbMPCs (Fig. 2f). This loss of adipogenic potential, reported for other mesenchymal cells in culture [27, 28], was attributed to the more extensive expansion that these cells required due to their lower presence in cord blood samples.

Since we intended to test MPCs as perivascular cells to engineer microvessel networks, we evaluated the ability of MPCs to differentiate towards a smooth muscle phenotype. As already shown, MPCs and mature SMCs shared a number of cellular markers including α-SMA, calponin, NG_2, and PDGF-Rβ (Supplementary Fig. 5 online). Although the definitive smooth muscle cell marker smMHC was absent in MPCs (Fig. 2g, h), both bmMPCs and cbMPCs were induced to express smMHC when directly co-cultured with cbEPCs (Fig. 2i, j). Importantly, induction did not occur when MPCs were indirectly co-cultured with cbEPCs using a Transwell culture system (Supplementary Fig. 6 online), consistent with previous reports that showed direct contact with endothelial cells is required for mesenchymal cell differentiation into SMCs [29, 30].

In vivo formation of human vascular networks

We have previously demonstrated the vasculogenic capacity of blood-derived EPCs both *in vitro* and *in vivo* [15, 31]. In these studies, the presence of vascular smooth muscle cells was crucial for formation of vascular networks. To answer the question of whether MPCs could act as perivascular cells, we implanted different combinations of cbEPCs and MPCs (either bmMPCs or cbMPCs) into nude mice for one week (Fig. 3). A total of $1.9x10^6$ cells was resuspended in 200 µl of Matrigel, using ratios of 100:0, 80:20, 60:40, 40:60, 20:80 and 0:100 (% cbEPCs:% MPCs), and injected subcutaneously. After harvesting the Matrigel implants (Fig. 3a-c), Hematoxylin and Eosin (H&E) staining revealed numerous vessels containing murine erythrocytes in implants containing both cbEPCs and

MPCs (Fig. 3e, g). The structures stained positive for human CD31 (Fig. 3d, f), confirming the lumens were lined by the implanted cells (the specificity of the anti-human CD31 antibody is shown in Supplementary Fig. 9 online). Implants of Matrigel alone were devoid of vessels (Supplementary Fig. 7 online) indicating the Matrigel itself was not responsible for the presence of vascular structures. As expected [15], implants with cbEPCs alone (Fig.3h) failed to form microvessels. Implants with only MPCs (Fig. 3i, j) presented infiltration of murine blood capillaries, but no human microvessels (Supplementary Fig. 9 online). The ability of human MPCs to recruit murine vessels into Matrigel may be explained by the secretion of VEGF from MPCs but not cbEPCs (Supplementary Fig. 8 online).

Microvessel density was determined by quantification of lumens containing red blood cells (Fig.3k). The extent of the engineered vascular networks was influenced by the ratio of EPCs to MPCs (Fig. 3k). A progressive increase in MPCs resulted in increased microvessel density and more consistent vascularization (Supplementary Table 1 online). When the ratio of EPC:MPC was 40:60, an average density of 119 ± 33 vessels/mm^2 and 117 ± 32 vessels/mm^2 with bmMPCs or cbMPCs, respectively, was achieved in all implants. These densities were significantly higher (P< 0.05) than those observed with MPCs alone, reaffirming the necessity of the endothelial component for the formation of human vessels in the implants.

Assembly of endothelial and mesenchymal progenitor cells in the vascular bed

In addition to the human CD31-positive lumenal structures, the engineered vessels were characterized by α-SMA staining of perivascular cells (Fig. 4a, b). With bmMPCs or cbMPCs, α-SMA-positive cells were detected both in proximity and adjacent to lumenal structures, suggesting an ongoing process of perivascular cell recruitment during vessel maturation [32-34]. In order to determine more precisely the contribution of each cell type, we implanted GFP-labeled cbEPCs with unlabeled MPCs. Anti-GFP staining clearly showed cbEPCs restricted to lumenal positions in the microvessel networks, while anti-α-SMA staining showed that the GFP-labeled vessels were covered by perivascular cells; this observation was valid with both sources of MPCs (Fig. 4c, d). Projections of whole-mount staining showed that the GFP-expressing cells formed extensive networks throughout the implants (Fig. 4e). Conversely, we implanted GFP-labeled bmMPCs with unlabeled cbEPCs to identify input MPCs without relying on anti-α-SMA. Sections were stained with anti-GFP and anti-CD31 antibodies: GFP-expressing cells were detected as perivascular cells surrounding human CD31+ lumens and as individual cells dispersed throughout the Matrigel implants (Fig. 4f).

Durability of the vascular bed

To test the durability of the engineered vascular beds *in vivo*, we evaluated implants of cbEPCs-bmMPCs (40:60) at 7, 14, 21 and 28 days after xenografting

(Fig. 5). H&E staining revealed the presence of lumenal structures containing erythrocytes in all implants at each time point (Fig. 5a-d). Microvessel quantification (Fig. 5e) revealed an initial reduction (statistically non-significant; P=0.105) in the number of patent blood vessels from 119 ± 33 vessels/mm^2 at day 7 to 83 ± 16 vessels/mm^2 at day 14. Microvessel densities remained stable thereafter (87 ± 21 vessels/mm^2 and 87 ± 32 vessels/mm^2 at days 21 and 28 respectively).

To further evaluate the engineered vascular bed, we used a luciferase-based imaging system to monitor perfusion of the Matrigel implants. cbEPCs were infected with lentivirus-associated vector encoding luciferase and implanted into immunodeficient mice in the presence or absence of bmMPCs. At one week and four weeks, mice were given the substrate, luciferin, by intraperitoneal injection (Fig. 5f). No bioluminescence was detected in implants with luciferase-expressing cbEPC alone, indicating that the substrate did not diffuse into the Matrigel. In contrast, a strong bioluminescent signal was detected in xenografts in which bmMPCs were co-implanted. This result, coupled with parallel histological data, confirmed that the presence of MPCs was crucial to achieve rapid perfusion of the implants. Importantly, the luciferase-dependent signal was still detected 4 weeks after implantation, a further indication of the long-lasting nature of the engineered vessels.

The cells within the Matrigel implants appeared to undergo a process of *in vivo* remodeling characterized by stabilization of total cellularity (Supplementary Fig. 10 online) and progressive restriction of α-SMA-expressing cells to perivascular locations (Fig. 5g-j), as expected in normal stabilized vasculature [34]. Finally, after 28 days *in vivo*, the presence of adipocytes was identified by staining with an anti-perilipin antibody (Supplementary Fig. 11 online), suggesting a process of integration between the implants and the surrounding mouse adipose tissue [35].

Vascular network formation using adult progenitor cells

As with cbEPCs, we previously reported that adult peripheral blood-derived EPCs (abEPCs) combined with mature SMCs at a ratio of 4:1(EPCs:SMCs), are vasculogenic *in vivo*, yet require higher seeding densities to achieve similar microvessel densities to those obtained with cbEPCs [15]. This apparent lower vasculogenic capacity of abEPCs has been reported recently by others [16]. We hypothesized that the combination of adult bmMPCs and abEPCs at an *optimized ratio* (Fig. 3k) would support the vasculogenic activity of abEPCs. Indeed, there are no previous reports on adult bmMPCs and abEPCs in the context of *in vivo* vasculogenesis. To evaluate this interaction, we isolated abEPCs as described [13-15], and confirmed their endothelial phenotype (Supplementary Fig. 12 online).

We then implanted a total of 1.9×10^6 cells (40% abEPCs and 60% bmMPCs) in Matrigel by subcutaneous injection into immunodeficient mice (Fig. 6). After

harvesting the implants at 7 days, H&E staining consistently (n=4) showed an extensive presence of blood vessels containing erythrocytes (Fig. 6a, b). In addition, these lumenal structures stained positive for human CD31 (Fig. 6d), confirming the lumens were formed by the implanted human abEPCs. Quantification of microvessel density (Fig. 6c) revealed that the use of 40% abEPCs resulted in a statistically significant (P<0.05) increase in the number of blood vessels (86 ± 26 vessels/mm^2) as compared to implants with bmMPCs alone (34 ± 25 vessels/mm^2). Moreover, the difference between implants composed of abEPCs:bmMPCs and those of cbEPCs:bmMPCs (119 ± 33 vessels/mm^2) was not statistically significant (P=0.158), indicating that the presence of sufficient number of bmMPCs supported the vasculogenic properties of abEPCs to the same extent as was achieved with cbEPCs.

DISCUSSION

Here, we show that human postnatal EPCs and MPCs isolated from either blood or bone marrow have an inherent vasculogenic ability that can be exploited to create functional microvascular networks *in vivo*. Using Matrigel as a supporting scaffold [15], we have shown that co-implantation of cbEPCs with either bmMPCs or cbMPCs into immunodeficient mice resulted in formation of extensive vascular networks after one week. Matrigel alone was inert. The presence of human EPC-lined lumens containing murine erythrocytes throughout the implants indicated not only a process of vasculogenesis from the two cell types, but also the formation of functional anastomoses with the host circulatory system. In addition,

MPCs were shown to reside in perivascular locations around the engineered lumens, confirming their active participation in blood vessel assembly. The extent of the engineered vascular networks was highly influenced by the ratio of EPCs to MPCs, with a progressive increase in vessel density and consistency of vascularized implants achieved when the contribution of MPCs was raised to 60% (Fig. 3). This was true for both abEPCs and cbEPCs (Fig. 6), demonstrating that both cord blood and adult peripheral blood are excellent sources of endothelial cells for tissue vascularization.

Previous studies suggested the possibility of using mature ECs derived from vascular tissue to create microvascular networks [7-9, 36]. However, the clinical use of mature ECs derived from autologous vascular tissue is limited by the difficulty of obtaining sufficient quantities of cells with minimal donor site morbidity [1]. Human ESCs have unlimited expansion capacity, but the therapeutic use of ESCs-derived ECs remains years away from the clinic. Most of these hurdles would be resolved if postnatal progenitor cells with expansion and functional potential were available from individual patients or from dedicated cell banks. In this regard, the *in vitro* expansion of blood-derived EPCs [12-15] and the recent confirmation of their ability to form vascular networks *in vivo* [15-17] have constituted major steps forward to resolve the problem of EC sourcing for therapeutic vasculogenesis.

Importantly, these studies have also shown that in order to produce high density and stable vascular networks, EPCs require co-implantation with perivascular cells. This is consistent with the substantial literature showing interactions between ECs and perivascular cells in the blood vessel wall are critical for normal vascular development [32-34]. In previous attempts to create vascular networks, either mature SMCs [15] or the mouse embryonic cell line 10T1/2 [16] were used to serve as perivascular cells; however, neither source is suitable for clinical application. Therefore, identification of MPCs as an appropriate perivascular cell source constitutes a crucial step in the development of therapeutic vasculogenesis. The numbers of human MPCs we were able to obtain in this study are likely to exceed, in the case of bone marrow, and be sufficient, in the case of cord blood, what would be needed for most autologous regenerative therapies.

This study has shown that successful *in vivo* vascularization depends on several distinct cellular functions. Firstly, both EPCs and MPCs must be present to initiate vasculogenesis, a process that was characterized by the formation of lumenal structures composed of human EPCs surrounded by α-SMA positive mesenchymal cells. Secondly, an angiogenic response from the host vasculature is needed so that host vessels will be available to form anastomoses with the nascent vasculature. In this regard, we propose that the implanted MPCs stimulated the host angiogenic response. This is based on 1) the ability of bmMPCs alone to recruit murine vessels into the Matrigel implant and 2) the

secretion of VEGF from MPCs in *in vitro* culture (Supplementary Fig. 8 online). EPCs did not secrete VEGF and did not stimulate murine vessel infiltration. Vascularization is achieved when the angiogenic and vasculogenic blood vessels meet, form anastomoses, and establish perfusion of the implants. The fact that perfusion occurred was supported by the presence of erythrocytes within the newly formed vasculature and the delivery of luciferin substrate from the peritoneal cavity to Matrigel implants containing both cbEPCs and bmMPCs. Subsequently, a process reminiscent of *in vivo* remodeling, characterized by a progressive restriction of α-SMA-expressing cells to perivascular locations, was seen, suggesting a normal stabilized vasculature [34]. Finally, our engineered vascular networks were found to remain patent and to maintain their microvessel densities for up to 4 weeks *in vivo*, confirming the capacity of EPC/MPC-derived vasculature to remain stable and functional [16].

In summary, we have demonstrated the feasibility of engineering vascular networks *in vivo* with human postnatal progenitor cells that can be obtained by noninvasive procedures. Our results constitute a major step forward in the development of clinical therapies that rely on vasculogenesis. Further efforts are required to implement these vascularization strategies into tissue regeneration and tissue engineering applications.

METHODS

Isolation and culture of EPCs

Human umbilical cord blood was obtained from the Brigham and Women's Hospital in accordance with an Institutional Review Board-approved protocol. Adult peripheral blood was collected from volunteer donors in accordance with a protocol approved by Children's Hospital Boston Committee on Clinical Investigation. EPCs were isolated from the mononuclear cell (MNC) fractions of both cord blood (cbEPCs; n=19) and adult peripheral blood (abEPCs; n=3) samples, and purified using CD31-coated magnetic beads as previously described [15]. EPCs were subcultured on fibronectin-coated (FN; 1 μg/cm^2; Chemicon International, Temecula, CA) plates using EPC-medium: EGM-2 (except for hydrocortisone; Lonza, Walkersville, MD) supplemented with 20% FBS (Hyclone, Logan, UT), 1x glutamine-penicillin-streptomycin (GPS; Invitrogen, Carlsbad, CA). EPCs between passages 5 and 7 were used for all the experiments.

Isolation and culture of MPCs

bmMPCs were isolated from the MNC fractions of a 25 mL human bone marrow sample (Cambrex Bio Science, Walkersville, MD). MNCs were seeded on 1% gelatin-coated tissue culture plates using EGM-2 (except for hydrocortisone, VEGF, bFGF, and heparin), 20% FBS, 1x GPS and 15% autologous plasma. Unbound cells were removed at 48 hours, and the bound cell fraction maintained in culture until 70% confluence using MPC-medium: EGM-2 (except for hydrocortisone, VEGF, bFGF, and heparin), 20% FBS, and 1x GPS. Commercially available bmMPCs (Cambrex) were used as control to those

isolated in our laboratory. Similarly, cbMPCs were isolated from the MNC fractions of 25 mL human cord blood samples (n=5). Unbound cells were removed at 48 hours, and the bound cell fraction maintained in culture using MPC-medium. cbMPCs emerged in culture forming mesenchymal-like colonies after one week. These cbMPCs colonies were selected with cloning rings and cultured separately from the rest of the adherent cells. Thereafter, both bmMPCs and cbMPCs were subcultured on FN-coated plates using MPC-medium. MPCs between passages 4 and 9 were used for all the experiments.

Cell expansion potential

cbEPCs and MPCs were isolated from 25 mL of either cord blood or bone marrow samples and serially expanded in culture using EPC-medium and MPC-medium respectively. All passages were performed by plating the cells onto 1 μg/cm^2 FN-coated tissue culture plates at either 5x10^3 cell/cm^2 (cbEPCs) or 1x10^4 cell/cm^2 (MPCs). Medium was refreshed every 2-3 days and cells were harvested by trypsinization and re-plated using the same culture conditions for each passage. Cumulative values of total cell number were calculated after 25, 40 and 60 days in culture by counting the cells at the end of each passage using a haemocytometer.

Flow cytometry

Cytometric analyses were carried out by labeling with phycoerythrin (PE)-conjugated mouse anti-human CD31 (Ancell, Bayport, MN), PE- conjugated

mouse anti-human CD90 (Chemicon International), fluorescein isothiocyanate (FITC)-conjugated mouse anti-human CD45 (BD PharMingen, San Jose, CA), FITC-mouse IgG_1 (BD PharMingen), and PE-mouse IgG_1 (BD PharMingen) antibodies (1:100). Antibody labeling was carried out for 20 minutes on ice followed by 3 washes with PBS/1% BSA/0.2 mM EDTA and resuspension in 1% paraformaldehyde in PBS. Flow cytometric analyses were performed using a Becton Dickinson FACScan flow cytometer and FlowJo software (Tree Star Inc., Ashland, OR).

Western blot

Cells were lysed with 4 mol/L urea, 0.5% SDS, 0.5% NP-40, 100 mmol/L Tris, and 5 mmol/L EDTA, pH 7.4, containing a protease inhibitor cocktail Complete Mini tablet (Roche Diagnostics, Indianapolis, IN). Lysates were subjected to 10% SDS-PAGE (10 μg of protein per lane) and transferred to Immobilon-P membrane. Membranes were incubated with respective primary antibodies, goat anti-human CD31 (1:500; Santa Cruz Biotechnology, Santa Cruz, CA), goat anti-human VE-cadherin (1:10,000; Santa Cruz Biotechnology), mouse anti-human α-SMA (1:2000; Sigma-Aldrich, St. Louis, MO), mouse anti-human calponin (1:500; Sigma-Aldrich), and mouse anti-human β-actin (1:10,000; Sigma-Aldrich) diluted in 1x PBS, 5% dry milk, 0.1% Tween-20, and then with secondary antibodies (1:5000; peroxidase-conjugated anti-goat or anti-mouse; Vector Laboratories, Burlingame, CA). Antigen-antibody complexes were visualized using Lumiglo and chemiluminescent sensitive film. SMCs isolated from human saphenous veins

and grown in DMEM, 10% FBS, 1x GPS, and 1x non-essential amino acids served as control.

Osteogenesis assay

Confluent MPCs were cultured for 10 days in DMEM low-glucose medium with 10% FBS, 1X GPS, and osteogenic supplements (1 µM dexamethasone, 10 mM β-glycerophosphate, 60 µM ascorbic acid-2-phosphate). Differentiation into osteocytes was assessed by alkaline phosphatase staining [18].

Chondrogenesis assay

Suspensions of MPCs were transferred into 15 ml polypropylene centrifuge tubes (500,000 cells/tube) and gently centrifuged. The resulting pellets were statically cultured in DMEM high-glucose medium with 1X GPS, and chondrogenic supplements (1X insulin-transferrin-selenium, 1 µM dexamethasone, 100 µM ascorbic acid-2-phosphate, and 10 ng/mL TGF-β1). After 14 days, pellets were fixed in 10% buffered formalin overnight, embedded in paraffin, and sectioned (7 µm-thick). Differentiation into chondrocytes was assessed by evaluating the presence of glycosaminoglycans after Alcian Blue staining. Sections of mouse articular cartilage served as control.

Adipogenesis assay

Confluent MPCs were cultured for 10 days in DMEM low-glucose medium with 10% FBS, 1X GPS, and adipogenic supplements (5 µg/mL insulin, 1 µM

dexamethasone, 0.5 mM isobutylmethylxanthine, 60 µM indomethacin). Differentiation into adipocytes was assessed by Oil Red O staining [18].

Smooth muscle differentiation assay

cbEPCs were co-cultured with either bmMPCs or cbMPCs (1:1 EPCs to MPCs ratio) at a density of $2x10^4$ cell/cm^2 on FN-coated plates using EPC-medium. After 7 days, immunofluorescence was carried out using rabbit anti-human vWF (1:200; DakoCytomation, Carpinteria, CA), and mouse anti-human smooth muscle myosin heavy chain (1:100; Sigma-Aldrich) antibodies, followed by anti-rabbit TexasRed-conjugated, and anti-mouse FITC-conjugated secondary antibodies (1:200; Vector Laboratories). Vectashield with 4,6-diamidino-2-phenylindole (DAPI; Vector Laboratories) was used as mounting medium. Monocultures of MPCs in EPC-medium served as control.

Retroviral transduction of cbEPCs and bmMPCs

GFP-labeled cells were generated by retroviral infection with a pMX-GFP vector using a modified protocol from Kitamura *et al.* [37]. Briefly, retroviral supernatant from HEK 293T cells transfected with Fugene reagent was harvested and both cbEPC and bmMPCs ($1x10^6$ cells) were then incubated with 5 mL of virus stock for 6 hr in the presence of 8 µg/mL polybrene. GFP-expressing cells were sorted by FACS, expanded under routine conditions, and used for *in vivo* vasculogenic assays.

In vivo vasculogenesis assay

The formation of vascular networks *in vivo* was evaluated using a xenograft model as previously described [15]. Briefly, a total of $1.9x10^6$ cells was resuspended in 200 µl of ice-cold Phenol Red-free Matrigel™ (BD Bioscience, San Jose, CA), at ratios of 100:0, 80:20, 60:40, 40:60, 20:80 and 0:100 (EPCs:MPCs). The mixture was implanted on the back of a six-week-old male athymic nu/nu mouse (Massachusetts General Hospital, Boston, MA) by subcutaneous injection using a 25-gauge needle. Implants of Matrigel alone served as controls. One implant was injected per mouse. Each experimental condition was performed with 4 mice.

Histology and immunohistochemistry

Mice were euthanized at different time points and Matrigel implants were removed, fixed in 10% buffered formalin overnight, embedded in paraffin, and sectioned. H&E stained 7 µm-thick sections were examined for the presence of lumenal structures containing red blood cells. For immunohistochemistry, 7-µm-thick sections were deparaffinized, and antigen retrieval was carried out by heating the sections in Tris-EDTA buffer (10mM Tris-Base, 2 mM EDTA, 0.05% Tween-20, pH 9.0). The sections were blocked for 30 minutes in 5-10% blocking serum and incubated with primary antibodies for 1 hour at room temperature. The following primary antibodies were used: mouse anti-human CD31 (for human microvessel detection; 1:20; DakoCytomation, M0823 Clone JC70A; blocking with horse serum), goat anti-human CD31 (for CD31 and α-SMA co-staining; 1:20; Santa Cruz Biotechnology; blocking with rabbit serum), mouse

anti-human α-SMA (1:750; Sigma-Aldrich; blocking with horse serum), rabbit anti-GFP antibody (1:4000; Abcam; blocking with goat serum), and mouse IgG (1:50; DakoCytomation; blocking with horse serum). Secondary antibody incubations were carried out for 1 hour at room temperature using either FITC- or TexasRed-conjugated antibodies (1:200; Vector Laboratories). For CD31 detection, biotinylated IgG /streptavidin-FITC conjugate (1:200; Vector Laboratories) incubations were carried out after primary antibodies. When double staining was performed, the sections were washed and blocked for 30 additional minutes in between the first secondary antibody and the second primary antibody. All the fluorescent-stained sections were counterstained with DAPI (Vector Laboratories). Projections of whole-mount GFP staining were performed on 100-µm-thick sections by confocal microscopy (71 sections over 50 µm). Additionally, horseradish peroxidase-conjugated mouse secondary antibody (1:200; Vector Laboratories) and 3,3'-diaminobenzidine (DAB) were used for detection of α-SMA, followed by hematoxilin counterstaining and Permount mounting.

Microvessel density analysis

Microvessels were quantified by evaluation of 10 randomly selected fields (0.1 mm^2 each) of H&E stained sections taken from the middle part of the implants. Microvessels were identified as lumenal structures containing red blood cells and counted. Microvessels density was reported as the average number of red blood cell-filled microvessels from the fields analyzed and expressed as vessels/mm^2.

Values reported for each experimental condition correspond to the average values ± S.D. obtained from at least four individual mice.

Luciferase assay

cbEPCs were infected with Lenti-pUb-fluc-GFP at a multiplicity of infection (MOI) of 10. The pUb-fluc-GFP was made based on the backbone of pHR-s1-cla. The CMV promoter was replaced by the ubiquitin promoter, followed by a firefly luciferase/GFP fusion gene [38]. Lentivirus was prepared by transient transfection of 293T cells. Briefly, pUb-fluc-GFP was cotransfected into 293T cells with HIV-1 packaging vector and vesicular stomatitis virus G glycoprotein-pseudotyped envelop vector (pVSVG). Collected supernatant was filtered using a syringe filter (0.45 µm) and concentrated by centrifuging at 5000g for 2 hours. The virus was titrated on 293T cells. The infectivity was determined by GFP expression and luciferase/GFP-expressing cbEPCs were further sorted by FACS, expanded under routine conditions, and used for *in vivo* vasculogenic assays. Luciferase/GFP-expressing cbEPCs were resuspended in 200 µl of Matrigel in the presence (40% cbEPC:60% bmMPCs) or absent of bmMPCs, at a total of $1.9x10^6$ cells. The mixture was implanted on the back of a six-week-old male nu/nu mouse by subcutaneous injection. One implant was injected per mouse. Each experimental condition was performed with 4 mice. At various intervals after implantation, the mice were imaged using an IVIS 200 Imaging System (Xenogen Corporation, Alameda, CA). Mice were anesthetized using an isofluorane chamber and were given the substrate, luciferin (2.5 mg/mL), by

intraperitoneal injection according to their weights (typically 250 µl/30 gr). Bioluminescence was detected in implants 30-40 min after luciferin administration, and the collected data analyzed with Live Image 3.0 (Xenogen Corporation).

Microscopy

Phase microscopy images were taken with a Nikon Eclipse TE300 inverted microscope (Nikon, Melville, NY) using Spot Advance 3.5.9 software (Diagnostic Instruments, Sterling Heights, MI) and 10x/0.3 objective lens. All fluorescent images were taken with a Leica TCS SP2 Acousto-Optical Beam Splitter confocal system equipped with DMIRE2 inverted microscope (Diode 405 nm, Argon 488 nm, HeNe 594 nm; Leica Microsystems, Wetzlar, Germany) using either 20x/0.7 imm, 63x/1.4 oil, or 100x/1.4 oil objective lens. Non-fluorescent images were taken with a Axiophot II fluorescence microscope (Zeiss, Oberkochen, Germany) equipped with AxioCam MRc5 camera (Zeiss) using either 2.5x/0.075 or 40x/1.0 oil objective lens.

Statistical analysis

The data were expressed as means ± SD. Where appropriate, analysis of variance (ANOVA) followed by two-tailed Student's unpaired t-tests were performed. *P* value < 0.05 was considered to indicate a statistically significant difference.

FIGURES LEGENDS

Figure 1. Phenotypic characterization of EPCs and MPCs.

(a) cbEPCs presented typical cobblestone morphology, while both (b) bMPCs and (c) cbMPCs presented spindle morphology characteristic of mesenchymal cells in culture (scale bars, 100 μm). (d) cbEPCs and MPCs were serially passaged and their *in vitro* expansion potential estimated by the accumulative cell numbers obtained from 25 mL of either cord blood or bone marrow samples after 25, 40 and 60 days in culture. (e) Flow cytometric analysis of cbEPCs, bmMPCs and cbMPCs for the endothelial marker CD31, mesenchymal marker CD90, and hematopoietic marker CD45. Solid gray histograms represent cells stained with fluorescent antibodies. Isotype-matched controls are overlaid in a black line on each histogram. Western blot analyses of cbEPCs, bmMPCs and cbMPCs for (f) endothelial markers CD31, and VE-cadherin, and (g) mesenchymal markers α-SMA, and Calponin. Expression of β-actin shows equal protein loading. SMCs isolated from human saphenous vein served as control.

Figure 2. Multilineage differentiation of MPCs.

(a) bmMPCs and (b) cbMPCs differentiation into osteocytes was revealed by alkaline phosphatase staining. (c) bmMPCs and (d) cbMPCs differentiation into chondrocytes was revealed by the presence of glycosaminoglycans, detected by Alcian Blue staining. The presence of adipocytes was assessed by Oil Red O staining, and it was evident in (e) bmMPCs, but absent in (f) cbMPCs. Smooth

muscle cell differentiation was evaluated by culturing MPCs in the absence or presence of cbEPCs (1:1 EPCs to MPCs ratio) for 7 days in EPC-medium. Induction of SMC phenotype was assessed by the expression of smMHC. Immunofluorescence staining with anti-vWF-Texas-Red and anti-smMHC-FITC, as well as nuclear staining with DAPI, revealed that smMHC was absent in both (g) bmMPCs and (h) cbMPCs, but it was induced in MPCs when co-cultured with cbEPCs (i, j). All scale bars correspond to 50 μm.

Figure 3. Formation of vascular networks *in vivo* with EPCs and MPCs.

A total of $1.9x10^6$ cells was resuspended in 200 μl of Matrigel using different ratios of cbEPCs and MPCs, and implanted on the back of six-week-old nu/nu mice by subcutaneous injection. Implants were harvested after 7 days and prepared for histological examination. (a, b) Macroscopic view of explanted Matrigel plugs seeded with 40% cbEPCs:60% bmMPCs and (c) 40% cbEPCs:60% cbMPCs (scale bars, 5 mm). (e, g) H&E staining revealed the presence of lumenal structures containing murine erythrocytes (yellow arrow heads) in implants where both cells types (cbEPCs and MPCs; 40:60) were used, but not in implants where (h) cbEPCs, (i) bmMPCs, and (j) cbMPCs were used alone (scale bars, 50 μm). Microvessels stained positive for human CD31 (d, f) (scale bars, 30 μm). Images are representative of implants harvested from at least four different mice. (k) Quantification of microvessel density was performed by counting erythrocyte-filled vessels in implants with ratios of 100:0, 80:20, 60:40, 40:60, 20:80 and 0:100 (cbEPCs:MPCs; n≥4 each condition). Each

bar represents the mean ± S.D. (vessels/mm^2) obtained from vascularized implants. * $P < .05$ compared to implants with bmMPCs alone (n=4). † $P < .05$ compared to implants with cbMPCs alone (n=4).

Figure 4. Specific location of EPCs and MPCs in the vascular bed.

Matrigel implants containing cbEPCs and MPCs (40:60 ratio) were evaluated after one week. Implants with (a) bmMPCs and (b) cbMPCs produced lumenal structures that stained positive for human CD31, confirming that those lumens were formed by the implanted cells. In addition, α-SMA-expressing cells were detected both in the proximity (white arrows) and around the lumenal structures (white arrow heads), (scale bars, 50 μm). Implants that utilized GFP-labeled cbEPC and either (c) bmMPCs or (d) cbMPCs produced GFP-positive lumenal structures (white arrow heads) covered by α-SMA-expressing perivascular cells, confirming that cbEPCs were restricted to the luminal aspect of the vessels (scale bars, 30 μm). (e) Projections of whole-mount staining showed that the GFP-expressing cells formed extensive networks throughout the implants (scale bar 100 μm). (f) Implants that utilized GFP-labeled bmMPC and unlabeled cbEPCs resulted in human CD31-positive lumenal structures with GFP-expressing cells adjacent to lumens (white arrow heads), confirming the role of MPCs as perivascular cells (scale bars, 50 μm). Images are representative of implants harvested from four different mice.

Figure 5. Durability of the vascular bed.

Matrigel implants containing cbEPCs and bmMPCs (40:60 ratio) were injected subcutaneously on the back of six-week-old nu/nu mice. H&E staining showed lumenal structures containing murine erythrocytes (yellow arrow heads) in implants after (a) 7, (b) 14, (c) 21, and (d) 28 days (scale bars, 50 μm; macroscopic view of explanted Matrigel plugs shown in insets; insets scale bars, 5 mm). (e) Quantification of microvessel density was performed by counting erythrocyte-filled vessels. Each bar represents the mean microvessel density value determined from four separate implants and mice ± S.D. (vessels/mm^2). (f) Additional implants were prepared with luciferase-labeled cbEPC in the presence or absence of unlabeled bmMPCs. Mice were imaged using an IVIS Imaging System, and bioluminescence detected 30-40 min after intraperitoneal injection of luciferin. In implants where cbEPCs and bmMPCs were co-implanted, bioluminescence was detected at 1 (image Min=-2.91x10^4., Max=2.67x10^5) and 4 (image Min=-3.29x10^4., Max=3.27x10^5) weeks, but not in those where cbEPCs were used alone. Immunohistochemical staining of α-SMA in implants after (g) 7, (h) 14, (i) 21, and (j) 28 days, revealed that α-SMA-expressing cells were progressively restricted to perivascular locations (black arrow heads), (scale bars, 50 μm). Images are representative of implants harvested from four different mice.

Figure 6. Vascular network formation using adult progenitor cells.

Matrigel implants containing 40% abEPCs and 60% bmMPCs (obtained from human adult peripheral blood and adult bone marrow samples respectively) were

injected subcutaneously on the back of six-week-old nu/nu mice and evaluated after one week. (a, b) H&E staining showed an uniform and extensive presence of lumenal structures containing murine erythrocytes (yellow arrow heads) throughout the implants (a scale bar, 500 μm; macroscopic view of explanted Matrigel plug shown in inset; inset scale bar, 5 mm; b scale bar, 50 μm). (c) Quantification of microvessel density was performed in implants seeded with bmMPCs in the absence or presence of either abEPCs or cbEPCs by counting erythrocyte-filled vessels. Each bar represents the mean microvessel density determined from four separate implants and mice ± S.D. (vessels/mm^2). * $P < .05$ compared to implants with bmMPCs alone (n=4). (d) Microvessels from implants containing 40% abEPCs and 60% bmMPCs stained positive for human CD31 (white arrow heads), confirming that those lumens were formed by the implanted cells (scale bars, 30 μm). Images are representative of implants harvested from four different mice.

ACKNOWLEDGMENTS

We thank Dr. Joseph C. Wu for providing construct of pUb-fluc-GFP (Department of Radiology and Molecular Imaging Program at Stanford, Stanford University School of Medicine), Dr. Masanori Aikawa for providing SMCs (Brigham and Women's Hospital), Elke Pravda for the confocal microscope imaging, Sandra R. Smith for VEGF analysis, Jill Wylie-Sears for technical assistance, and Kristin Johnson for figures preparation. This research was supported by funding from the US Army Medical Research and Materiel Command (W81XWH-05-1-0115).

AUTHOR CONTRIBUTIONS

J.M.M.-M. designed, executed and interpreted all experiments and wrote the first draft of the paper. M.E.D.O., contributed immunohistochemistry and technical assistance; S.-Y.K. contributed retroviral transduction and technical assistance with mouse studies; Z.A.K. contributed intellectual advice and technical assistance with mouse studies; L.Y. contributed lentiviral transduction; P.O. involved in conceptual design of lentiviral transduction and luciferase assay; J.B. was involved in conceptual design of this project, interpretation of experimental results, and writing and editing drafts of the manuscript and figures.

COMPETING INTERESTS STATEMENT

The authors declare that they have no competing financial interest.

REFERENCES

1. Jain, R.K., Au, P., Tam, J., Duda, D.G. & Fukumura, D. Engineering vascularized tissue. *Nat Biotechnol* **23**, 821-823 (2005).

2. Isner, J.M. & Asahara, T. Angiogenesis and vasculogenesis as therapeutic strategies for postnatal neovascularization. *J Clin Invest* **103**, 1231-1236 (1999).

3. Isner, J.M. et al. Clinical evidence of angiogenesis after arterial gene transfer of phVEGF165 in patient with ischaemic limb. *Lancet* **348**, 370-374 (1996).

4. Lee, H. et al. Local delivery of basic fibroblast growth factor increases both angiogenesis and engraftment of hepatocytes in tissue-engineered polymer devices. *Transplantation* **73**, 1589-1593 (2002).

5. Li, X. et al. Revascularization of ischemic tissues by PDGF-CC via effects on endothelial cells and their progenitors. *J Clin Invest* **115**, 118-127 (2005).

6. Rafii, S. & Lyden, D. Therapeutic stem and progenitor cell transplantation for organ vascularization and regeneration. *Nat Med* **9**, 702-712 (2003).

7. Koike, N. et al. Tissue engineering: creation of long-lasting blood vessels. *Nature* **428**, 138-139 (2004).

8. Nor, J.E. et al. Engineering and characterization of functional human microvessels in immunodeficient mice. *Lab Invest* **81**, 453-463 (2001).

9. Schechner, J.S. et al. In vivo formation of complex microvessels lined by human endothelial cells in an immunodeficient mouse. *Proc Natl Acad Sci U S A* **97**, 9191-9196 (2000).

10. Levenberg, S. et al. Engineering vascularized skeletal muscle tissue. *Nat Biotechnol* **23**, 879-884 (2005).

11. Wang, Z.Z. et al. Endothelial cells derived from human embryonic stem cells form durable blood vessels in vivo. *Nat Biotechnol* **25**, 317-318 (2007).

12. Asahara, T. et al. Isolation of putative progenitor endothelial cells for angiogenesis. *Science* **275**, 964-967 (1997).

13. Ingram, D.A. et al. Identification of a novel hierarchy of endothelial progenitor cells using human peripheral and umbilical cord blood. *Blood* **104**, 2752-2760 (2004).

14. Lin, Y., Weisdorf, D.J., Solovey, A. & Hebbel, R.P. Origins of circulating endothelial cells and endothelial outgrowth from blood. *J Clin Invest* **105**, 71-77 (2000).

15. Melero-Martin, J.M. et al. In vivo vasculogenic potential of human blood-derived endothelial progenitor cells. *Blood* **109**, 4761-4768 (2007).

16. Au, P. et al. Differential in vivo potential of endothelial progenitor cells from human umbilical cord blood and adult peripheral blood to form functional long-lasting vessels. *Blood* (2007).

17. Yoder, M.C. et al. Redefining endothelial progenitor cells via clonal analysis and hematopoietic stem/progenitor cell principals. *Blood* **109**, 1801-1809 (2007).

18. Pittenger, M.F. et al. Multilineage potential of adult human mesenchymal stem cells. *Science* **284**, 143-147 (1999).

19. Simper, D., Stalboerger, P.G., Panetta, C.J., Wang, S. & Caplice, N.M. Smooth muscle progenitor cells in human blood. *Circulation* **106**, 1199-1204 (2002).

20. Kim, J.W. et al. Mesenchymal progenitor cells in the human umbilical cord. *Ann Hematol* **83**, 733-738 (2004).

21. Le Ricousse-Roussanne, S. et al. Ex vivo differentiated endothelial and smooth muscle cells from human cord blood progenitors home to the angiogenic tumor vasculature. *Cardiovasc Res* **62**, 176-184 (2004).

22. Lee, O.K. et al. Isolation of multipotent mesenchymal stem cells from umbilical cord blood. *Blood* **103**, 1669-1675 (2004).

23. Traktuev, D. et al. A Population of Multipotent CD34-Positive Adipose Stromal Cells Share Pericyte and Mesenchymal Surface Markers, Reside in a Periendothelial Location, and Stabilize Endothelial Networks. *Circ Res* (2007).

24. Marion, N.W. & Mao, J.J. Mesenchymal stem cells and tissue engineering. *Methods Enzymol* **420**, 339-361 (2006).

25. Madsen, C.S. et al. Smooth muscle-specific expression of the smooth muscle myosin heavy chain gene in transgenic mice requires 5'-flanking and first intronic DNA sequence. *Circ Res* **82**, 908-917 (1998).

26. Miano, J.M., Cserjesi, P., Ligon, K.L., Periasamy, M. & Olson, E.N. Smooth muscle myosin heavy chain exclusively marks the smooth muscle lineage during mouse embryogenesis. *Circ Res* **75**, 803-812 (1994).

27. Digirolamo, C.M. et al. Propagation and senescence of human marrow stromal cells in culture: a simple colony-forming assay identifies samples with the

greatest potential to propagate and differentiate. *Br J Haematol* **107**, 275-281 (1999).

28. Wall, M.E., Bernacki, S.H. & Loboa, E.G. Effects of serial passaging on the adipogenic and osteogenic differentiation potential of adipose-derived human mesenchymal stem cells. *Tissue Eng* **13**, 1291-1298 (2007).

29. Antonelli-Orlidge, A., Saunders, K.B., Smith, S.R. & D'Amore, P.A. An activated form of transforming growth factor beta is produced by cocultures of endothelial cells and pericytes. *Proc Natl Acad Sci U S A* **86**, 4544-4548 (1989).

30. Hirschi, K.K., Rohovsky, S.A. & D'Amore, P.A. PDGF, TGF-beta, and heterotypic cell-cell interactions mediate endothelial cell-induced recruitment of 10T1/2 cells and their differentiation to a smooth muscle fate. *J Cell Biol* **141**, 805-814 (1998).

31. Wu, X. et al. Tissue-engineered microvessels on three-dimensional biodegradable scaffolds using human endothelial progenitor cells. *Am J Physiol Heart Circ Physiol* **287**, H480-487 (2004).

32. Darland, D.C. & D'Amore, P.A. Blood vessel maturation: vascular development comes of age. *J Clin Invest* **103**, 157-158 (1999).

33. Folkman, J. & D'Amore, P.A. Blood vessel formation: what is its molecular basis? *Cell* **87**, 1153-1155 (1996).

34. Jain, R.K. Molecular regulation of vessel maturation. *Nat Med* **9**, 685-693 (2003).

35. Fukumura, D. et al. Paracrine regulation of angiogenesis and adipocyte differentiation during in vivo adipogenesis. *Circ Res* **93**, e88-97 (2003).

36. Shepherd, B.R. et al. Rapid perfusion and network remodeling in a microvascular construct after implantation. *Arterioscler Thromb Vasc Biol* **24**, 898-904 (2004).

37. Kitamura, T. et al. Efficient screening of retroviral cDNA expression libraries. *Proc Natl Acad Sci U S A* **92**, 9146-9150 (1995).

38. Wu, J.C. et al. Proteomic analysis of reporter genes for molecular imaging of transplanted embryonic stem cells. *Proteomics* **6**, 6234-6249 (2006).

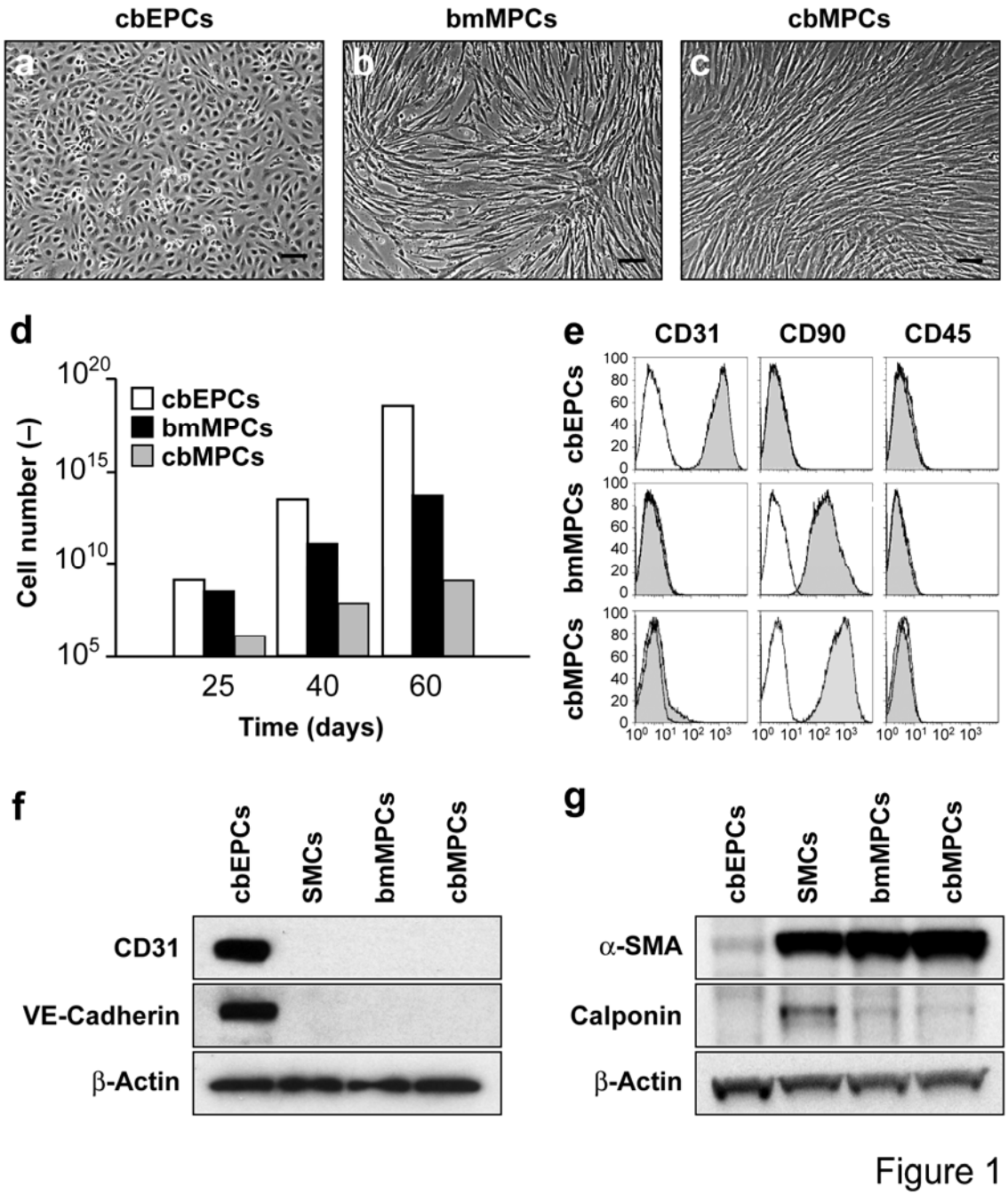
cbEPCs
bmMPCs
cbMPCs
a
b
c
d
Cell number (–)
10^{20}
10^{15}
10^{10}
10^{5}
cbEPCs
bmMPCs
cbMPCs
25
40
60
Time (days)
e
CD31
CD90
CD45
cbEPCs
bmMPCs
cbMPCs
100
80
60
40
20
0
10^0 10^1 10^2 10^3
f
cbEPCs
SMCs
bmMPCs
cbMPCs
CD31
VE-Cadherin
β-Actin
g
cbEPCs
SMCs
bmMPCs
cbMPCs
α-SMA
Calponin
β-Actin

Figure 1

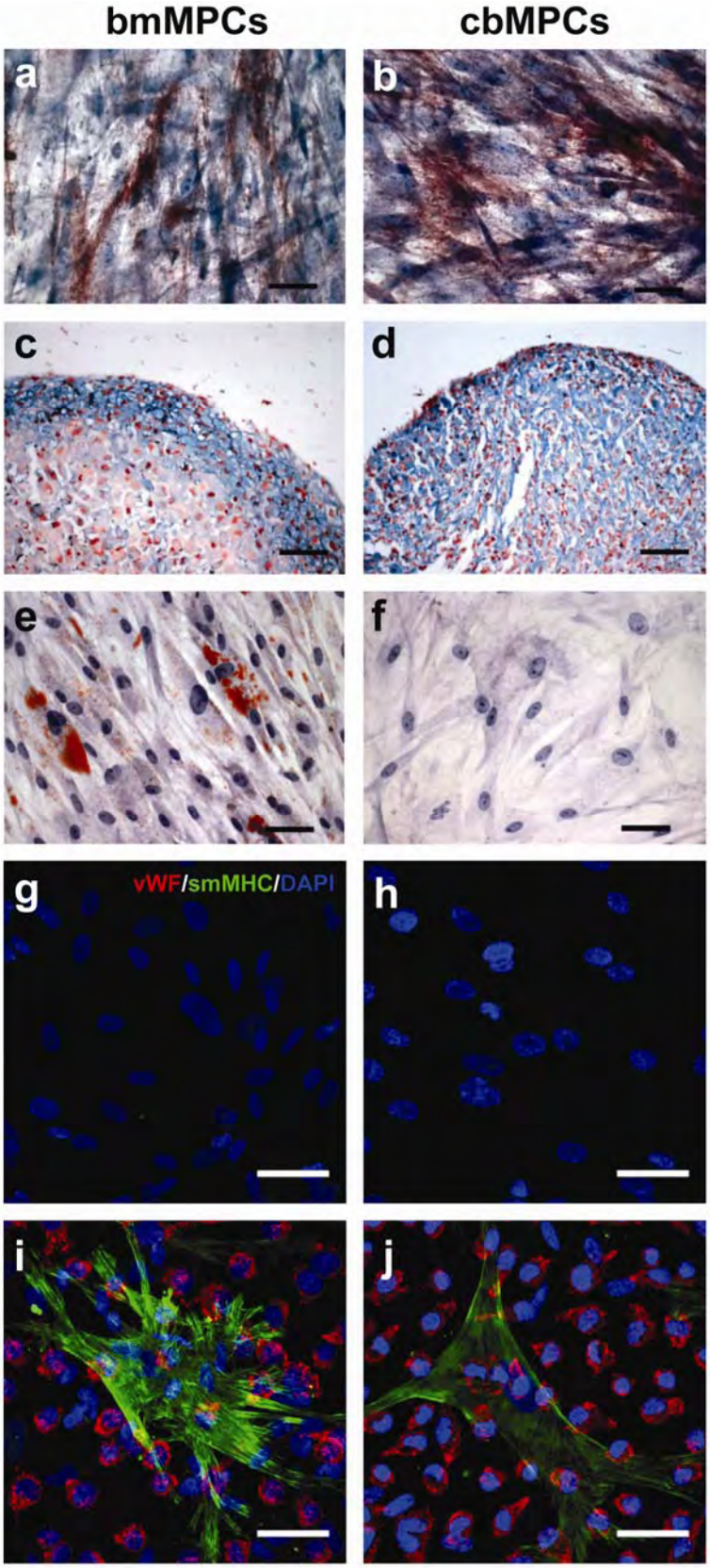

Figure 2

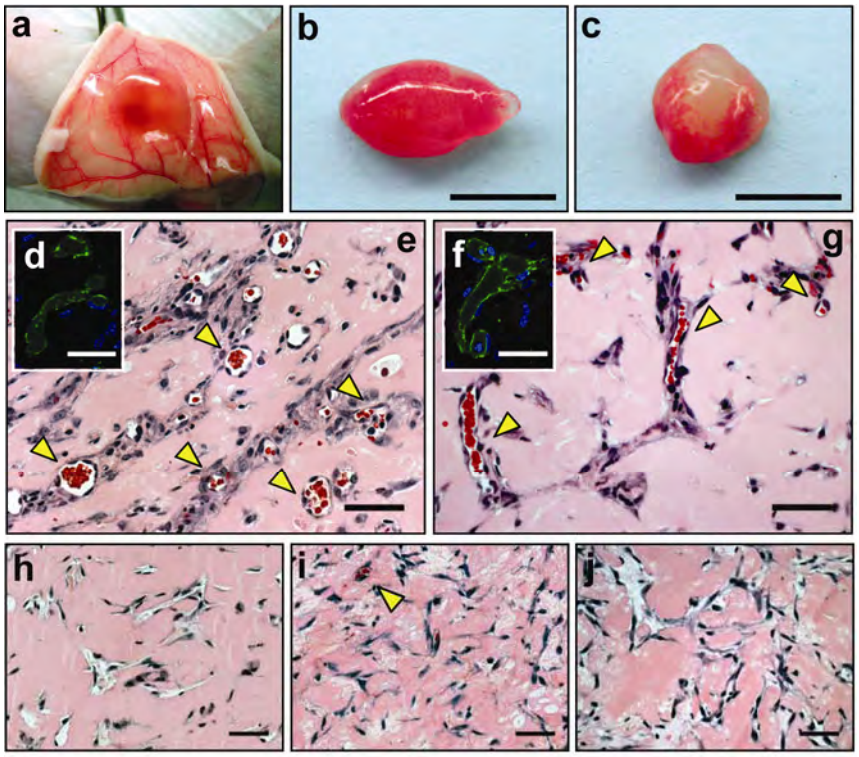
a
b
c
d
e
f
g
h
i
j

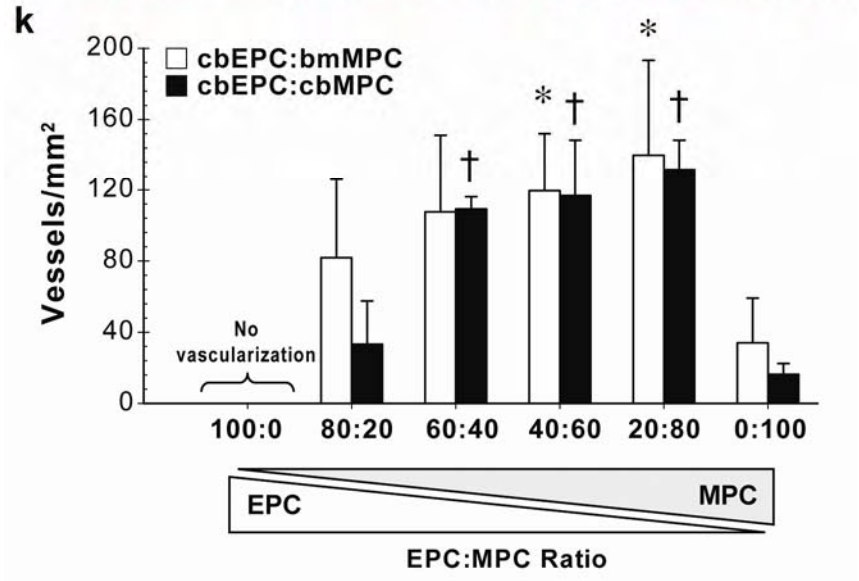
k
cbEPC:bmMPC
cbEPC:cbMPC
Vessels/mm²
200
160
120
80
40
0
No vascularization
100:0
80:20
60:40
40:60
20:80
0:100
*
†
EPC
MPC
EPC:MPC Ratio

Figure 3

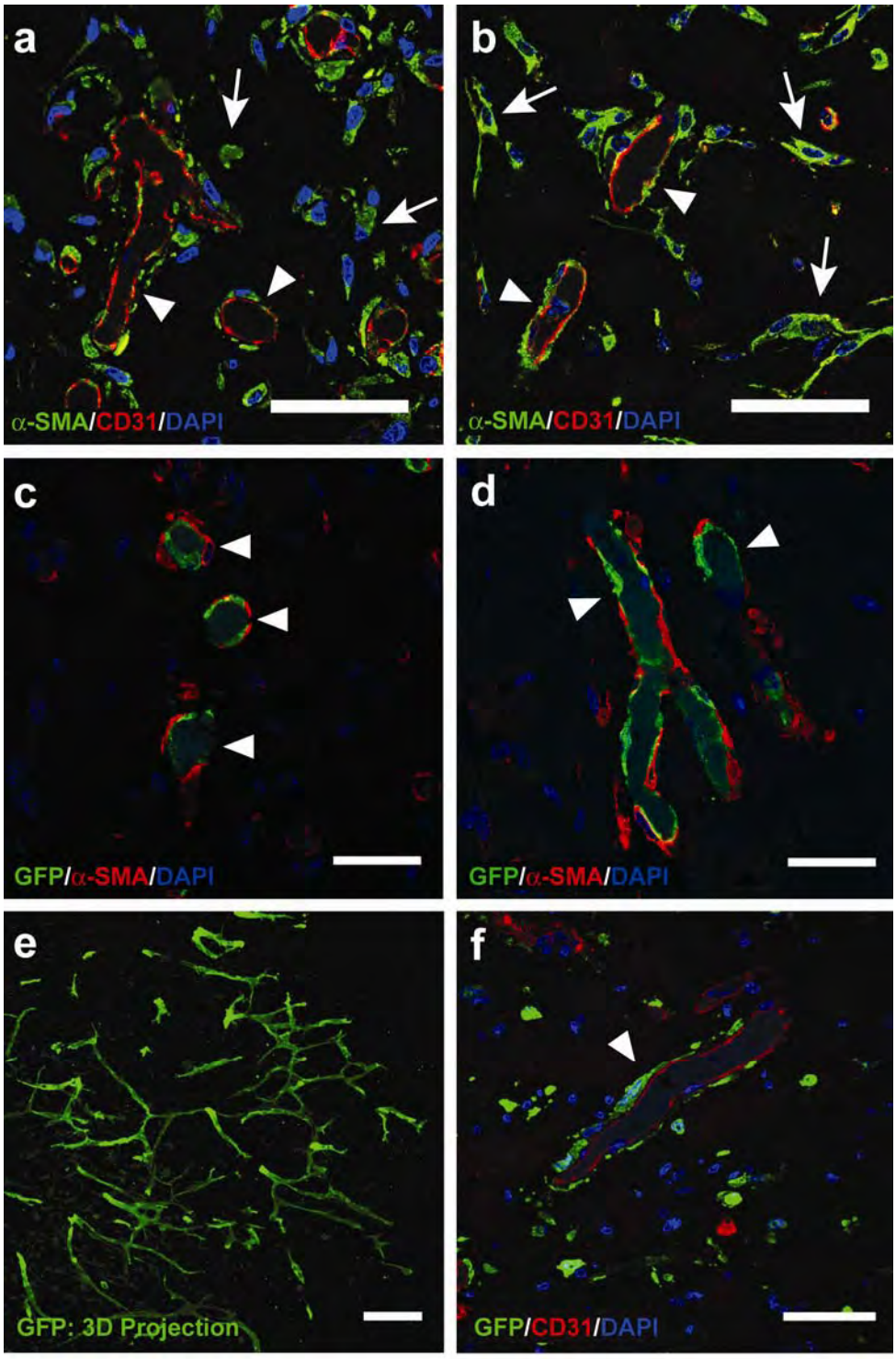
a
α-SMA/CD31/DAPI
b
α-SMA/CD31/DAPI
c
GFP/α-SMA/DAPI
d
GFP/α-SMA/DAPI
e
GFP: 3D Projection
f
GFP/CD31/DAPI

Figure 4

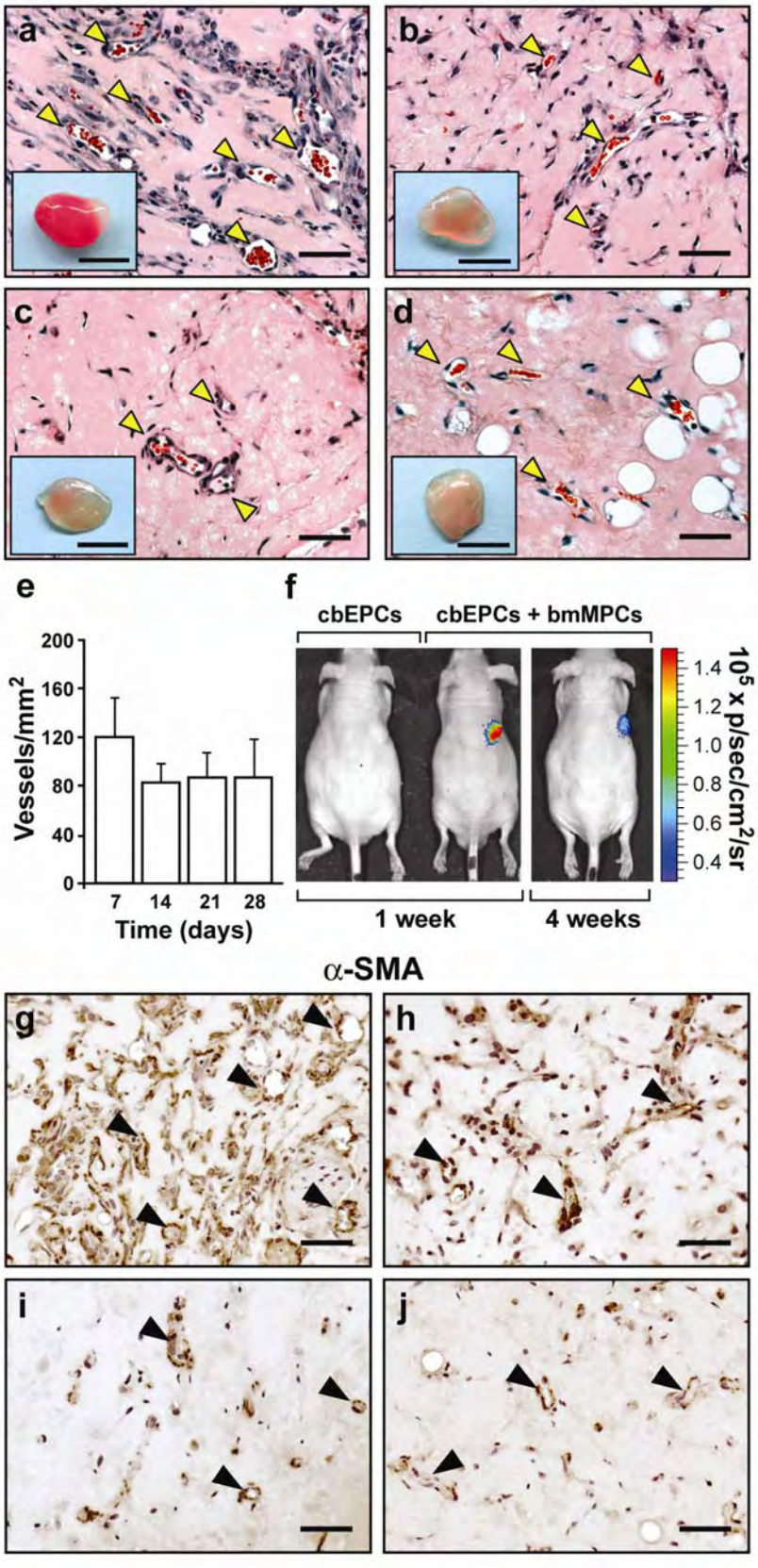
a
b
c
d
e
f
cbEPCs
cbEPCs + bmMPCs
Vessels/mm2
200
160
120
80
40
0
7
14
21
28
Time (days)
1 week
4 weeks
10^5 x p/sec/cm^2/sr
1.4
1.2
1.0
0.8
0.6
0.4
α-SMA
g
h
i
j

Figure 5

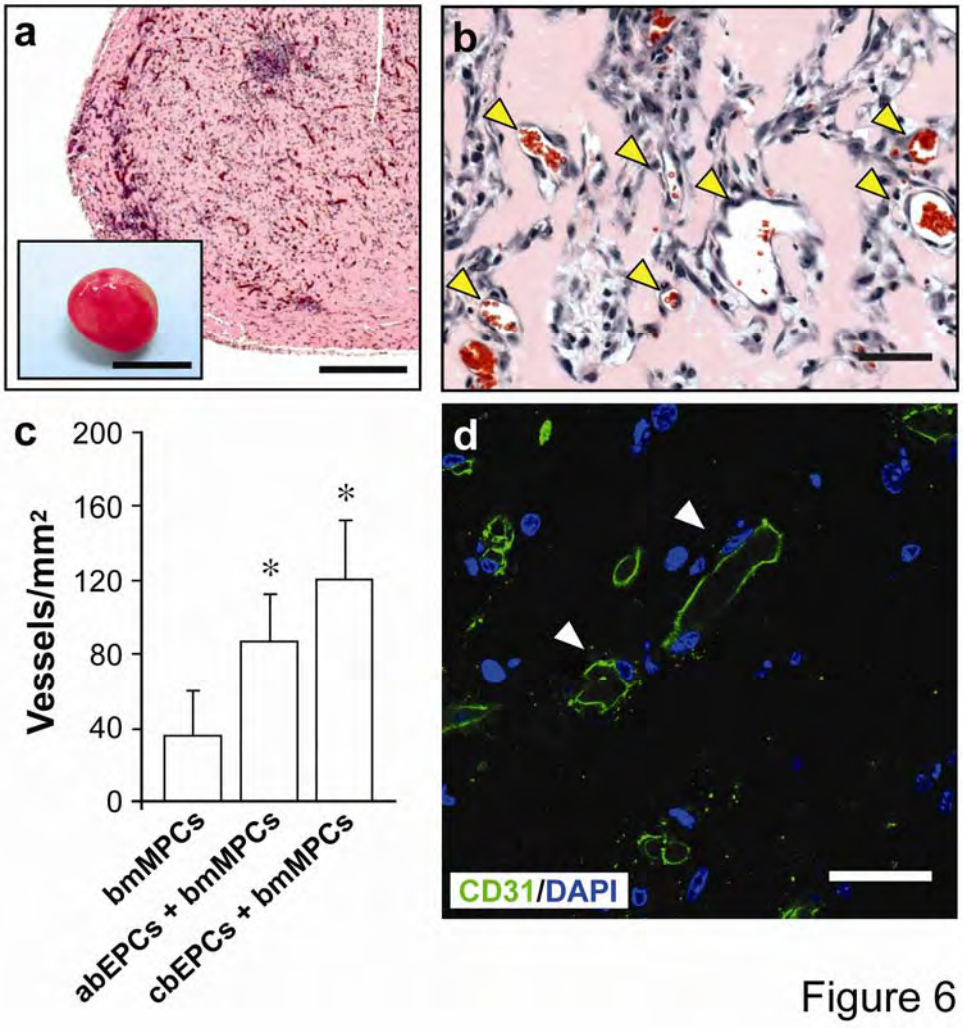
a
b
c
200
160
120
80
40
0
Vessels/mm²
*
*
bmMPCs
abEPCs + bmMPCs
cbEPCs + bmMPCs
d
CD31/DAPI

Figure 6